U.S. Department
of Transportation
Federal Railroad
Administration

Experimental Investigations of Dynamic Buckling of CWR Tracks

Office of Research and
Development
Washington DC 20590

G. Samavedam
A. Kish
D. Jeong

Transportation Systems Center
Cambridge MA 02142

DOT/FRA/ORD-86/07
DOT-TSC-FRA-85-3

November 1986
Final Report

Technical Report Documentation Page

1. Report No	2. Government Accession No	3. Recipient's Catalog No.
DOT/FRA/ORD-86/07		

4. Title and Subtitle	5. Report Date
Experimental Investigations of Dynamic Buckling of CWR Tracks	November 1986
	6. Performing Organization Code: DTS-76
7. Author(s): G. Samavedam*, A. Kish, and D. Jeong	8. Performing Organization Report No.: DOT-TSC-FRA-85-3
9. Performing Organization Name and Address: U.S. Department of Transportation, Research and Special Programs Administration, Transportation Systems Center, Cambridge, MA 02142	10. Work Unit No. (TRAIS): RR519/R5304
	11. Contract or Grant No.
12. Sponsoring Agency Name and Address: U.S. Department of Transportation, Federal Railroad Administration, Office of Research and Development, Washington, DC 20590	13. Type of Report and Period Covered: Final Report, Sep 1983 - Jan 1986
	14. Sponsoring Agency Code: RRS-31

15. Supplementary Notes: *Foster-Miller, Inc., 350 Second Avenue, Waltham, MA 02254

16. Abstract

Thermal buckling of railroad tracks in the lateral plane is an important problem in the design and maintenance of continuous welded rail (CWR) tracks. The severity of the problem is manifested through the large number of derailments which are attributable to track buckling, indicating a need for developing better control on the allowable safe temperature increase for CWR tracks.

The work reported here is a part of a major investigation conducted by the Transportation Systems Center for the Federal Railroad Administration on the thermal buckling of CWR tracks in the lateral plane with the objective of developing guidelines and recommendations for buckling prevention.

This report presents the results of a series of track dynamic buckling tests investigating the influences of vehicle induced loads on the thermal buckling behavior of tangent and curved tracks. Comparisons between theoretical predictions and experimental results are given, and conclusions of practical significance regarding the buckling safety of CWR tracks under dynamic conditions are presented.

17. Key Words	18. Distribution Statement
Track Buckling, Dynamic Buckling, Lateral Stability, Margin of Safety, Continuous Welded Rails	DOCUMENT IS AVAILABLE TO THE PUBLIC THROUGH THE NATIONAL TECHNICAL INFORMATION SERVICE, SPRINGFIELD VIRGINIA 22161

19. Security Classif. (of this report)	20. Security Classif. (of this page)	21. No. of Pages	22. Price
UNCLASSIFIED	UNCLASSIFIED	132	

PREFACE

This report was sponsored by the U.S. Department of Transportation, Federal Railroad Administration, Office of Research and Development, Washington, DC.

The report presents the results of a series of track dynamic buckling tests conducted in the fall of 1983 and 1984 for the purpose of quantifying the lateral buckling mechanism for CWR tracks under dynamic conditions. The tests constitute a major part of the Transportation Systems Center's (TSC) track stability research program being conducted for the Federal Railroad Administration (FRA) for the purpose of developing guidelines and specifications for the prevention of track buckling induced derailments.

The tests were conducted in concert with the Association of American Railroads (AAR) at the Transportation Test Center, under contract DTFR-53-820C-00282, Task Orders No. 10 and No. 17, and with Foster-Miller, Inc. (FMI) under contract DTRS57-83-C-00071. The data reduction and analysis was performed jointly by TSC and FMI.

Thanks are due to Messrs. W. B. O'Sullivan and H. Moody of the FRA for their support throughout the various phases of the test program, and to R. Smith and A. Sluz of the TSC for their test planning and on-site test conduct support.

Acknowledgements are also due to Messrs. L. Daniels and D. Read of the AAR for their efforts in conducting the tests, with special thanks and appreciation to Mr. Read for his dedication, cooperation and hard work throughout the test program.

METRIC CONVERSION FACTORS

Approximate Conversions to Metric Measures

Symbol	When You Know	Multiply by	To Find	Symbol
LENGTH				
in	inches	*2.5	centimeters	cm
ft	feet	30	centimeters	cm
yd	yards	0.9	meters	m
mi	miles	1.6	kilometers	km
AREA				
in^2	square inches	6.5	square centimeters	cm^2
ft^2	square feet	0.09	square meters	m^2
yd^2	square yards	0.8	square meters	m^2
mi^2	square miles	2.6	square kilometers	km^2
	acres	0.4	hectares	ha
MASS (weight)				
oz	ounces	28	grams	g
lb	pounds	0.45	kilograms	kg
	short tons (2000 lb)	0.9	tonnes	t
VOLUME				
tsp	teaspoons	5	milliliters	ml
Tbsp	tablespoons	15	milliliters	ml
fl oz	fluid ounces	30	milliliters	ml
c	cups	0.24	liters	l
pt	pints	0.47	liters	l
qt	quarts	0.96	liters	l
gal	gallons	3.8	liters	l
ft^3	cubic feet	0.03	cubic meters	m^3
yd^3	cubic yards	0.76	cubic meters	m^3
TEMPERATURE (exact)				
°F	Fahrenheit temperature	5/9 (after subtracting 32)	Celsius temperature	°C

*1 in. = 2.54 cm (exactly). For other exact conversions and more detail tables see NBS Misc. Publ. 286, Units of Weights and Measures. Price $2.25 SD Catalog No. C13.10:286.

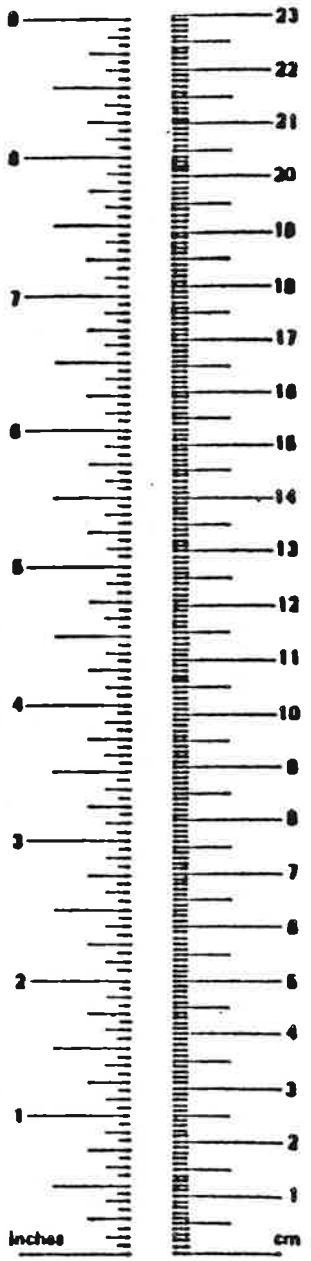

Approximate Conversions from Metric Measures

Symbol	When You Know	Multiply by	To Find	Symbol
LENGTH				
mm	millimeters	0.04	inches	in
cm	centimeters	0.4	inches	in
m	meters	3.3	feet	ft
m	meters	1.1	yards	yd
km	kilometers	0.6	miles	mi
AREA				
cm^2	square centimeters	0.16	square inches	in^2
m^2	square meters	1.2	square yards	yd^2
km^2	square kilometers	0.4	square miles	mi^2
ha	hectares (10,000 m^2)	2.5	acres	
MASS (weight)				
g	grams	0.035	ounces	oz
kg	kilograms	2.2	pounds	lb
t	tonnes (1000 kg)	1.1	short tons	
VOLUME				
ml	milliliters	0.03	fluid ounces	fl oz
l	liters	2.1	pints	pt
l	liters	1.06	quarts	qt
l	liters	0.26	gallons	gal
m^3	cubic meters	36	cubic feet	ft^3
m^3	cubic meters	1.3	cubic yards	yd^3
TEMPERATURE (exact)				
°C	Celsius temperature	9/5 (then add 32)	Fahrenheit temperature	°F

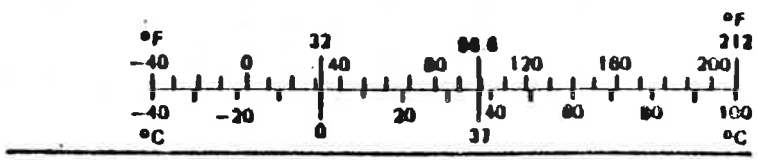

TABLE OF CONTENTS

TABLE OF CONTENTS (Continued)

LIST OF ILLUSTRATIONS

LIST OF ILLUSTRATIONS (Continued)

LIST OF ILLUSTRATIONS (Continued)

LIST OF ILLUSTRATIONS (Continued)

LIST OF TABLES

EXECUTIVE SUMMARY

The increased utilization of continuous welded rail (CWR) tracks in the United States has resulted in a large number of accidents attributable to train derailments induced by thermal buckling of railroad tracks. In an effort to improve the safety of CWR tracks, experimental and analytic investigations are being conducted by the Transportation Systems Center (TSC) supporting the safety mission of the Federal Railroad Administration (FRA). This report describes a part of these investigations dealing with the dynamic buckling behavior of CWR tracks.

Specifically, the work described here presents the results of a series of track dynamic buckling tests conducted in the fall of 1983 (Phase I) and the fall of 1984 (Phase II), which investigated the influence of vehicle induced loads on the thermal buckling of tangent and curved tracks with the following objectives:

a. To verify the dynamic safe temperature increase concept proposed in the dynamic buckling theory

b. To study the effect of track uplift in between trucks of long cars, and verify analytical predictions on dynamic buckling behavior

c. To assess lateral and vertical load influence on misalignment growth mechanisms in combination with high thermal loads

The thermal load was generated by artificially heating the rails, and the vehicle/load influence was provided by short train consists operating at various speeds up to 40 mph. Measurements included the various elements of track characterization, rail temperature, rail longitudinal forces, lateral

and vertical displacements, and wheel/rail loads. Based on the results of these tests, the following major conclusions are drawn:

a. The "static safe temperature" criterion by itself is not sufficient to ensure the buckling safety of CWR tracks under traffic. Dynamic buckling response must be included in the determination of safety limits for buckling prevention.

b. To minimize growth of misalignments of tracks with initial imperfections when subjected to traffic and high thermal loads, tracks must have an "adequate" lateral resistance. This resistance can be determined analytically by stipulating the tracks to have a certain specified "margin of safety," defined as the difference between the dynamic buckling and safe temperatures.

c. The margin of safety concept was partially verified experimentally on a 5 degree curve by comparing the dynamic stability under inadequate lateral resistance to one with "minimally acceptable" lateral resistance.

d. The central bending wave producing vertical uplift displacement between the trucks of a car is, to a large extent, responsible for the growth of the lateral misalignments, hence for the progressive buckling of weak tracks. The effect of this uplift wave influence caused by a long hopper car is more pronounced than one caused by a locomotive. The resulting loss in lateral resistance due to uplift is a key contributor to dynamic instability.

e. The experimental results are in good agreement with the theoretical concepts and analyses used for the prediction of dynamic buckling behavior of CWR tracks.

LIST OF SYMBOLS AND ABBREVIATIONS

x	longitudinal distance from center of track
E	Young's modulus for rail steel
A	rail cross-sectional area
I	rail area moment of inertia about vertical axis
ΔT	rail temperature increase (above the stress-free temperature)
ΔT_s	safe temperature increase (above the stress-free temperature)
ΔT_B	buckling temperature increase (above the stress-free temperature)
P	rail compressive force in the buckled zone
P	compressive rail force in the rails
P_L	applied lateral force in track resistance test
w	lateral deflection
U	axial displacement in the buckled zone
u	axial displacement in the adjoining zone
v	vertical deflection
w'	primes denote derivatives with respect to x
$\dot{w}$	dots denote derivatives with respect to θ
α	coefficient of thermal expansion
F_o	constant track lateral resistance
f_o	constant track longitudinal resistance
2ℓ	test track length
$2L$	buckling length
$2L_o$	length of initial misalignment
δ_o	initial misalignment amplitude
k_v	track modulus (units: lb/in/in abbreviated as psi)
R	radius of curvature
L/V	ratio of lateral to vertical load
μ	friction coefficient between ties and ballast
k_e	end stiffness
f_1	longitudinal resistance inside heated zone
f_2	longitudinal resistance outside heated zone

1. INTRODUCTION

A major concern of the Federal Railroad Administration (FRA) and the railroad industry is the buckling safety of tracks with continuous welded rails (CWR) subjected to thermal and vehicle loads. The FRA has been sponsoring a research program through the Transportation Systems Center (TSC) for the development of performance based safety specifications and guidelines for prevention of the CWR track buckling. The work reported here is a part of this research program.

In an earlier work (1), an experimental validation of the 'static' theory developed in (2-3) was presented. The work involved both tangent and curved tracks, and buckling was caused by thermal loads induced by rail heating in the absence of vehicle loads.

In a recent work (4), the influence of vehicle loads on thermal buckling of CWR tracks has been studied theoretically. The theoretical results show that the vehicle influences can be significant, particularly on the buckling temperature. Further, the track response characteristic (temperature increase versus the track lateral deflection curve) can be very much different from that in the 'static' case. The theory predicts also that the 'margin of safety,' i.e., the difference between the dynamic buckling and the safe temperature, (see Figure G-1), is reduced in the presence of vehicle loads, and in fact can be zero, unless an adequate amount of lateral resistance is maintained in the track. Tracks with a low margin of safety can buckle out progressively under the combined effects of thermal and vehicle loads.

An important dynamic buckling consideration used in the theory (4) is based on the assumption that in the central zone between the leading and the trailing trucks of cars, the track

lateral resistance is altered significantly due to the vertical wheel loads. At some distance away from the trucks, there can be a reduction in the lateral resistance due to lift off or reduced pressure between ties and ballast. The reduction in the lateral resistance could be sufficient to cause buckling of the track. Therefore, the central bending wave between the trucks is an important characteristic in the dynamic buckling analysis.

Some of the parameters influencing the stability of CWR tracks under vehicles are: the truck center spacing, the track vertical stiffness, the tie ballast friction coefficient, and the lateral and vertical wheel loads. The track curvature, imperfections and the unloaded track lateral and longitudinal resistances are also important, as in the case of the static theory.

As a part of the TSC's track stability research program, dynamic buckling tests were designed and conducted to experimentally verify the dynamic buckling theories and concepts. These tests were conducted in two phases at the Transportation Test Center (TTC).

Phase I tests were conducted in the months of October and November of 1983. The results of this program were used to conduct preliminary analyses and verification studies and to define Phase II tests which were conducted in August-September of 1984.

The tests were performed on a tangent and on a 5 degree curved segment of the balloon loop (Figure 1). The test length (heated zone) of the segments was 200m in Phase I and 300m in Phase II. The test segments were of wood tie and cut spike construction with channel type of anchors, slag ballast and 136 RE continuous welded rail (Figure 2).

SITE DESCRIPTION

- o 136RE CWR rail
- o 7" x 9" x 8'6" wood ties
- o cut spikes
- o 14" AREA 'A' punch plates
- o channel type anchors every tie
- o recently tamped slag ballast
- o 12"-15" shoulders
- o Curved site: 5 degree curve with 4 inches of superelevation and 0.5% grade
- o Tangent site: 0.8% grade
- o Loop is designed for 45 mph operation

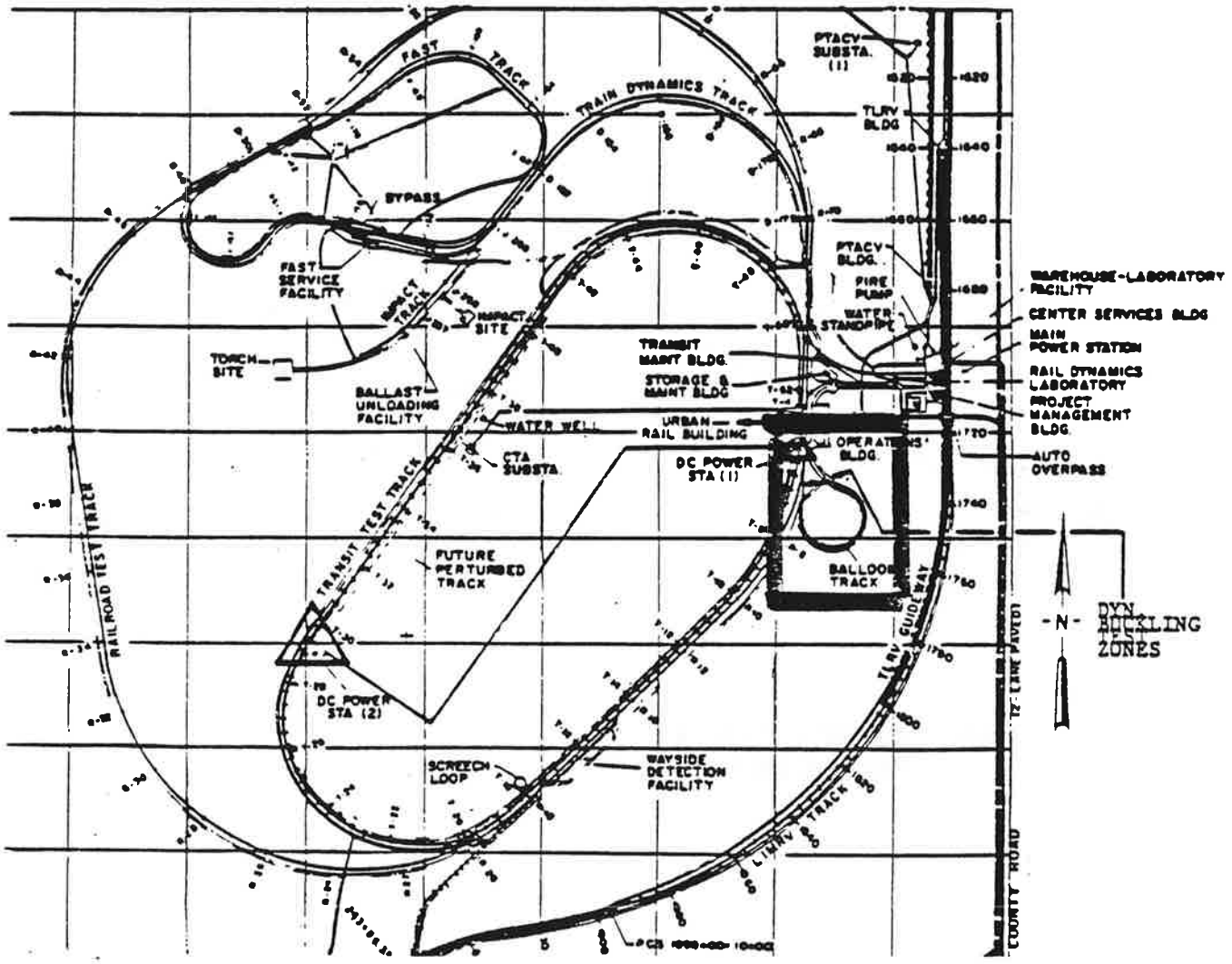

FIGURE 1. SITE LOCATION

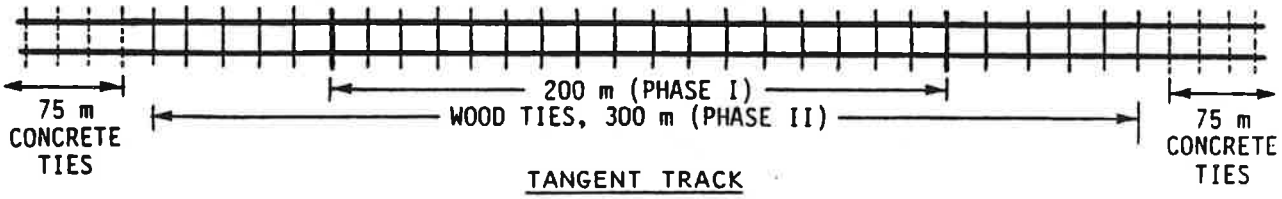

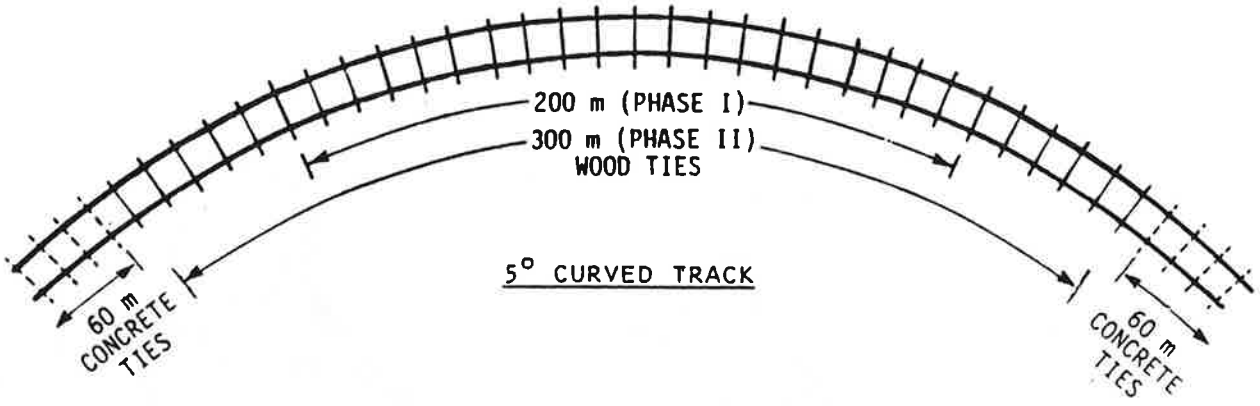

NOTE: CONCRETE TIES IN PHASE II ONLY

FIGURE 2. TEST SEGMENTS

As in the previous static buckling tests on the Southern Railway at The Plains (1), the compressive force in the rails was artificially induced by passing direct current of the order of 6,500A. However, there was a fundamental difference in the source for this current. Whereas in the static tests, the required current was drawn from the alternators of diesel locomotives, at TTC power was drawn from two substations. The former method provided a mobile source of rail heating which could be utilized to test any track in service such as the tracks tested on the Southern Railway. The latter method, although restricted to the locations near the substations, provided a 'laboratory' type of environment for buckling tests. In the early stages of Phase I, only one substation was used and some difficulties were experienced in obtaining a continuous output of current of the order of 6,500A. A second substation which was at some distance away from the test tracks was subsequently coupled in parallel with the first to give the required output. The running rails of the transit tracks were used to draw the current from the second substation.

The purpose of this document is to present the Phase I and Phase II dynamic buckling experiments, including test objectives, methodology, instrumentation, test results and results of relevant analysis verification studies.

For convenience, Phase I and II tests will be described in separate sections of this report; however, a unified theme is maintained in the presentation and the conclusions are integrated. Certain theoretical concepts and some explanations of the terminology used in this report are presented in the Glossary of Terms.

2. PHASE I TESTS

The tests were conducted in accordance with the requirements defined in (5) and as per the test plan (6).

2.1 OBJECTIVES

The main objectives of Phase I tests were:

a. To prove the existence of the central bending wave in between the trucks of a car, which tends to lift the rails and ties, causing changes in the local lateral resistance.

b. To check for the safety of the tangent and curved tracks under moving vehicles, when the rails are heated up to the theoretical dynamic safe temperature levels

c. To determine the dynamic buckling strength of tangent and curved tracks, under a locomotive, a hopper car and with no car (static buckling strength).

To achieve the foregoing objectives, a series of tests were conducted on tangent and curved tracks. The test operations and the test conduct will be presented in the following paragraphs. Track characterization tests were first carried out with the purpose of determining the required input parameters for the dynamic buckling analysis (4).

2.2 TRACK CHARACTERIZATION

The important parameters include rail neutral temperature, lateral and longitudinal resistances, vertical track modulus, and the tie ballast friction coefficient.

2.2.1 Rail Neutral Temperature

To establish a known and uniform rail neutral temperature, the track was destressed. The track was already welded at one end of the test zone and gaps were left at the other end. The rail anchors were removed and the rails were allowed to "breathe." To enhance the breathing, a rail vibrator was employed.

The gaps at the other end were intended to be closed by field welds when the rail temperature would be around 80°F. This was difficult to achieve in practice, because the rail temperature was changing during the welding operation. Prior to welding, each of the strain gauge readings was first taken by means of a portable strain indicator box. The box was disconnected from the strain gauge circuit, and the latter was connected immediately to the signal conditioning unit in the data van. The strain gauge readings from the portable strain indicator box were used in the data van to provide the references (zeros).

Analysis of the temperature and rail force data showed that the neutral temperature of the two rails were not equal in some experiments. Additional problems were created by asymmetric distribution of forces. This was partly attributable to inadequate destressing and partly to instrumentation errors.

The tangent track was destressed at a rail average temperature of 70°F to 75°F for the safe temperature test, and about 80°F for the buckling temperature determination test. The curve was destressed at rail temperature of 76°F.

2.2.2 Lateral Resistance

This parameter is determined from the Track Lateral Pull Test (TLPT). As in the previous static tests (1), the setup for this test consists of the lateral pull rig, Figure 3, and a bulldozer to provide the reaction. A load cell was used to

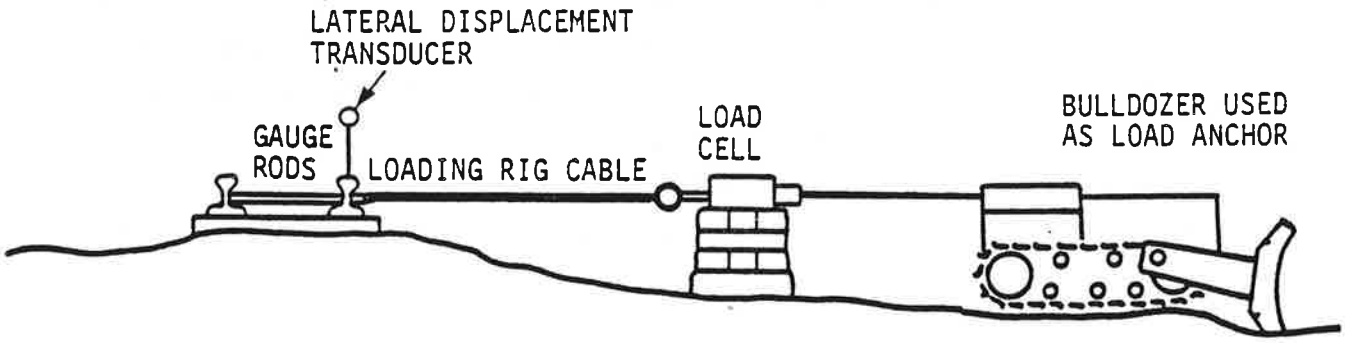

FIGURE 3. TRACK LATERAL PULL TEST RIG (TLPT)

measure the lateral force and a string pot to measure the lateral displacement at the point of load application. The load was applied to the track gradually using the hydraulic pump, until a maximum rail deflection of about 2 in. was reached. The output of the load cell and the string pot was displayed on an X-Y plotter in engineering units.

Figure 4 shows the data obtained for the tangent and curved tracks, which had 12 to 15 in. shoulder and tamped slag ballast.

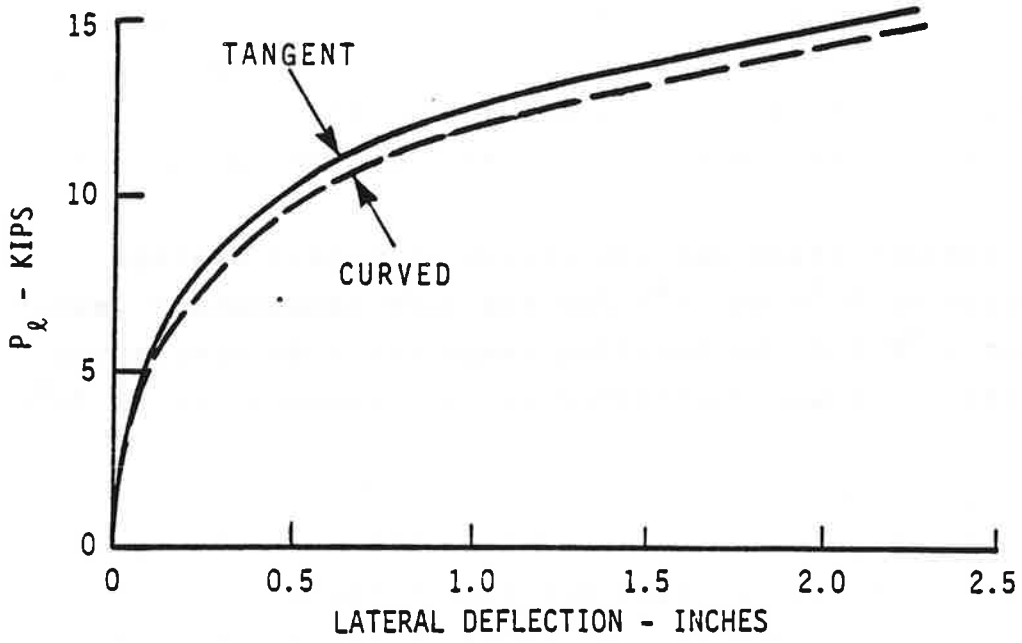

FIGURE 4. FORCE - DEFLECTION RELATIONSHIP (TANGENT TRACK)

The data has been reduced to determine the bilinear lateral resistance using the algorithm described in Reference (7). The resistance values are shown in Figure 5.

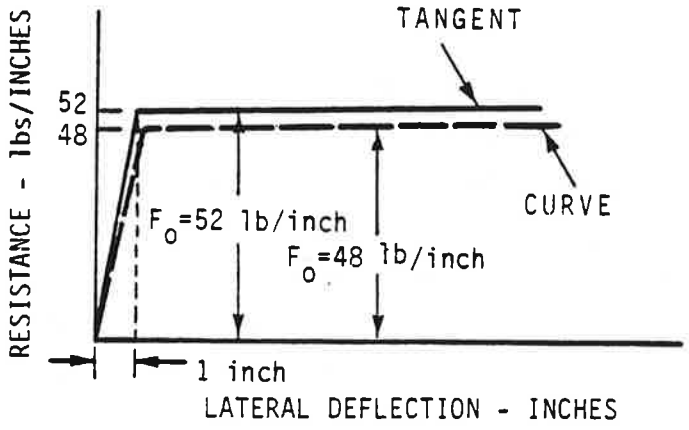

FIGURE 5. REDUCED LATERAL RESISTANCE (TAMPED SLAG BALLAST, 12 TO 15 in. SHOULDER)

2.2.2.1 Tie-Ballast Friction Coefficient - This parameter is required in the dynamic buckling analysis for the computation of lateral resistance distribution under vehicle loads. To determine this, 16 concrete ties were placed across the rails at intervals of 30 in, providing a total distributed load of 13.6 kips. The lateral resistance in the loaded zone was measured as in the lateral resistance tests. The friction coefficient μ is evaluated using the formula

$$\mu = \frac{\text{(Loaded Resistance - Unloaded Resistance)}}{\text{Vertical Load Per Unit Length}}$$

The lateral resistance of the loaded tangent track was found to be 75 lb/in.; the unloaded resistance is 52 lb/in. as before. The friction coefficient works out to be about 0.81. The same value is used for the curved track.

2.2.3 Longitudinal Resistance

Before the rail ends were welded, attempts were made to pull the rails longitudinally and monitor the longitudinal

forces and displacements for the determination of the longitudinal resistance. These attempts were not successful due to the equipment failure. However, the resistance parameter was determined from the data collected from the safe and buckling temperature determination tests. (The instrumentation and test methodology will be described later.)

The rail force distributions measured in the tangent track tests are shown in Figure 6. As indicated, the two distributions correspond to the two different anchoring patterns employed in the tests. Initially, every other tie was anchored in the safe temperature test. The ends of the heated section showed substantial longitudinal movement. It was thought desirable to increase the longitudinal resistance and hence decrease the end movement. In subsequent tests, therefore, every tie was anchored. The force distribution for the curve is shown in Figure 7.

The resistance is determined by the force gradient under the assumption that it is constant. For the tangent track, it is found to be 23.5 lb/in. of track length (420 kg/m) when every other tie was anchored, and 35.4 lb/in. (634 kg/m) when every tie was anchored.

The force distribution for the curved track is shown in Figure 7. The longitudinal resistance is determined to be 46.9 lb/in. (840 kg/m) (every tie in the curve was anchored).

2.2.3.1 End Stiffness - This is the relationship between the rail force at the end of the test zone and the longitudinal rail displacement at the end. For the finite track analysis (Appendix A), this stiffness is an important parameter. The stiffness characteristic as determined in the experiments is seen in Figures 8 and 9 for the tangent and the curve, respectively.

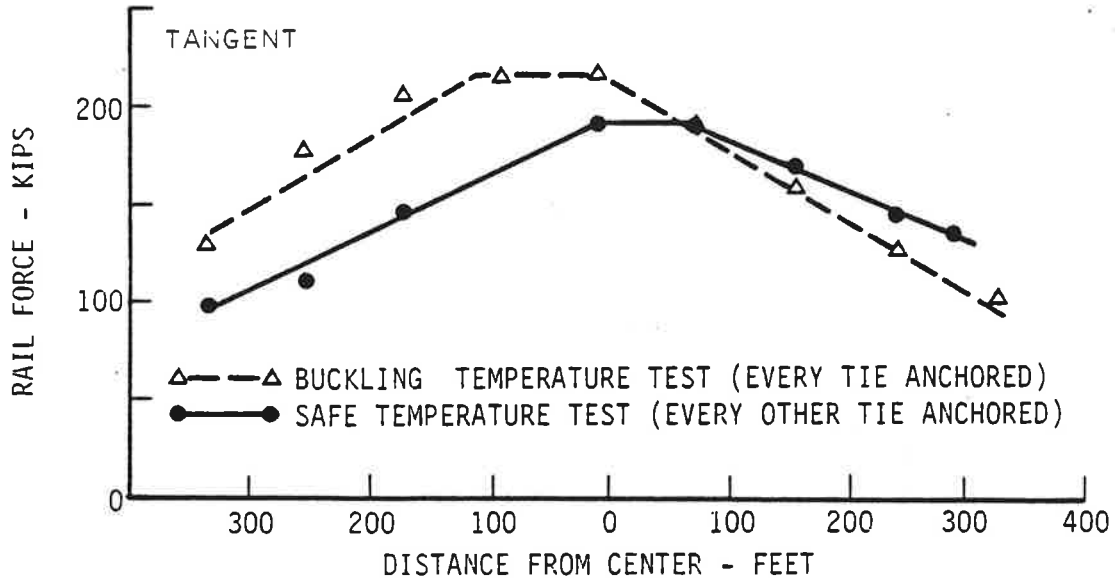

FIGURE 6. RAIL FORCE DISTRIBUTION IN TANGENT TRACK

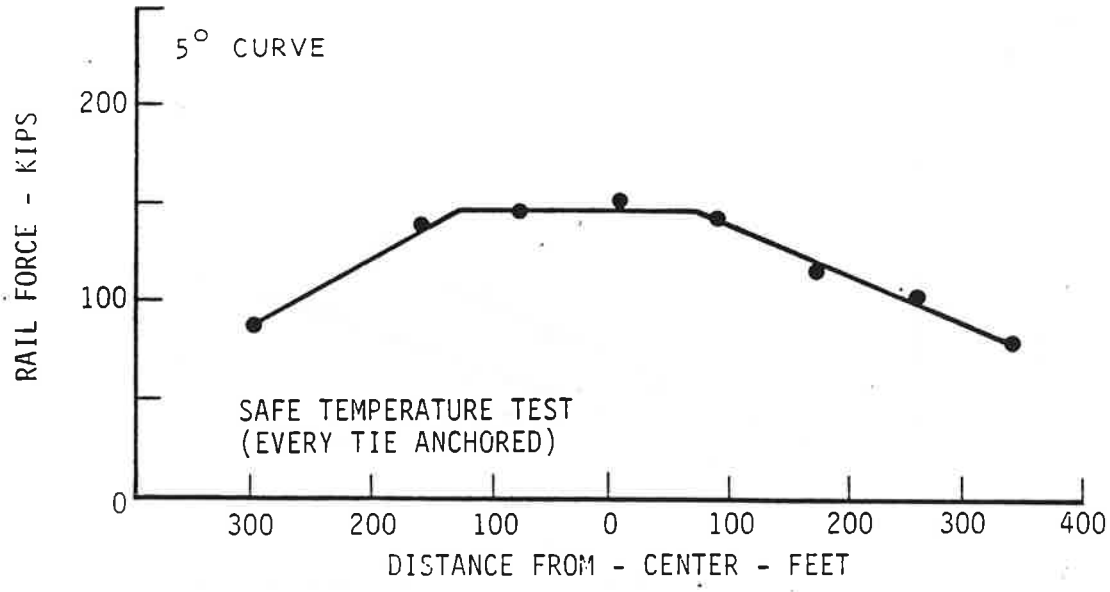

FIGURE 7. RAIL FORCE DISTRIBUTION IN CURVED TRACK

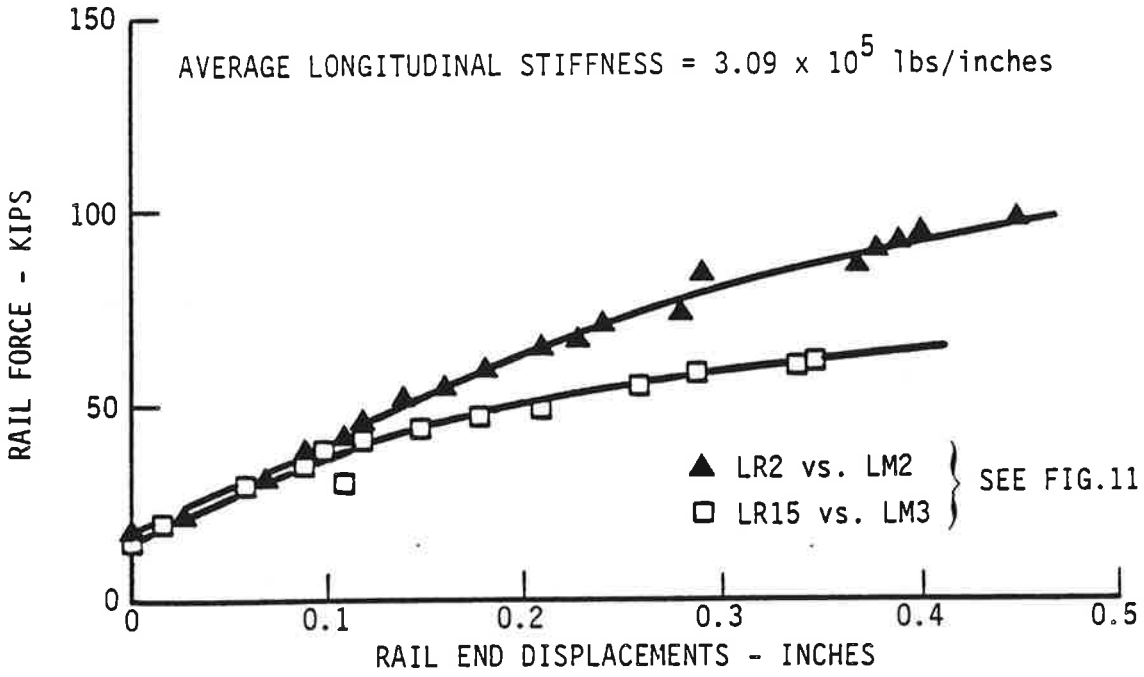

FIGURE 8. END STIFFNESS CHARACTERISTIC (TANGENT)

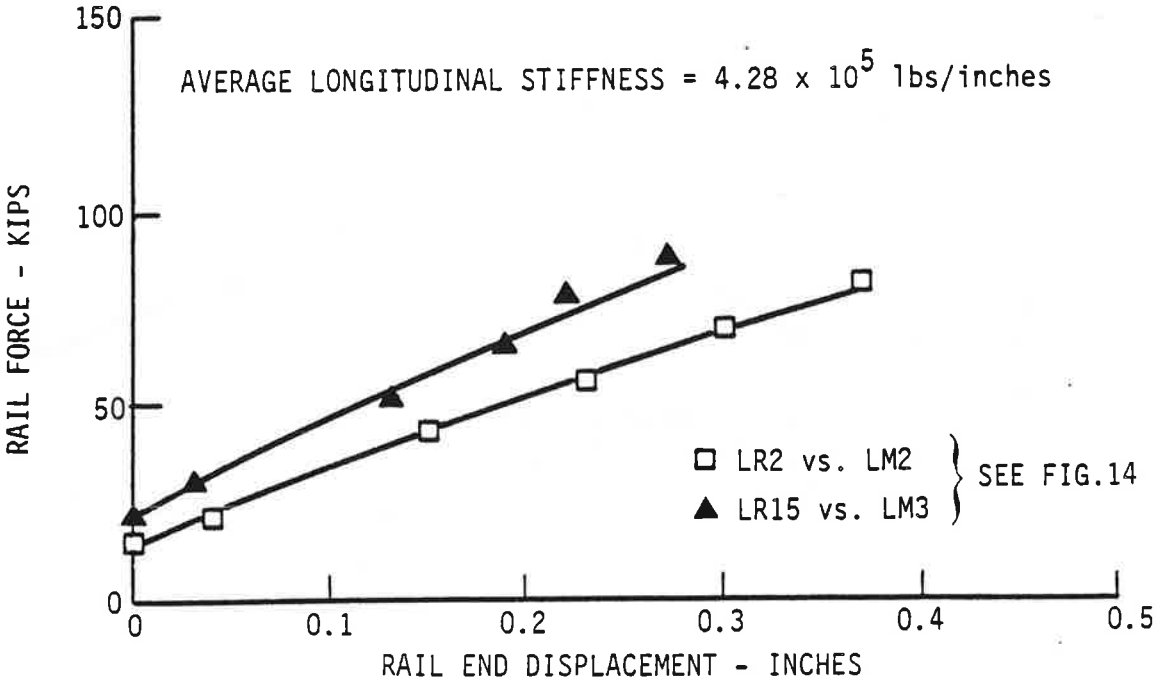

FIGURE 9. END STIFFNESS CHARACTERISTIC (CURVE)

The end stiffness is also dependent on the longitudinal resistance outside the test zone. Although the external resistance was not directly measured, it could be estimated on the basis of the stiffness relationship described in Appendix A. Calculations have shown that the average longitudinal resistance outside the test zones is 44 lb/in. for the tangent track and 52 lb/in. for the curved track. The average values are required in the analysis, which assumes equal stiffness values at both ends. It may be noted that the external resistance is higher than the internal (inside the test zone), as one would expect since the test zone was tamped and the outside zone was not.

2.2.4 Vertical Track Modulus

Vertical deflections of the ties under the Hopper car were measured using LVDTs. The results for the tangent track are shown in Figure 10.

The best theoretical fit of the experimental data gives a value of K_v = 3000 psi. As seen from Figure 10, the scatter is significant near the center of the vehicle. According to Hetenyi's (8) analysis, there will be a "lift off" in the central zone. This was apparently too small (less than 0.01 in.) to be measurable by the instrumentation setup used in the experiment.

The vertical modulus value K_v = 3000 psi was verified also by the TTC Track Modulus 605 car measurements. The modulus for the curved track was also found to be approximately the same value as for the tangent track.

From the point of view of realizing the first objective of quantifying the uplift (subsection 2.1), the experiment was not conclusive. Additional attempts were therefore made in Phase II to improve the measurement accuracy as described later.

2.3 MEASUREMENTS

In addition to the track parameters referred to in subsection 2.1, the following quantities were measured during the buckling tests.

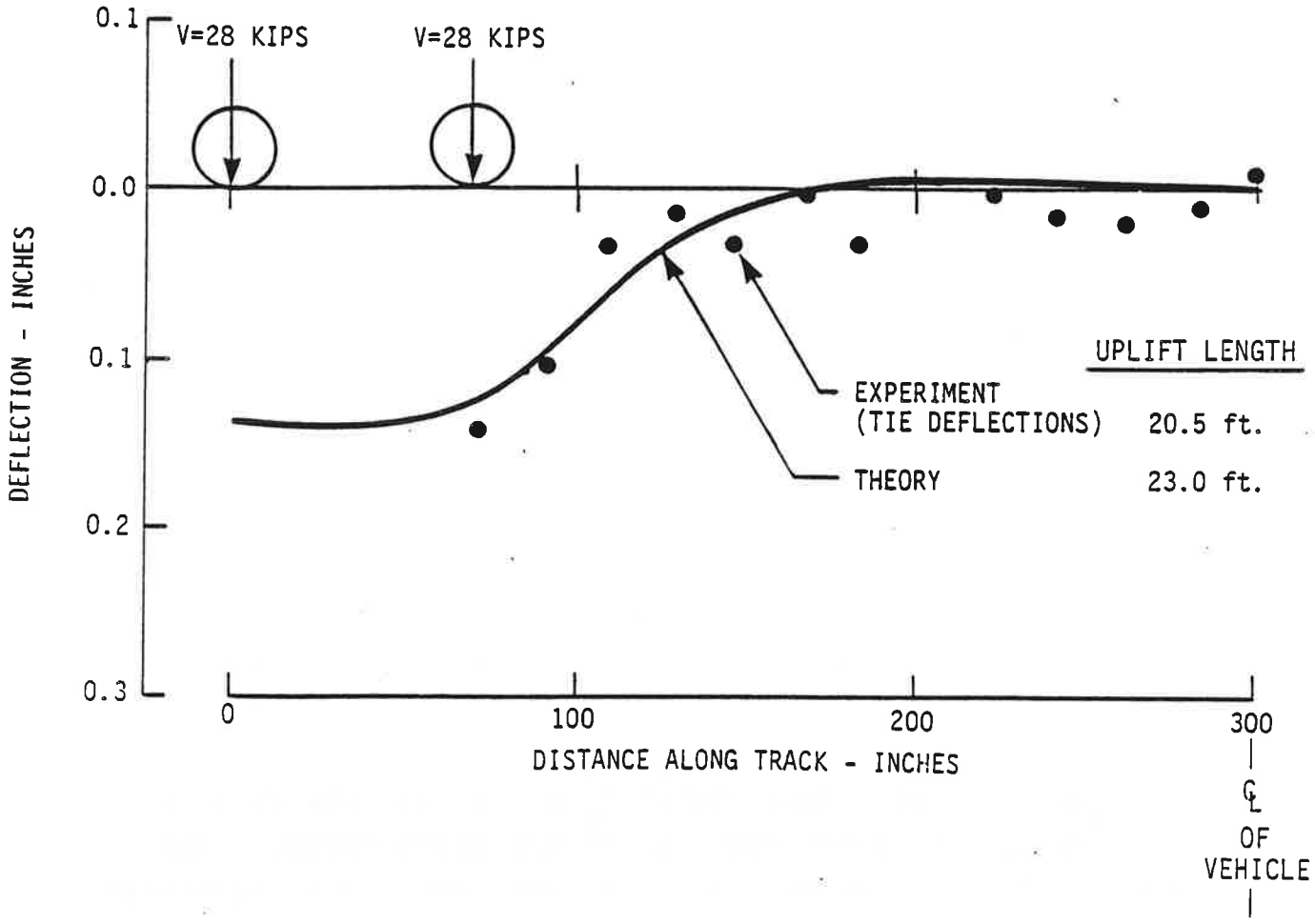

FIGURE 10. VERTICAL DEFLECTION UNDER HOPPER CAR (TANGENT TRACK)

Rail Temperature was measured using the thermocouples spot welded to the rail web; the temperature was continuously monitored during the heating tests, and the values in ^{o}F were printed on the datalogger output (HP9826 Multiprogrammer).

Longitudinal Rail Force was measured using the standard four-arm strain gauge bridge configuration (2 longitudinal gauges and 2 vertical gauges (1), as done in The Plains tests). The gauge circuit gives the mechanical strain after compensating for thermal strains. The rail force is calculated using the formula

$$P = \frac{AEe}{2(1+\nu)}$$

where

A = rail cross sectional area
E = modulus = 30×10^6 psi
ν = Poisson's ratio = 0.3
e = bridge output in mechanical strain

The datalogger was programmed to yield the rail force in kips. The force was continuously monitored during the tests at various locations on the two rails.

Displacement - The lateral displacements of the track were measured with respect to a fixed "reference rail" using rotary potentiometer. The longitudinal displacements of the rails at the ends were also measured using the same type of instrument. The vertical displacements of the rails and the ties were measured using the LVDTs (Linear Variable Differential Transformer). All the instruments were connected to the datalogger.

Vertical Loads on the rails due to vehicles were measured using the standard four-arm strain gauge bridge circuit as indicated in Reference (6).

Lateral Load - The lateral load generated on the rail, as the wheel negotiated the lateral imperfections, was measured using the standard strain gauge bridge circuit, as described in Reference (6).

2.3.1 Instrumentation Deployment

Table 1 provides a list of the different measurements made and the instrumentation notation used in the tests. The instrumentation deployment for the tangent track is shown in Figure 11 for the safe temperature test, and Figure 12 for the buckling temperature test. Figures 13 and 14 show the instrument deployment for the curved track tests.

The instrumentation was connected to the signal conditioning units in the data van, which was situated near the center of the test zone. The outputs from the signal conditioning units were connected to a 24-channel datalogger, which was programmed for output in engineering units. A backup magnetic tape recorder was also used.

2.4 TESTS ON TANGENT TRACK

The procedures used for the determination of the dynamic safe and buckling temperatures of the tangent track are described briefly here. The test results and comparisons with the theoretical predictions are also presented.

2.4.1 Safe Temperature Test

The objective of this test was to investigate the safety of the tangent track when heated up to the theoretical dynamic safe temperature and subjected to traffic. The test concept was to establish "buckling safety" by allowing multiple passes at different speeds, when the rails were at the theoretical

safe temperature and monitoring the misalignments. The theoretical dynamic safe temperature increase was analytically determined to be 75°F, using the parameters measured in the track characterization tests.

TABLE 1. MEASUREMENTS AND INSTRUMENTATION NOTATION FOR PHASE I

MEASUREMENT	METHOD	RANGE	SYMBOL ON MAP	DATA LOGGER SYMBOL
1. Longitudinal Rail Force	Strain Gauge	±300 Kips	▲	LR
2. Rail Temperature	Rail Thermo-couple	0° to 350° F	○	RT
3. Lateral Rail Displacements	Rotary Poten-tiometer	0 to 25 in.	○	LD
4. Longitudinal Rail Displacements to Ground	Rotary Poten-tiometer	-2.5 to +2.5 in.	⊠	LM
5. Vertical Wheel Loads	Vertical Load Gauge	0 to 40 Kips	⬡	RV
6. Vertical Displacemeents to Ground	LVDT	-1 to +1 in.	⊠	VT

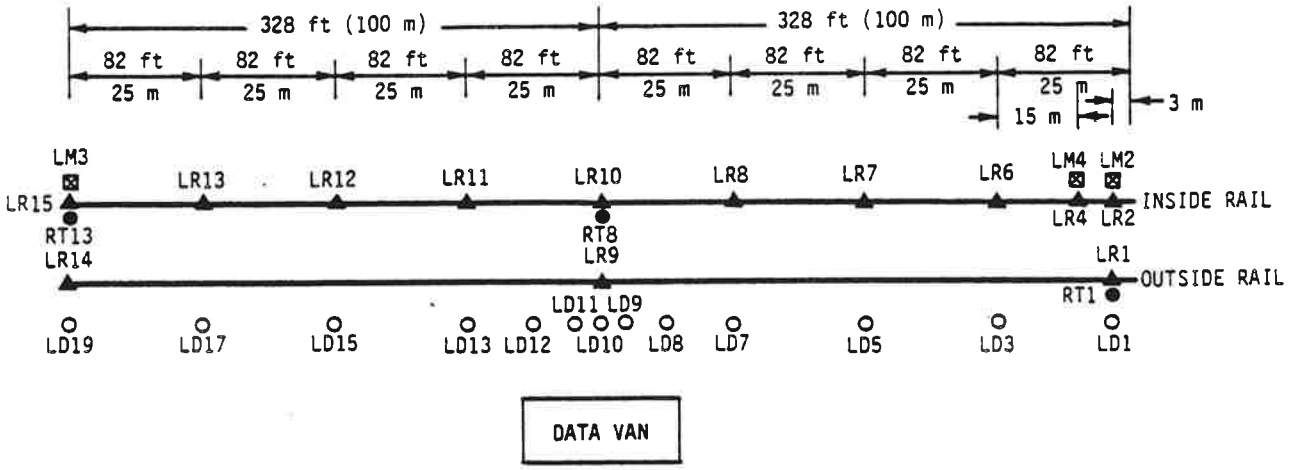

FIGURE 11. INSTRUMENTATION DEPLOYMENT FOR SAFE TEMPERATURE TEST (TANGENT TRACK)

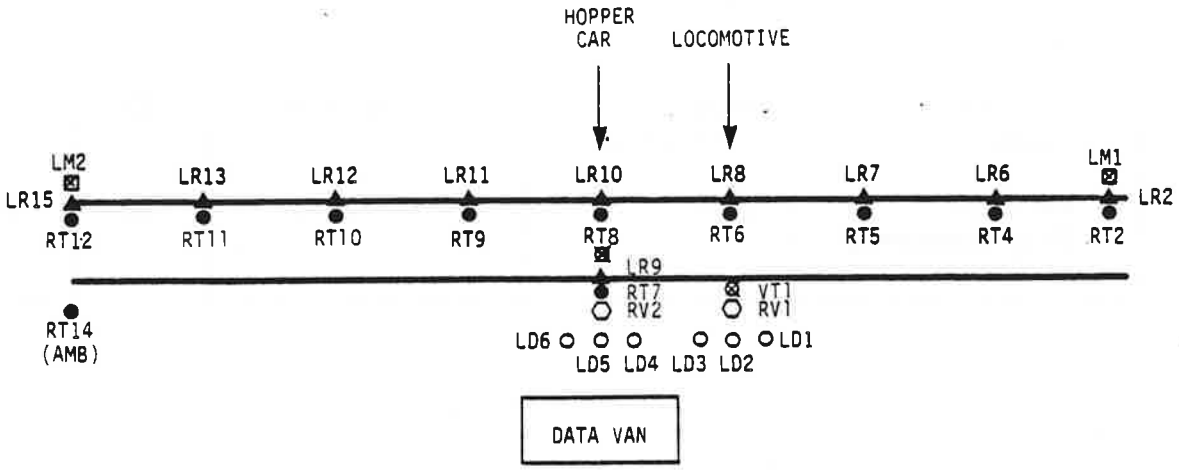

FIGURE 12. INSTRUMENTATION DEPLOYMENT FOR EXPLOSIVE BUCKLING TEST (TANGENT TRACK)

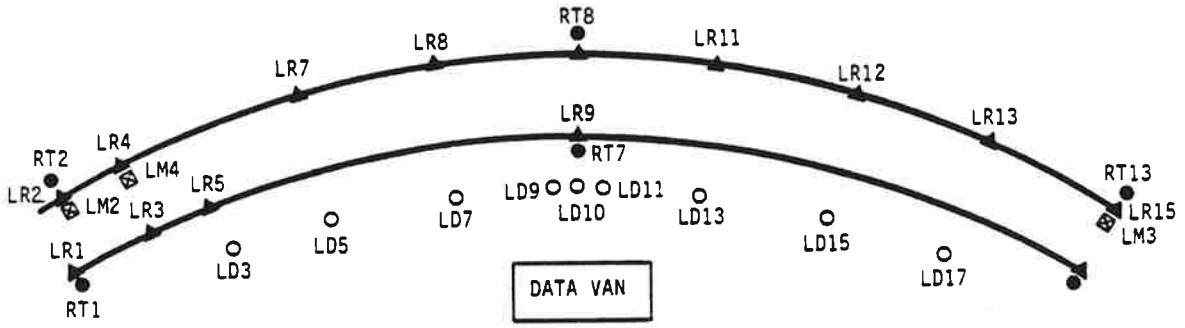

FIGURE 13. INSTRUMENTATION DEPLOYMENT FOR SAFE TEMPERATURE TEST (CURVED TRACK)

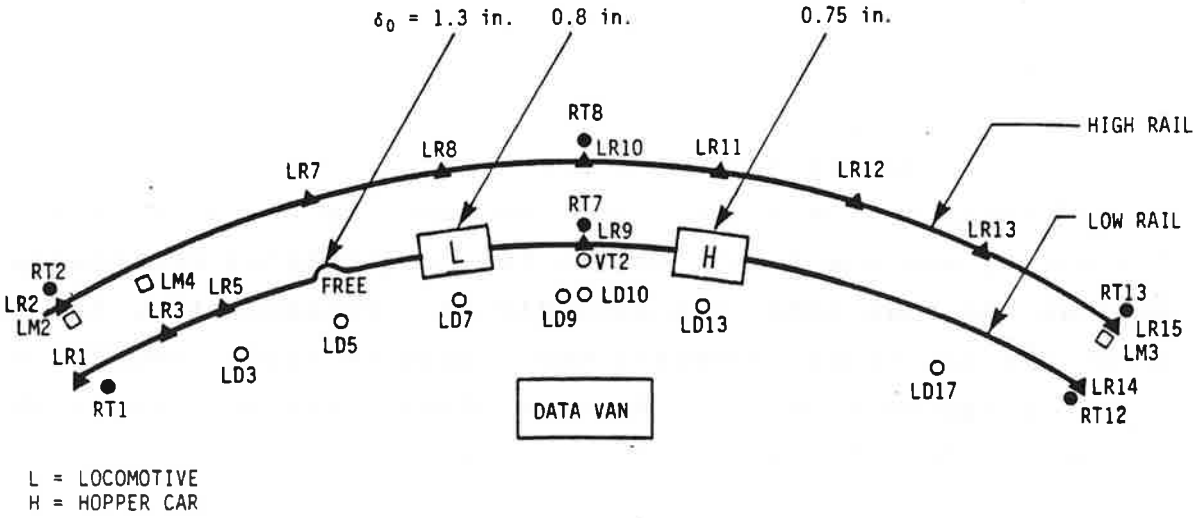

FIGURE 14. INSTRUMENTATION DEPLOYMENT FOR EXPLOSIVE BUCKLING TEST (CURVED TRACK)

The track was heated initially to 150°F, which was 75°F over its neutral temperature. A 10-car train including a GP-40 locomotive, eight fully loaded hopper cars, and a tank car made forward and return passes over the test zone at 10 mph. The rail heating was cut off during the train passage over the track. The rails were reheated to the temperature increase of 75°F and a 20 mph pass (forward and return) was made. After this, the 30 and 40 mph runs were also made with the rails reheated in between the runs to keep the rails at 75°F temperature increase over the neutral temperature.

Throughout this test, the lateral alignment of the track was carefully monitored by means of the lateral displacement transducers at several locations. Train passes were allowed after making sure that the track misalignments were not dangerously large after the previous passes.

2.4.1.1 Analysis of Results - No significant lateral movements were noticed in the track during or soon after the train passage. The track, therefore, withstood the vehicle traffic at the peak force (190 kips/rail) corresponding to the dynamic safe temperature of 75°F. However, this force was not uniform and dropped from the center to the ends in a triangular manner. The nonuniform force build-up was due to the inadequate length of the heated zone, and the low end stiffness. The latter was the result of the low longitudinal resistance outside the test zone (see Appendix A). Consequently, the test track did not truly represent the "infinite track" condition, which is appropriate in buckling studies since it gives lower buckling strength than the finite track condition.

The theoretical results for the infinite track are shown in Figure 15. The expected force levels at the dynamic safe temperatures corresponding to different vehicles in the consist are shown in Figure 16. Although the temperature and force levels reached in the test (viz. 75°F, 190 kips/rail) were

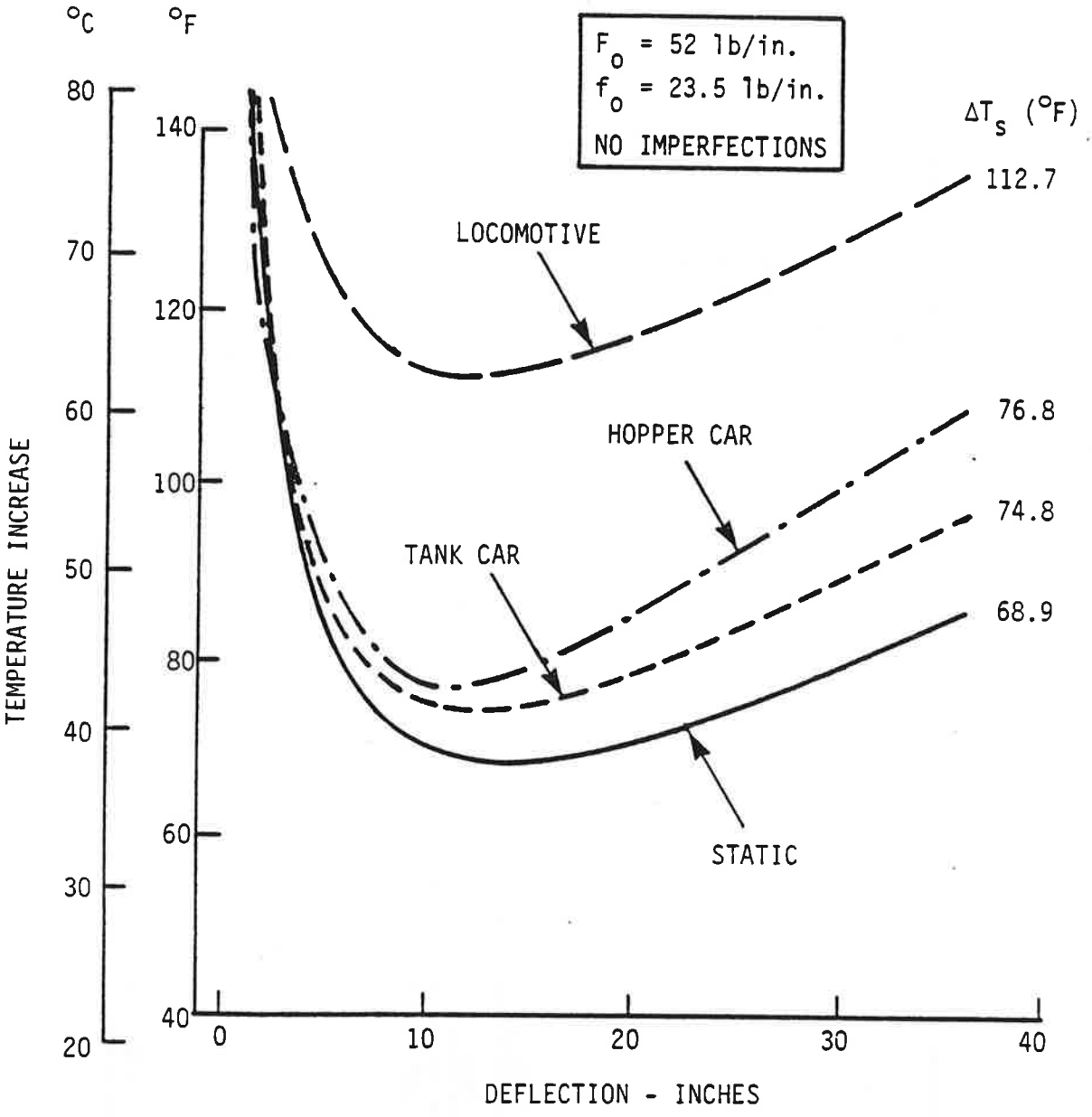

FIGURE 15. BUCKLING RESPONSE OF THE INFINITE TRACK THEORY (TANGENT TRACK)

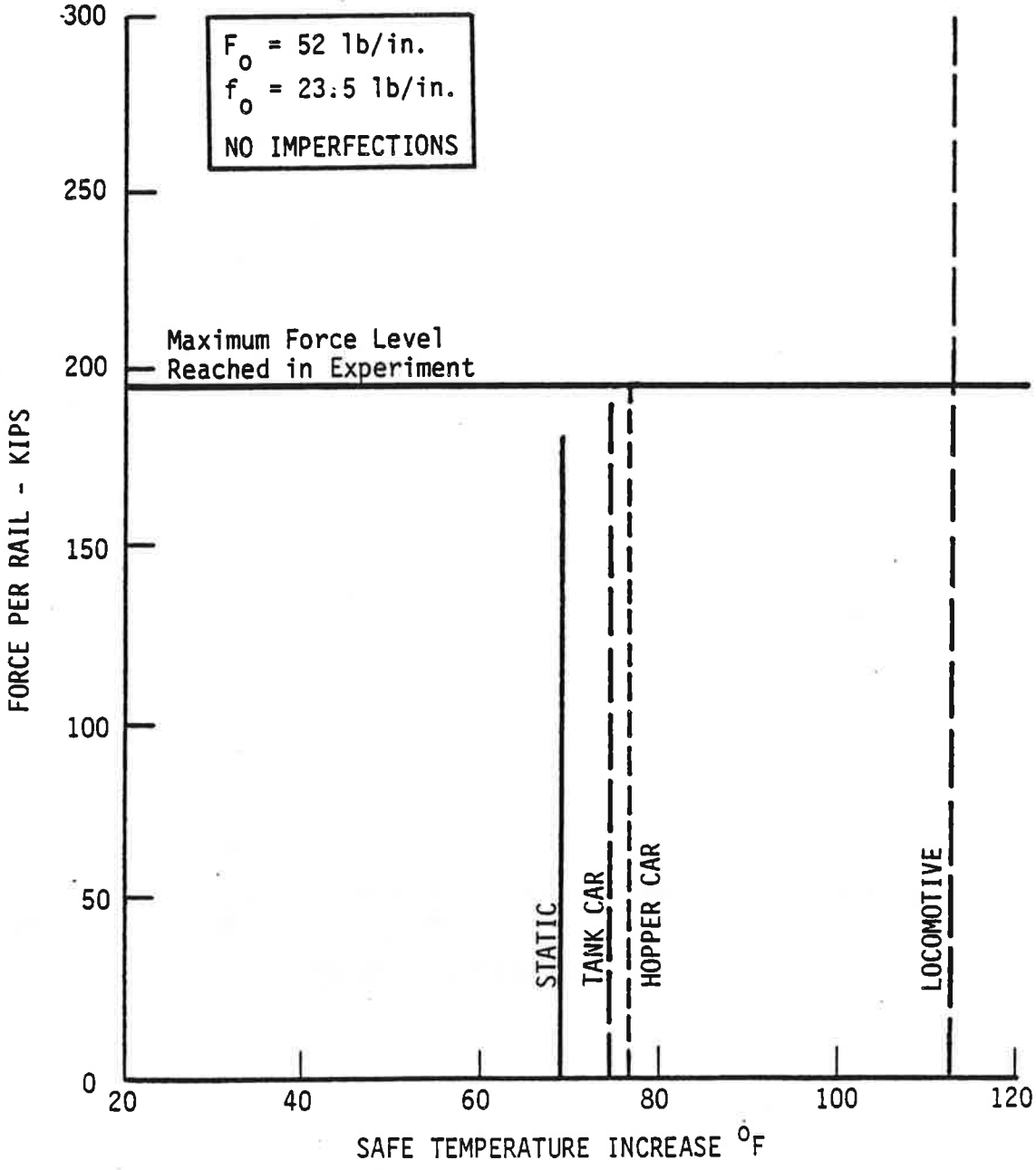

FIGURE 16. MAXIMUM SAFE FORCES FOR THE INFINITE TRACK THEORY (TANGENT TRACK)

adequate for testing the infinite track, they were lower than the levels required for the verification of the finite track buckling strength as indicated in Figure 17.

Although it was not possible to establish the validity of the dynamic safe temperature from this test, the results showed the right trend and the track was safe at least within 23°F of the theoretical safe temperature. The dynamic safe temperature verification test was repeated in Phase II, as described later.

2.4.2 Explosive Buckling Test

The objective of this test was to determine the buckling strength of the track under the influence of stationary vehicles (locomotive and hopper car) and compare it with the static buckling strength of CWR tracks.

It was initially planned to set up three equal imperfections at the same time in the test zone. Two of the imperfections would be under the vehicles (locomotive and hopper car), and the third one would be free of vehicles. The dynamic buckling strength could be assessed from the response of the track under the vehicles, while the "free" imperfection would yield the static buckling strength. Due to the fact that the force buildup in the test zone was nonuniform, it was not possible to find more than two locations of equal rail force level. Hence, it was decided during the test program to exclude the static buckling assessment and study the vehicle influence only.

Each of the imperfections was 0.75 in. over a length of 32 ft. A hopper car and the locomotive were spotted over the imperfection as shown in Figure 12. The rails were heated gradually. (Insulating pads were kept underneath the wheels of the vehicles to isolate them electrically from the rails during rail heating.) An explosive buckling occurred under the hopper car at a temperature increase of 167°F. The rail forces and displacements were monitored during and after buckling.

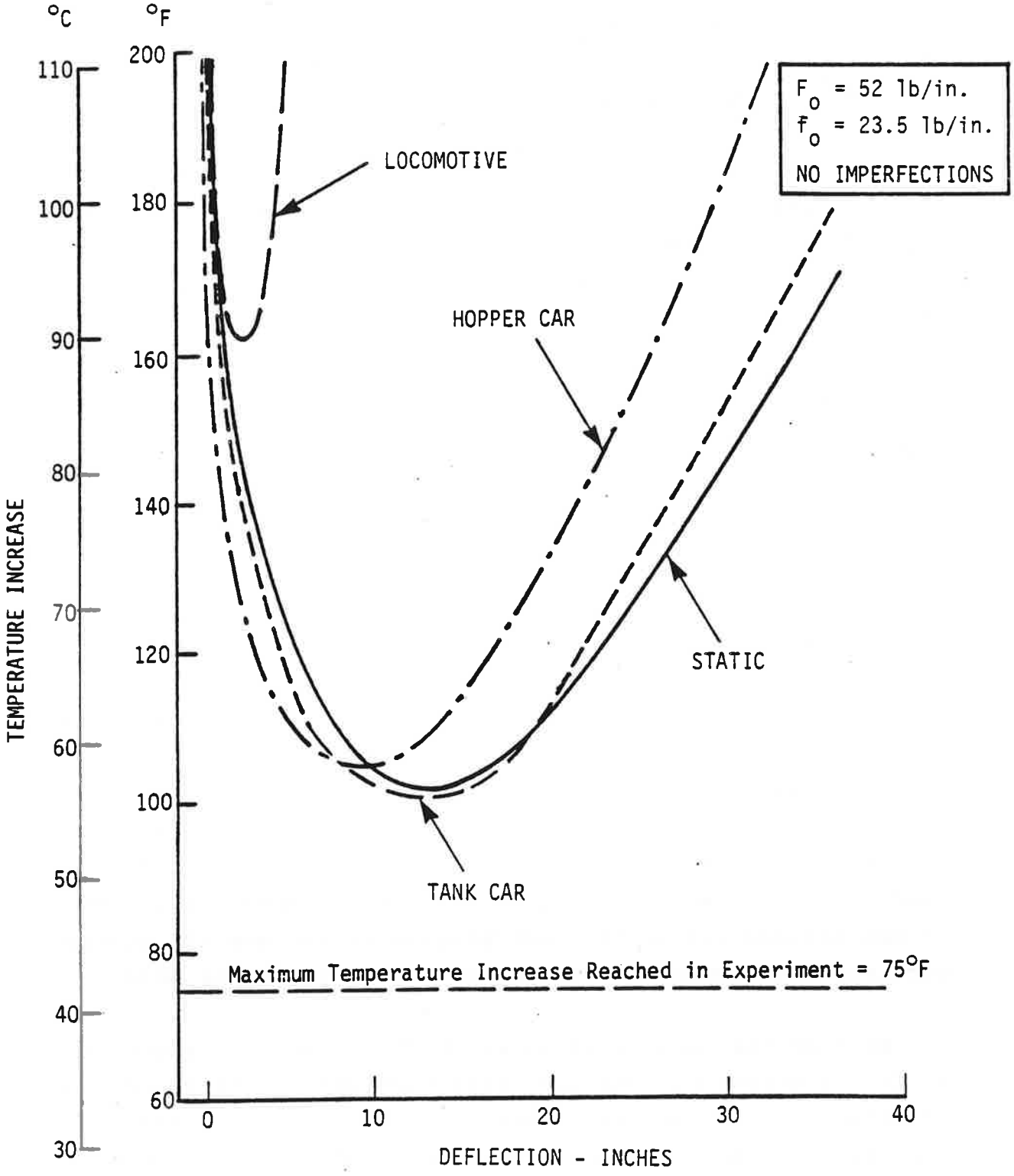

FIGURE 17. BUCKLING RESPONSE OF TEST TRACK (FINITE TRACK THEORY, TANGENT TRACK)

2.4.2.1 Analysis of Results - The experimental value of the dynamic buckling temperature for the hopper was 167°F over the neutral temperature; the rail force under the vehicle being 364 kips/rail. The corresponding theoretical values are 158°F and 370 kips/rail as indicated in the response curves in Figure 18.

The buckled shape is shown in Figure 19. The maximum buckling deflection is seen to be 26 in. The buckling deflections predicted are 31 in. by the finite track theory and 45 in. by the infinite track theory. The lower deflections in the finite track theory is due to lower levels of strain energy stored in the track when compared to that of the infinite track.

The rail force distribution before and after buckling is seen in Figure 20. A large drop in the rail force under the hopper car can also be seen in this figure. The drop in force under the locomotive, which was in a close proximity to the hopper, was due to the longitudinal movement of the rails and not due to any lateral movement under the locomotive. Likewise, the drop in force in the track segment on the left side of the locomotive (Figure 20) was due to the longitudinal movement of the rails towards the buckle under the hopper. This longitudinal movement would be greater than the corresponding movement of the right side segment, which was restrained by the locomotive to some extent.

The growth of the initial lateral deflections under the locomotive and the hopper are plotted in Figure 21. Clearly, the track under the locomotive was more stable laterally than under the hopper car. This is attributed to the shorter uplift regime under the locomotive, as discussed in the dynamic buckling theory (4).

Another important observation was made on the vertical uplift of the track under the hopper car. As indicated in

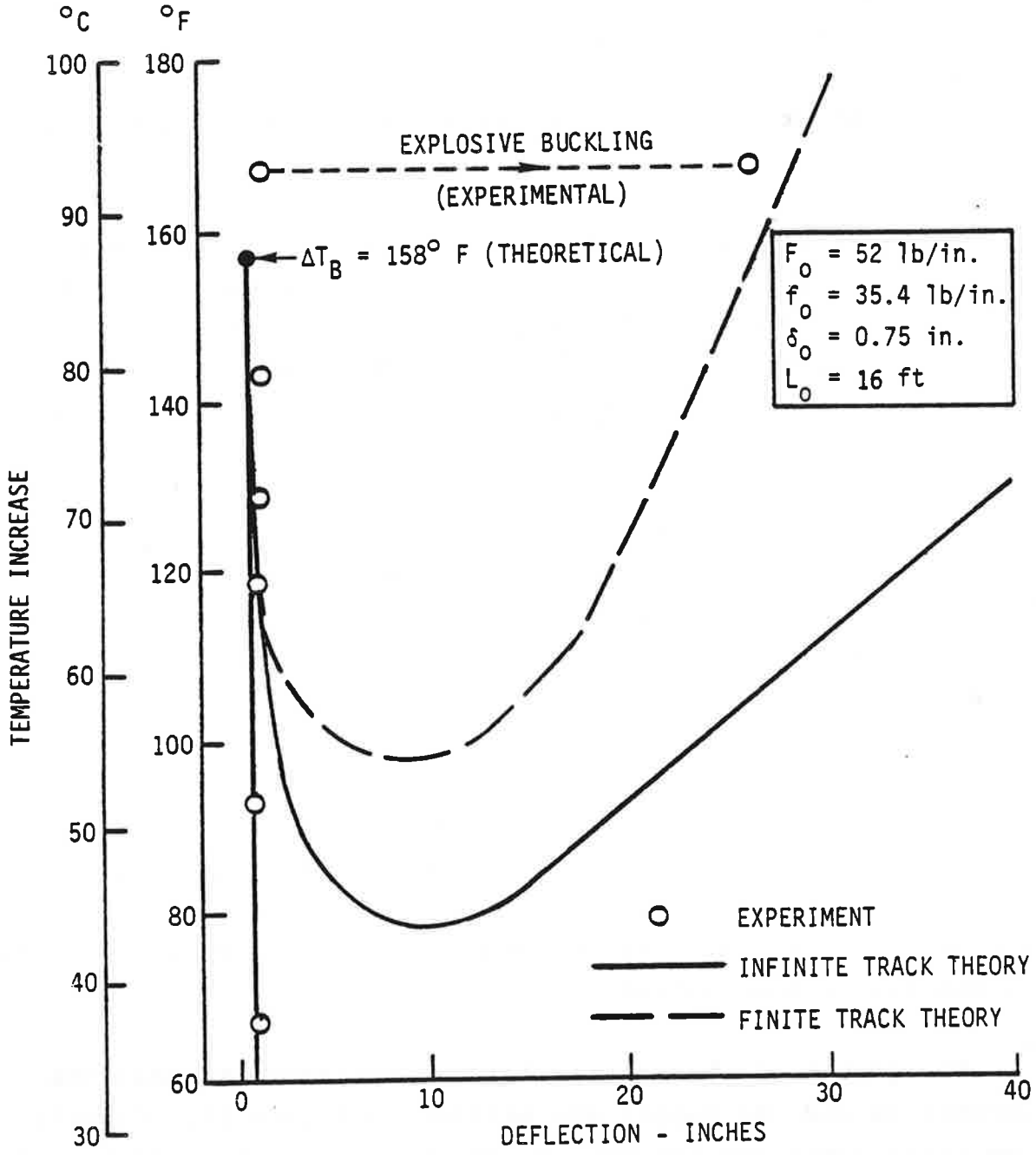

FIGURE 18. BUCKLING RESPONSE OF TANGENT TRACK UNDER HOPPER CAR

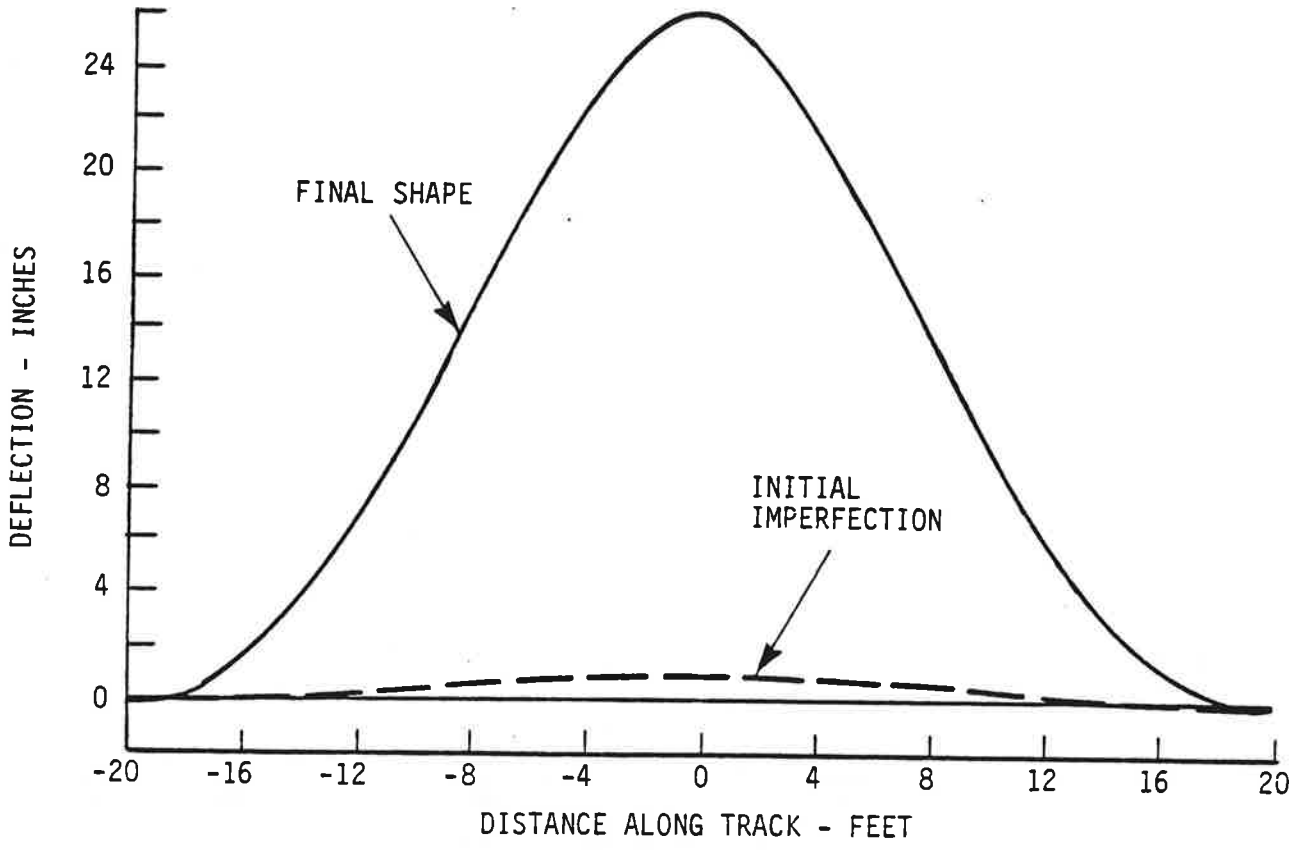

FIGURE 19. BUCKLED SHAPE OF TANGENT TRACK UNDER HOPPER CAR

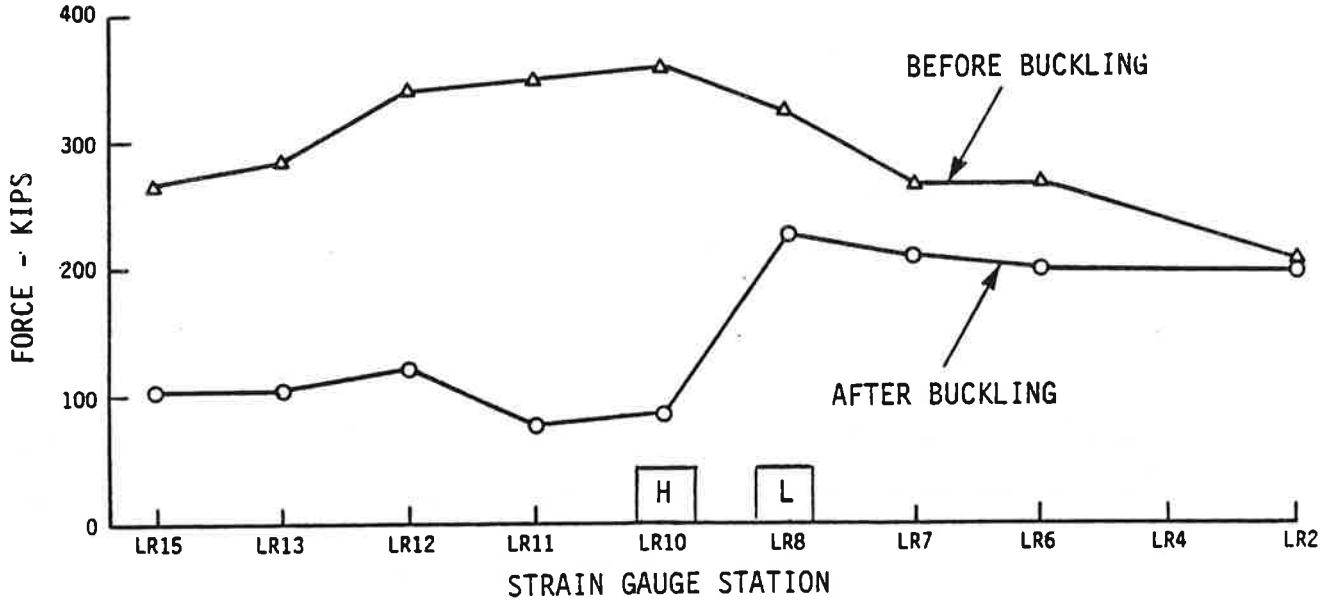

H = HOPPER CAR
L = LOCOMOTIVE

FIGURE 20. RAIL FORCE DISTRIBUTION BEFORE AND AFTER BUCKLING (TANGENT TRACK)

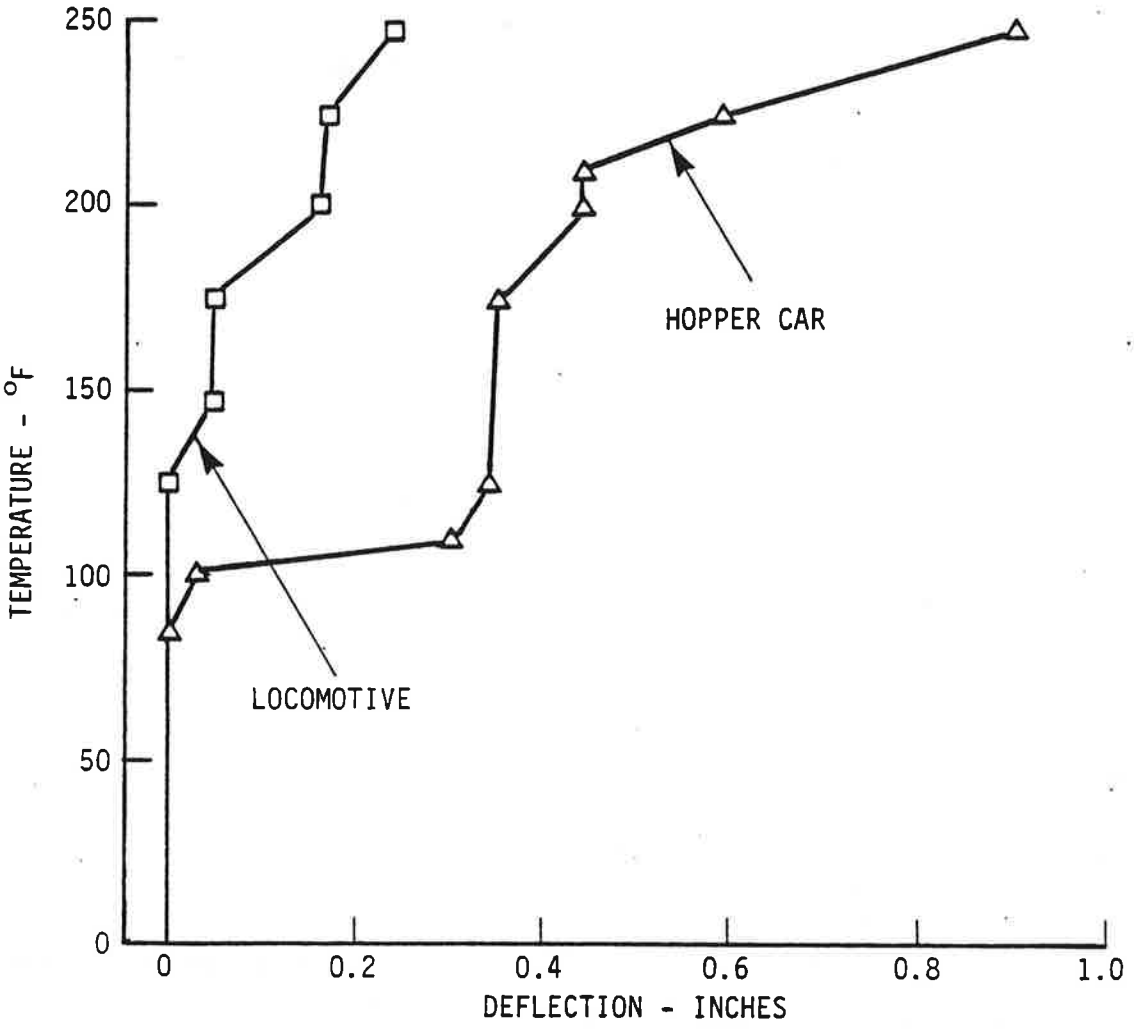

FIGURE 21. PREBUCKLING LATERAL SHIFT UNDER LOCOMOTIVE AND THE HOPPER CAR (TANGENT TRACK)

Figure 22, vertical uplift of the central tie occurred simultaneously with its lateral displacement as the rail temperature increased. The uplift was significant, though initially it was too small to be detected due to the vehicle load alone. Therefore, the central bending wave, augmented by thermal loads, plays a key role in the dynamic buckling of tracks.

2.5 TESTS ON CURVED TRACK (PHASE I)

The tests performed on the curve will be described in the following sections. The first test was intended for the verification of the dynamic safe temperature concept for a 5 degree curve. Due to certain difficulties as explained later, this aim was not properly realized in the test. The test was repeated to confirm the results obtained in the first attempt.

The second major test on the curve was intended to compare the relative dynamic buckling strengths of the curved track under the hopper car and the locomotive.

2.5.1 Safe Temperature Test

The test was intended to demonstrate that the curved track could withstand the vehicle traffic without developing unduly large lateral deflections, when the rails were heated up to the dynamic safe temperature. This aim was consistent with the dynamic buckling theory (4) and it was implied that the theoretical dynamic response characteristic would show a distinct dynamic safe temperature. For this specific test segment, however, the theoretical response happened to be 'progressive' and it was difficult to identify a safe temperature (as it could be done for the tangent track tested previously). This was due to the low lateral resistance and the imperfections of the curve which were not identified in advance of the test.

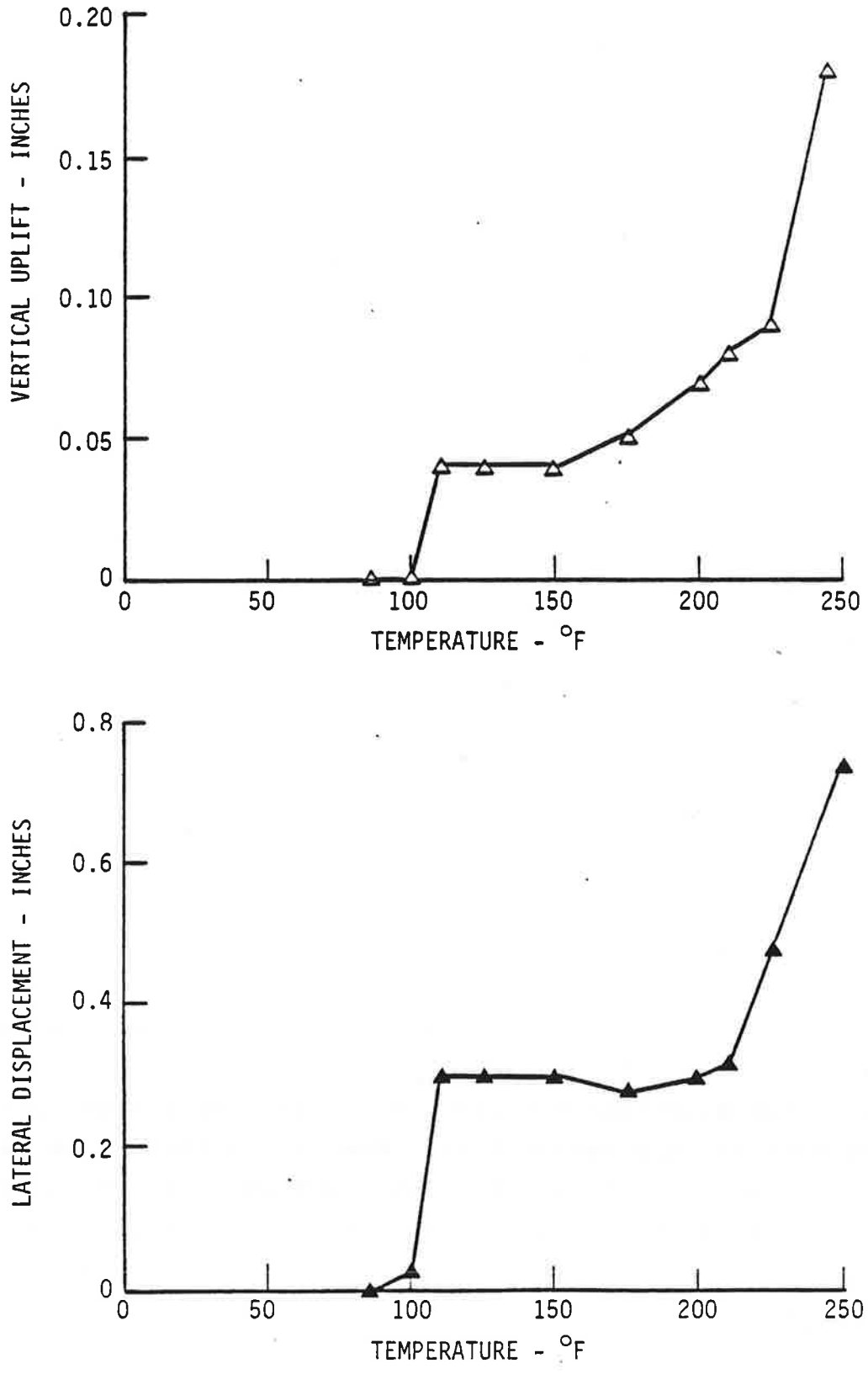

FIGURE 22. VERTICAL UPLIFT AND LATERAL SHIFT OBSERVED IN BUCKLING TEST UNDER THE CENTER OF THE HOPPER CAR (TANGENT TRACK)

Nevertheless, it was decided to conduct a test in which the rails would be heated up to the "theoretical safe temperature increase for the perfect track" and subjected to the ten-car train traffic. The lateral deflection with temperature increase would be monitored and compared with the theoretical results.

The track was heated initially to a temperature of about 76^{o}F over its stress free temperature (which was also about 76^{o}F). This resulted in a force of about 170 kips/rail at the center. The initial misalignment at the center was about 0.3 in. at the stress free temperature and it grew only by about 0.1 in. due to the heating. At the ends where the initial imperfections were of the same order as at the center, however, the static heating resulted into lateral deflection increments of the order of 0.2 in.

The ten-car consist was sent over the track at a speed of 10 mph. The rails cooled off to some extent while the consist made the pass. When the consist was at the center of the track, the rail temperature was about 69^{o}F over the stress free value and the compressive force in each rail was about 158 kips. The track shifted laterally by about 0.8 in. in the central zone. A return pass was made at the same speed, after heating the rail to the same temperature as in the forward pass. The misalignments grew to 1.7 in. No further passes were made at this temperature. However, a third pass was made at a reduced temperature of about 60^{o}F over the stress free value. The lateral misalignment grew to about 2 in. at a location near the center. No further passes were made on the track, as the imperfection level reached was considered to be large enough to induce buckling under the train.

2.5.1.1 Analysis of Results - The growth of lateral imperfection at the center due to static rail heating was tolerable

but that due to the passage of the train consist was not considered to be safe. Figure 23 shows the lateral imperfection growth observed during the test. Figure 24 shows the theoretical response for the curve treated as a finite track. The theoretical results show that the dynamic response is progressive, which is in reasonable agreement with the test observations.

Figure 25 shows the analytic results for the infinite track. Compared to finite track, the infinite track gives lower values of safe temperatures and larger deflections. If the infinite track conditions were to prevail in the test (i.e., longer heated zone, larger end stiffness), more severe growth of the lateral imperfections would have resulted.

The test was repeated after realignment and consolidation using the FAST consist and again similar results were obtained.

Another test was done to make sure that the observed growth of lateral imperfections was not due to the (L/V) effect. The (L/V) was found to be negligible (less than 0.25).

The test results could be explained reasonably by the dynamic theory (4). The important finding from this experiment is that for a proper application of the safe temperature concept for an assurance against buckling, it is necessary to have a distinct dynamic safe temperature in the theoretical response curve. Figure 25 also shows that statically the track appears to be safe, though dynamically it is not. Further aspects of this requirement are explored in Phase II.

2.5.2 Explosive Buckling Test

The purpose of this test was to assess the relative dynamic buckling strengths of tracks under the locomotive and the hopper car, and also to compare the dynamic buckling strengths with the static buckling strength.

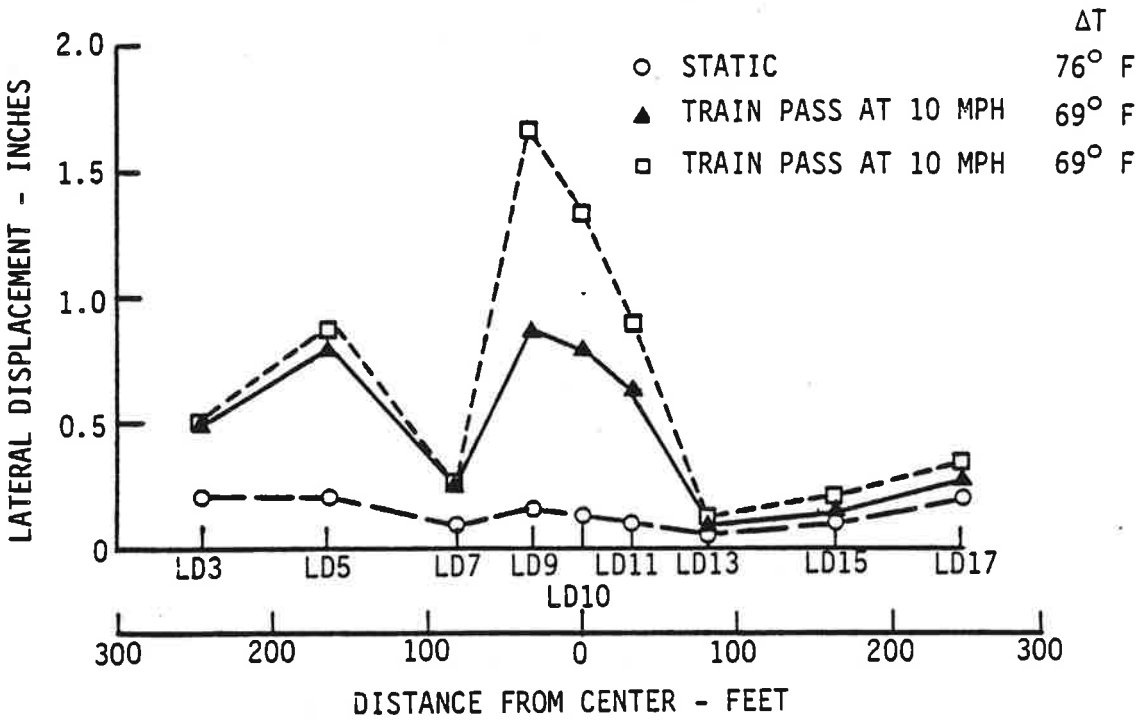

FIGURE 23. LATERAL DEFLECTION OF CURVED TRACK

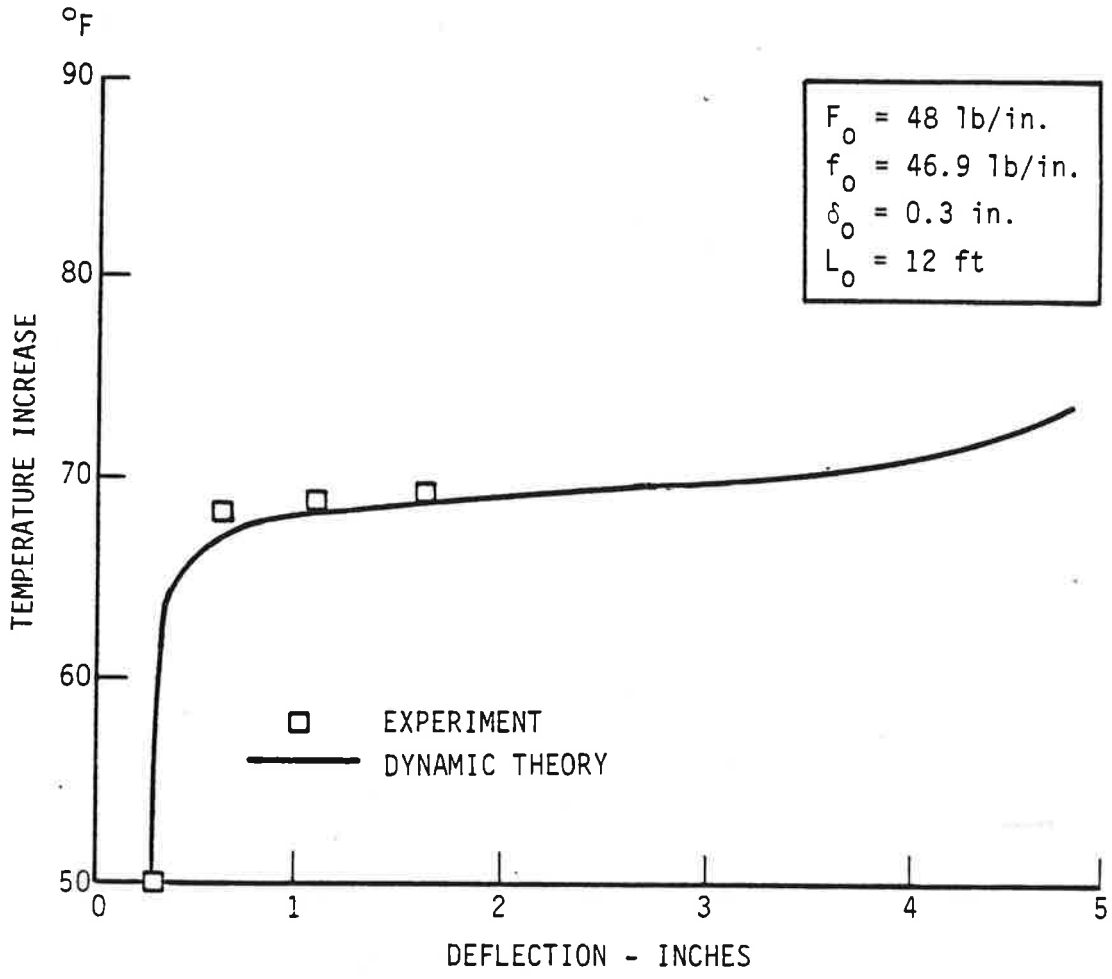

FIGURE 24. DYNAMIC BUCKLING RESPONSE OF CURVE (FINITE TRACK THEORY)

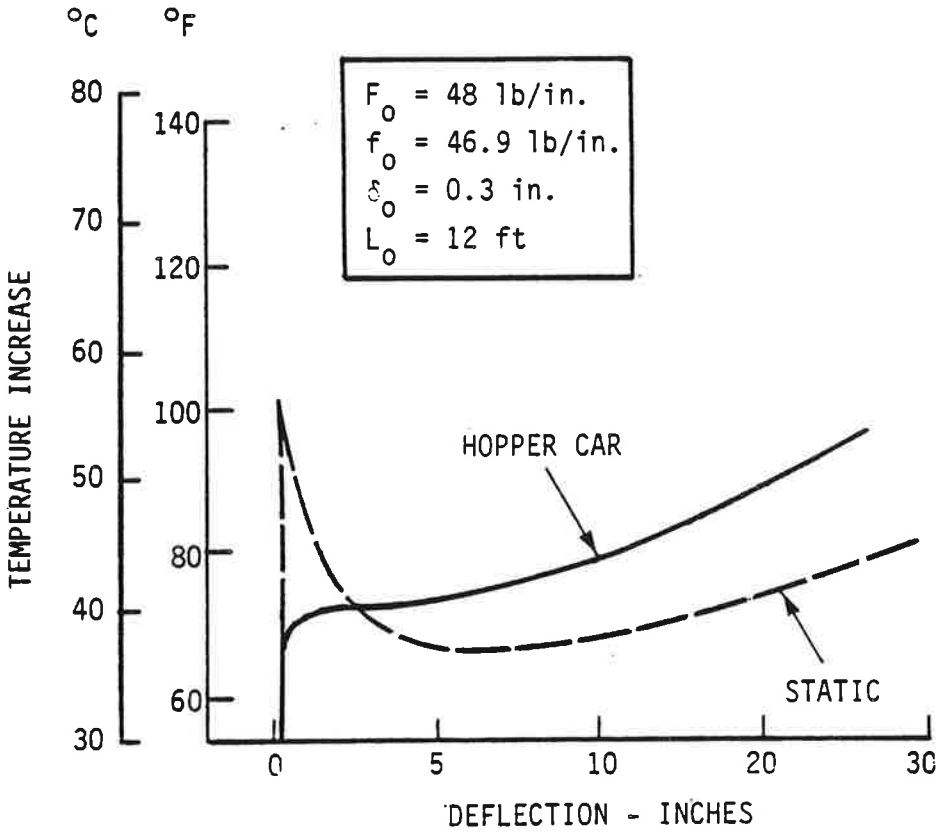

FIGURE 25. BUCKLING RESPONSE OF CURVED TRACK (INFINITE TRACK THEORY)

Three lateral imperfections were placed in the track, two of which were under the locomotive and the hopper car (Figure 14). The third imperfection was free of vehicles and intended to represent the static buckling strength. The imperfection amplitudes under the locomotive and the hopper car were 0.8 in. and 0.75 in. respectively, whereas the free imperfection had 1.3 in. for its amplitude. These differences were not intended and were due to test difficulties in setting up and controlling the imperfection amplitudes.

The track was heated to about 93^{o}F over its stress free temperature. This gave a force of about 190 kips/rail at the center and 174 kips/rail at the free imperfection. The track buckled explosively under the free imperfection, resulting in a buckling deflection of 6 inches.

2.5.2.1 Analysis of Results - The track buckled at the free imperfection which was more severe than those under the vehicles. Figure 26 shows the response curves from the finite track theory. The lengths of imperfections under vehicles were not measured and therefore taken equal to that at the free imperfection. It must be noted that the actual force distribution in the test track was more complex than assumed in the theory (see Figure A-1), because of the uneven prebuckling longitudinal movements. Further, the free imperfection was not at the center of the track. These factors were not included in the theoretical results shown in Figure 26. The theory predicts a buckling force of about 160 kips/rail at the free imperfection and a deflection of about 7 in. The corresponding test results were 174 kips/rail and 6 in. deflection.

If the conditions at all the three imperfection locations were identical in regard to the lateral resistance (before the vehicles were spotted), imperfection amplitudes and lengths, and the levels of the rail force, then according to the dynamic buckling theory, Reference (4), the track should have buckled

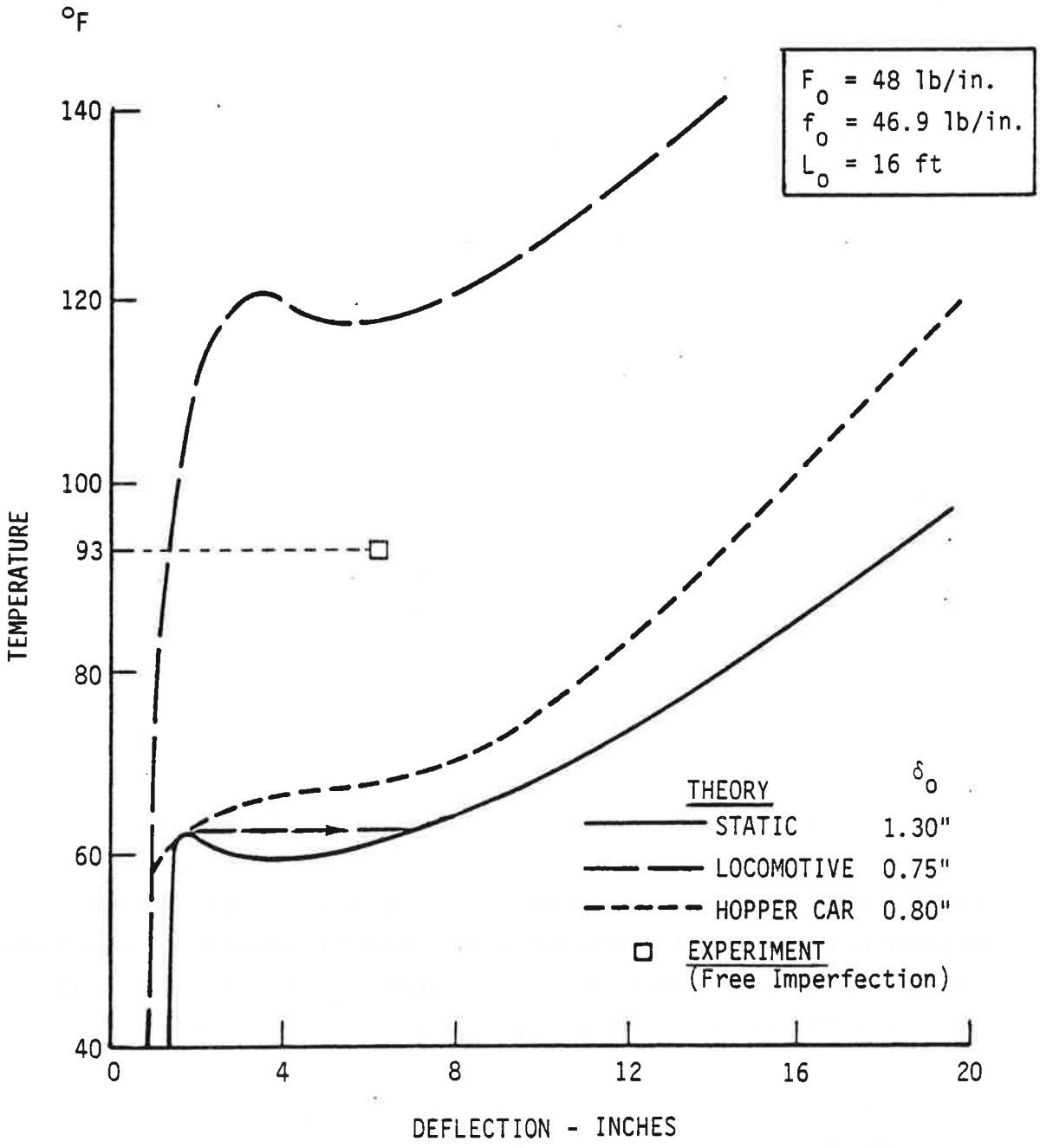

FIGURE 26. BUCKLING RESPONSE OF CURVED TRACK (FINITE TRACK THEORY)

under the hopper car. Although the experiment did not yield this result, it is satisfactory to know that the theory accounts for the observed static buckling response.

2.6 OBSERVATIONS FROM PHASE I RESULTS

a. The CWR track subjected to thermal loads is more stable under the GP-40 locomotive than under the hopper car. The explosive buckling test (subsection 2.4.2) provides a good evidence for this conclusion, which is also expected from the dynamic buckling theory. The stability under the vehicle is influenced by the truck center spacing among other parameters. In general, the smaller the truck center spacing is, the greater will be the track lateral stability.

b. Although the safe temperature test on the tangent track did not yield any result that contradicted the theory, the temperatures and the forces reached were inadequate for "finite track" considerations. Consequently, this test should be regarded as inconclusive.

c. The 5 degree curve is weaker than the tangent track for the same lateral resistance, as seen from the test results presented here. The relative weakness is both in its lower static and dynamic buckling strengths.

d. If the theoretical response curve does not show a distinct dynamic safe temperature, i.e., exhibits progressive buckling response, then there will be difficulties in conducting a successful dynamic safe temperature test. The curved track test suffered from this disadvantage. For a distinct dynamic safe temperature, a distinct dynamic buckling temperature

should also exist eliminating any possibility of progressive buckling. Further implications of this, lead to the concept of the margin of safety, as discussed in Phase II.

e. The dynamic buckling theory (4) assumes that the track "lifts" off (partially or fully) over some length in the central zone under the vehicles, thereby reducing the lateral resistance. Although an attempt was made to measure the "lift off" of the track under the vehicle load, when the track was at its neutral temperature, the test only marginally substantiated the theoretical assumptions, due to the extremely fine accuracy required. However, the "lift off" was clearly noticeable at higher temperatures. Thus, the central bending wave augmented by the thermal loads is an attributable cause of the dynamic buckling.

f. The results of the finite track tests and analysis overestimate the actual buckling strength of CWR tracks. This becomes an important consideration in the design and conduct of buckling tests and in the practical application of the data from tests with "short" test section lengths.

3. PHASE II TESTS

Phase II dynamic buckling tests on the same tangent and curved tracks segments as in Phase I were conducted during August and September 1984, in accordance with the test requirements definition given in Reference (9).

There were some significant changes between the two phases of activity in regard to some of the test concepts, track preparation and instrumentation requirements and the train consist. Some of the specific changes were:

a. The length of the heated zones was increased to 300m from the 200m length used in Phase I, for a better simulation of the infinite track condition and for creating a central zone of constant rail force.

b. The "outside" zones were stiffened longitudinally by replacing the wood ties with concrete ties and using unit anchors. Every tie was anchored to increase the longitudinal resistance. The tracks were consolidated by using the FAST consist for about 0.125 MGT of traffic, to increase their lateral and longitudinal strength.

c. The ten-car train consist used in Phase I was reduced to two cars (hopper car and the GP-40 locomotive) to facilitate a better monitoring of individual truck influences.

d. Resistance temperature detectors (RTD) were used in place of the thermocouples to measure the rail temperature. Instrumentation and measurements were simplified but better accuracy was sought.

3.1 OBJECTIVES

The following paragraphs describe the Phase II test objectives. A brief technical background on each of the objectives is included for clarification of the basic issues involved in the dynamic buckling tests.

Objective (i): Verification of dynamic safe temperature

As in Phase I, the aim was to demonstrate that the track heated up to its dynamic safe temperature increase can withstand vehicle traffic without developing unduly large misalignments. This aim could not be fully realized in Phase I tests due to difficulties in the generation of a constant force buildup in the track. The track longitudinal resistance was low both inside and outside the test zones in Phase I, causing large longitudinal movements at the ends, and nonuniform force distribution at the center.

It was therefore decided to increase the track end stiffness, as well as the overall heated length so as to obtain a constant force, proportional to rail temperature, over a central zone of 50 to 100m. The test length was increased from 200 to 300m, with concrete ties with unit anchors providing the required increase in longitudinal resistance in the outside zones. In the case of the tangent track, the concrete ties were laid for about 75m at both ends, whereas for the curve they were limited to 60m on either end due to practical constraints at the site. The basis for the increased track length and external resistance is provided in Appendix B.

Objective (ii): Determination of progressive dynamic buckling characteristic

The aim was to let the tangent track buckle progressively (by weakening its lateral resistance and providing a large

lateral imperfection) and determine an approximate value of the dynamic safe temperature from the response curve.

One of the problems faced in the verification of track buckling theory is that the safe temperature cannot be explicitly determined experimentally. When the track with imperfections buckles explosively, it does so at the buckling temperature $\Delta T_{B,dyn}$ and then snaps into its post buckled equilibrium configurations (as shown in Figure 27). The safe temperature $\Delta T_{S,dyn}$ is not realizable in the explosive buckling, but can be approached in the progressive buckling tests, which require large initial imperfections in the case of the tangent track.

The entire progressive characteristic (including an approximate value of the safe temperature) is experimentally determinable and a direct comparison with the theoretical curve can also provide a good validation of the dynamic theory developed (4).

To achieve this objective a given lateral imperfection was placed in the track and a hopper car was stationed over the imperfection. As the track was heated, the progressive characteristic was recorded and subsequently compared with the theoretical predictions.

Since buckling safety criteria depends heavily on theoretically predicted safe temperature, the determination of even an approximate value by an experiment has been considered to be a very important part of the analysis verification studies.

Objective (iii): Verification of margin of safety concept for curved track

The aim was to assess the curved track safety subjected to thermal and vehicle loads in terms of its 'margin of safety' which is defined as the difference between the dynamic buckling and safe temperatures increase values.

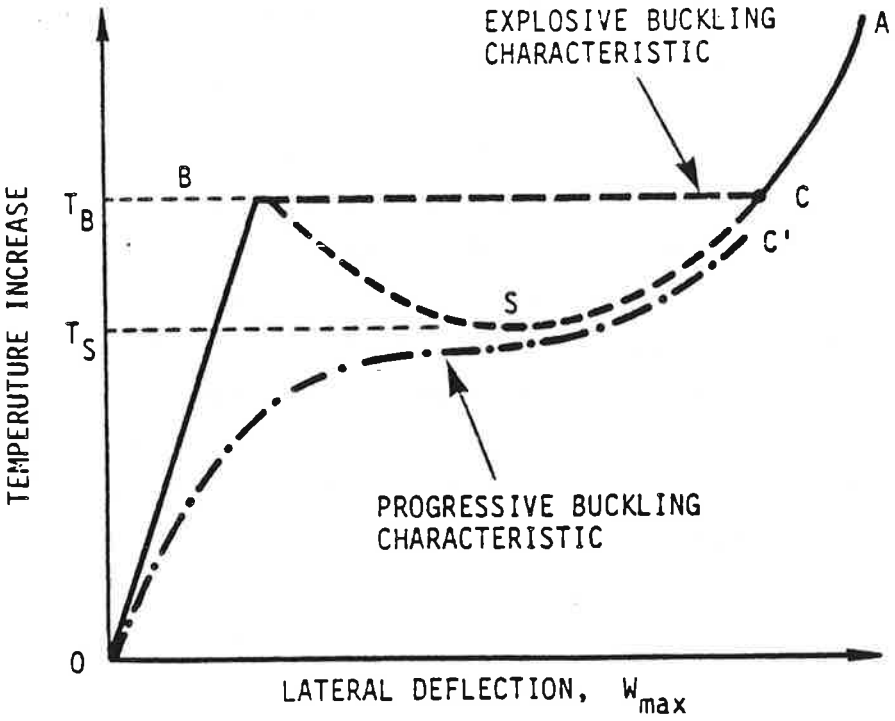

FIGURE 27. EXPLOSIVE AND PROGRESSIVE RESPONSE CHARACTERISTIC

A perfect track has a very high margin of safety. In the presence of lateral imperfections, this margin reduces significantly. Figure 28 shows a plot of the theoretical margin of safety for the assumed imperfection shown in the figure, as a function of the track lateral resistance and curvature. Track conditions represented by points well above the zero margin of safety line, are supposed to be safe for carrying traffic, even when the rails are heated up to the dynamic safe temperature. Conversely, if the point representing a track falls on or below this safety line, the track is unsafe for carrying traffic at elevated termperatures.

To achieve the objective, two experiments were planned and executed. In these experiments, all parameters except the lateral resistance were kept constant. The resistance was such as to assure safe conditions (finite margin of safety) in the first experiment and was subsequently reduced to provide unsafe conditions (zero margin of safety) in the second experiment.

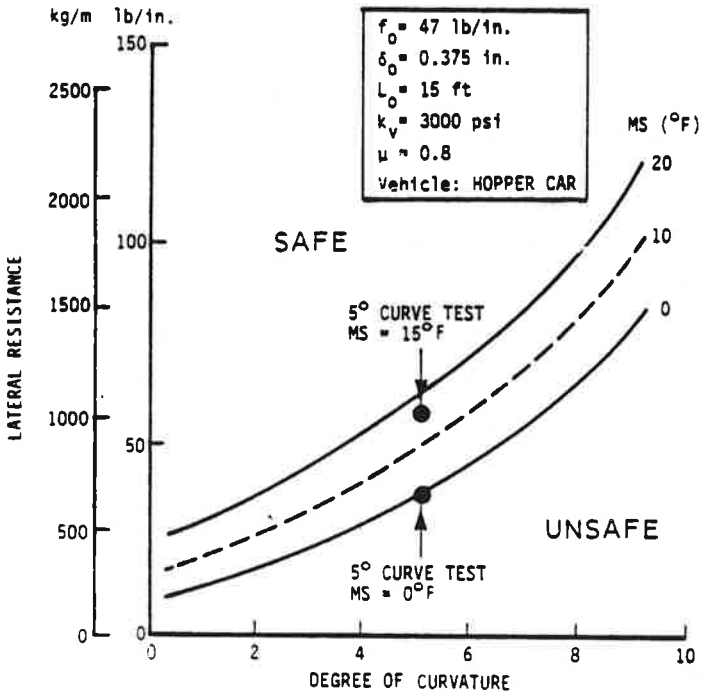

FIGURE 28. MARGIN OF SAFETY AS A FUNCTION OF CURVATURE AND LATERAL RESISTANCE

Objective (iv): Identification of principal causes of misalignment growth

The aim was to show that the main cause of the lateral imperfection growth is the central bending wave between the trucks.

The growth of lateral imperfection under traffic is attributable to two major factors: 1) L/V effect and 2) precession and/or central bending wave which can reduce the lateral resistance in the imperfection zone as the vehicle moves over, and hence the rails under compression laterally shift into a new equilibrium configuration.

As regards to L/V effect, observations in Phase I indicated that for small imperfections (less than 0.375 in. over 30 ft) the L/V effect at low speeds is small, hence the growth of

imperfections in the initial stage may be largely attributed to "uplift" due to the bending wave.

The relative contributions to the growth of imperfections by the precession, recession and central bending waves were not known; however, the central bending wave was expected to be a significant contributor in the case of "long" cars, and the precession wave in the case of the locomotive.

To achieve this objective, experiments were planned on the 5 degree curve. An imperfection amplitude of 0.375 in. was set. A consist of a locomotive and a hopper car made passes over the test track, and the growth of imperfection was monitored with temperature increase. Using vertical and lateral force gages output on a strip chart recorder, the imperfection growth was related to specific wheel passes. Thus, the contributions of precession, recession and central bending waves and (L/V) ratio were monitored.

3.2 TRACK CHARACTERIZATION

As in Phase I, the purpose of track characterization was to determine the track parameters required as inputs in the dynamic analysis (4). A brief description of the measurement of the parameters and the results are presented here.

3.2.1 Rail Neutral Temperature

The tracks were destressed to provide a uniform reference neutral temperature in the test zone and to establish "zeroes" for the strain gages. The tangent track destressing was done somewhat differently from that used in Phase I. The rails were welded at the ends of the test segment. The two rails at the center were cut and the anchors were removed. This resulted in a larger gap than expected and required two additional cuts (one for each rail) before final welding. The rail temperature during this midday operation was changing rapidly due to solar

heating, and this resulted in an uneven neutral temperature in the track. The neutral temperature at the center of the track was 95°F.

The curved track destressing was done differently from that of the tangent. The rails were cut at the ends of the test zone. The anchors were removed and the rails were vibrated to facilitate the breathing of rails. The welds were poured, and the rail vibration continued (except near the ends while the welds were being poured). The strain gages were zeroed, and the rails were reanchored. During this operation, the temperature remained steady at 78°F due to the prevailing cloudy conditions resulting in a uniform stress free temperature of 78°F, for the curved track.

3.2.2 Lateral Resistance

This parameter is measured using the Track Lateral Pull test (TLPT), as done previously in Phase I.

The results obtained for the tangent track were shown in Figure 29. The higher resistance (64.8 lb/in.) was for the consolidated condition (0.125 MGT of traffic) used in the Safe Temperature test (subsection 3.4.1), and the lower value (53.9 lb/in.) was for the tamped condition used for the Progressive Buckling test (subsection 3.4.2). The tamped track represents an extremely weak condition (from a lateral stability point of view) produced in certain track maintenance operations. To induce progressive buckling, such a condition was required in the track.

The resistance results for the curved track are shown in Figure 30. Here, the values are for the two conditions, viz., partially consolidated and the lift tamped, and for two different locations, i.e., center and another location about 123 ft from the center (designated as A) which showed a buckle not anticipated before the commencement of the test. The measurement at the center was done before the test, whereas at A, it was after the test.

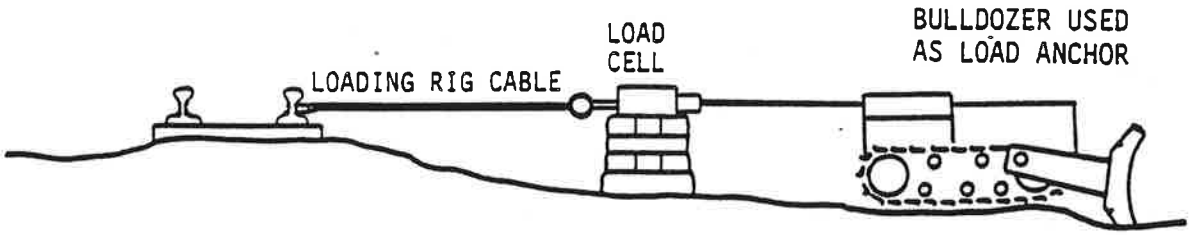

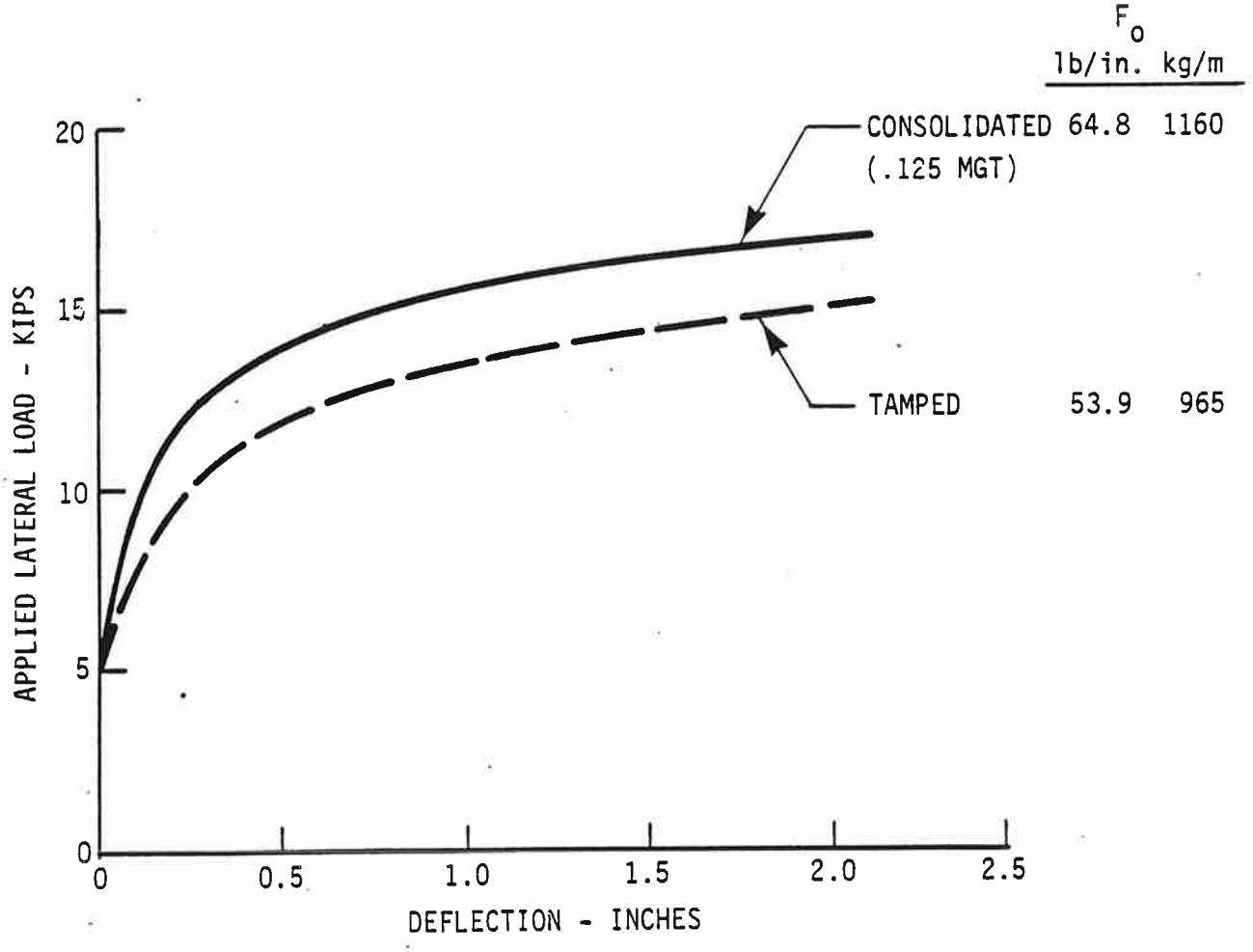

FIGURE 29. MEASUREMENT OF LATERAL RESISTANCE, F_o (TANGENT)

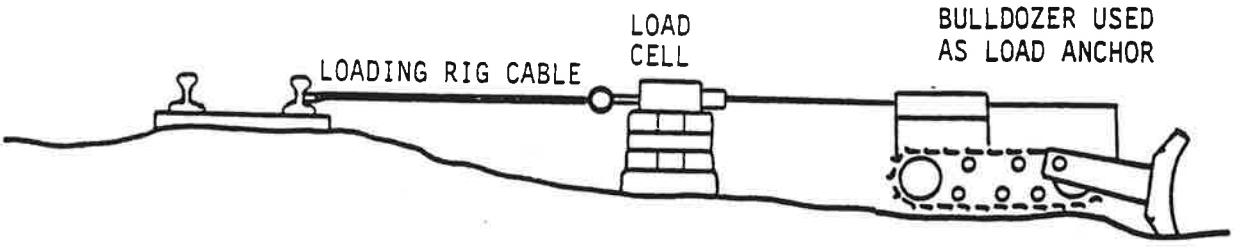

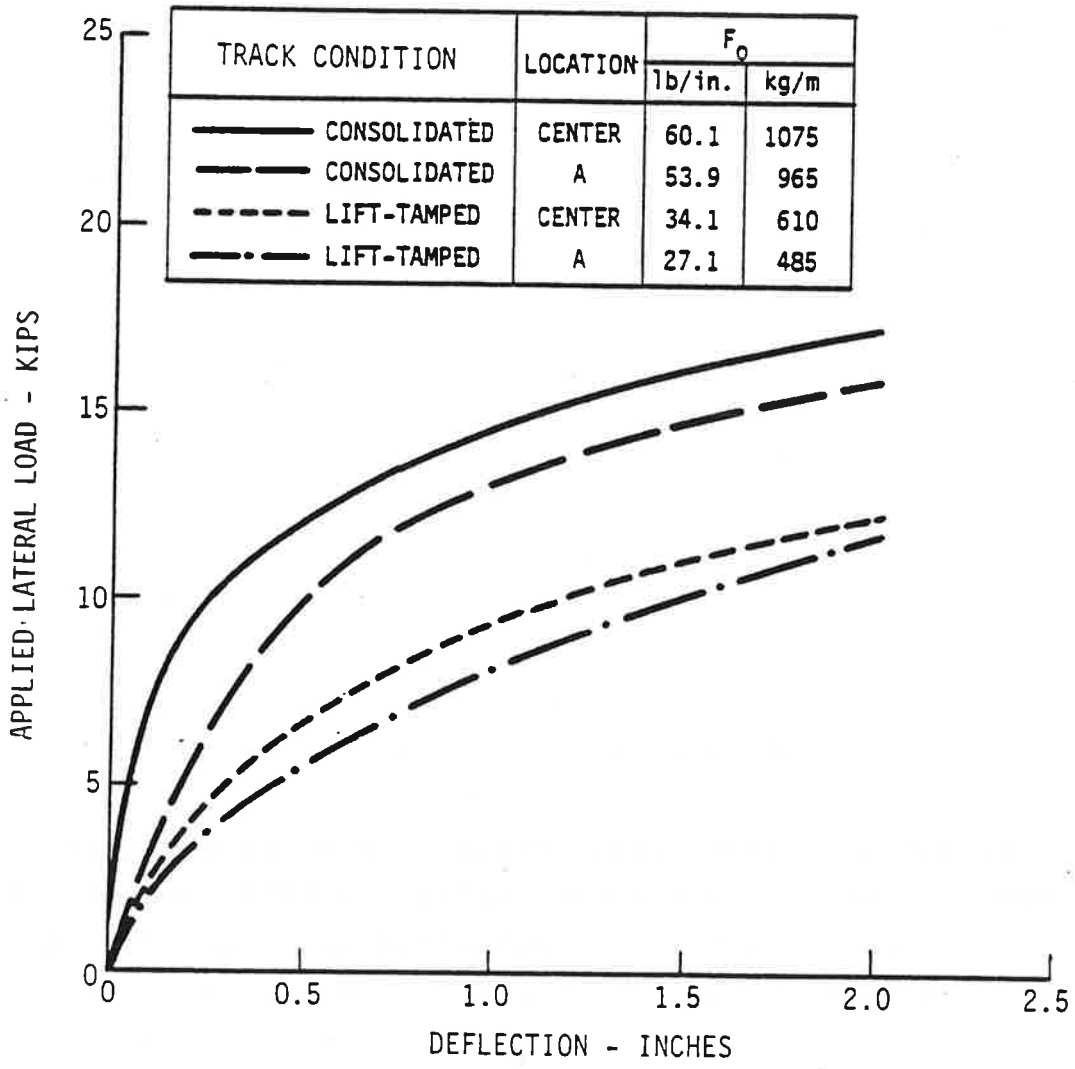

FIGURE 30. MEASUREMENT OF LATERAL RESISTANCE, F_o (CURVE)

The partially consolidated condition was used in the test on the curve with a finite margin of safety (subsection 3.5.1), and the tamped condition was for the track with no margin of safety (subsection 3.5.2). As seen in Figure 30, the values measured at the center were 60.1 lb/in. (partially consolidated and 34.1 lb/in.(lift-tamped).

Tie Ballast Friction Coefficient

No measurement was made to determine the tie-ballast friction coefficient to minimize disturbance to the track. The value of 0.8 in Phase I was assumed for the purpose of analysis of Phase II results.

3.2.3 Longitudinal Resistance

The longitudinal resistances for the tangent and curved tracks were determined from the rail force gradients along the track, as in Phase I.

Tangent Track Longitudinal Resistance

Before the consolidation of the track, force gradients were created in the test zone, by heating the rails using the electric current. This gave a value of 36.3 lb/in. (650 kg/m,) the same as determined in Phase I for every tie anchored.

The ballast was later consolidated to a 0.125 MGT level inside and outside the test zones, using the FAST consist. The longitudinal resistance for this condition was deduced from the rail force measurements made in the Safe Temperature test (subsection 3.4.1). Figure 31 shows the force distribution, from which the average longitudinal resistance is estimated to be about 53.1 lb/in. (950 kg/m) for every tie anchored.

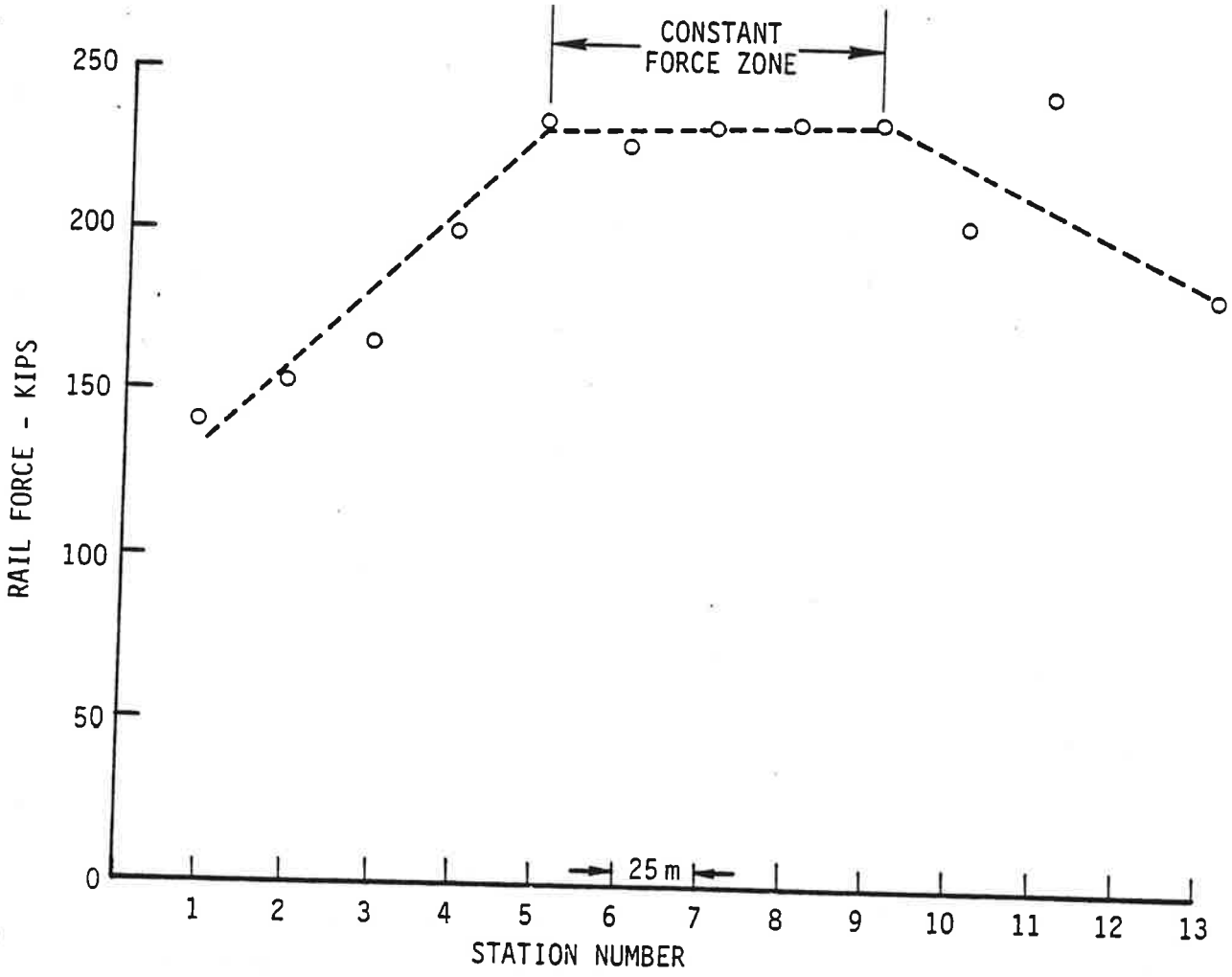

FIGURE 31. RAIL FORCE DISTRIBUTION AT $\Delta T = 90^{o}F$ (TANGENT TRACK)

Curved Track Longitudinal Resistance

Figure 32 shows the rail force distribution observed in the curved track test (subsection 3.5.1). The track was consolidated by about 0.125 MGT of FAST consist traffic, and every tie was anchored. From this distribution, the average longitudinal resistance worked out to be 55.9 lb/in. (1000 kg/m).

Figure 33 shows the rail force distribution observed for the curved track with no margin of safety (subsection 3.5.2). The track was lift-tamped. The average resistance works out to be 31.3 lb/in. (560 kg/m) for every tie anchored.

End Stiffness

The longitudinal force-deflection relationship measured in the tests on the tangent track is shown in Figure 34. The two ends had almost equal stiffness. The longitudinal resistance outside the heated zone works out to be about 85 lb/in.

For the curved track, the results are plotted in Figure 35. The end stiffness for the curve was seen to be higher than that of the tangent. This was presumably due to the greater care and effort put in consolidating the outside zones of the curve prior to the track characterization. The longitudinal resistance in the outside zone works out to be over 140 lb/in. The high longitudinal resistance is due to concrete ties and special rail/tie fasteners used and is required to gain greater end stiffness.

Because of the high end stiffness and the increased length of the heated zone, the test segments in Phase II were good

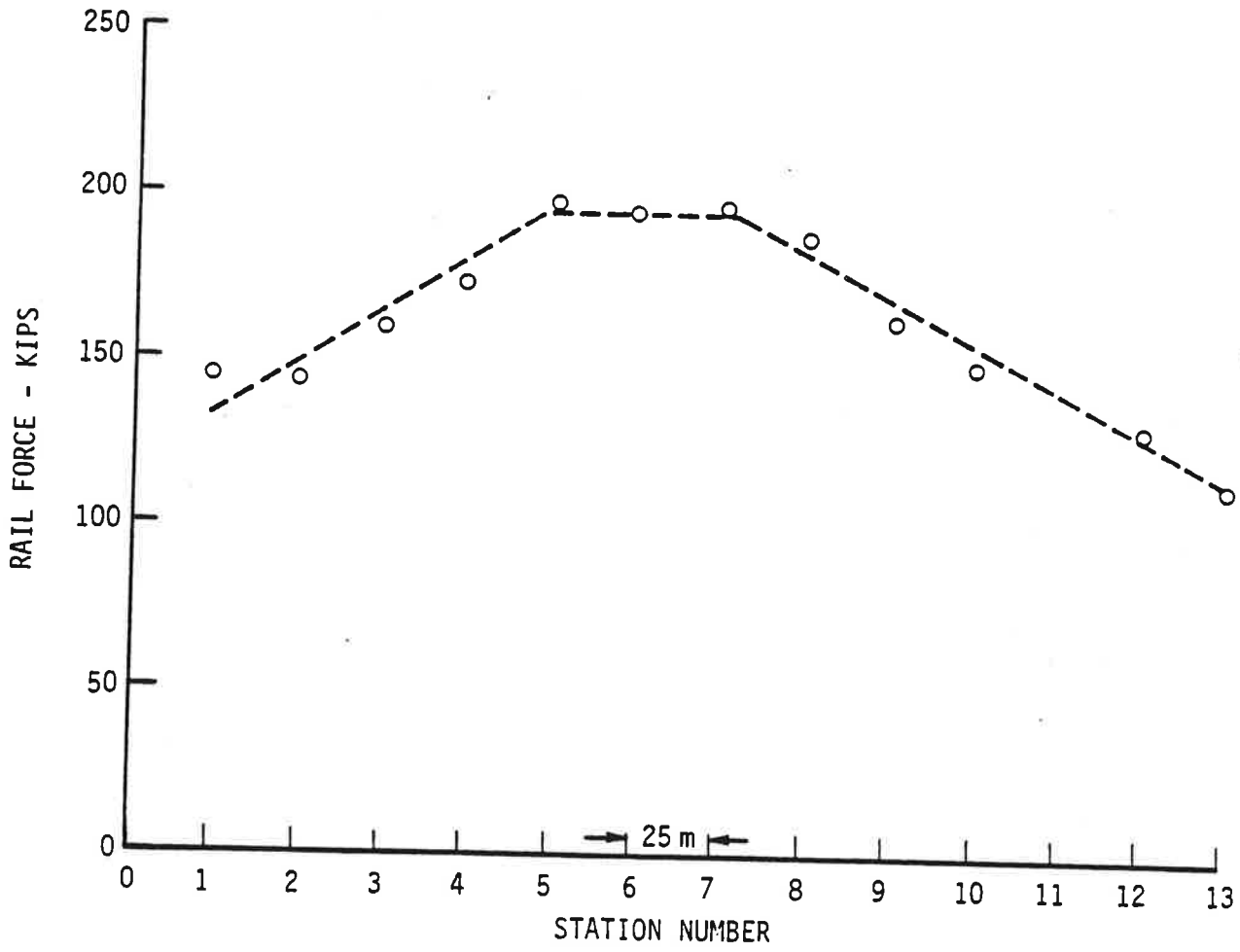

FIGURE 32. RAIL FORCE DISTRIBUTION AT $\Delta T = 75^{\circ}F$
(CURVED TRACK, CONSOLIDATED)

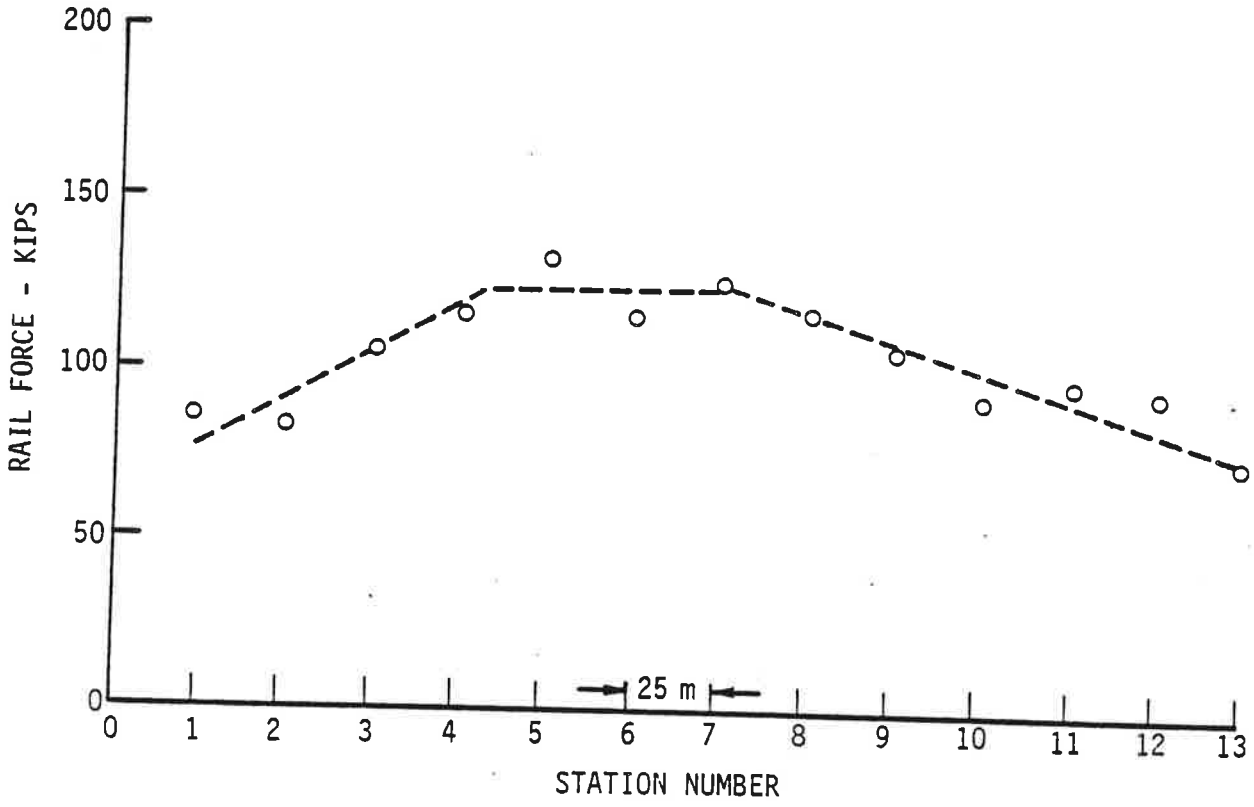

FIGURE 33. RAIL FORCE DISTRIBUTION AT $\Delta T = 50^{o}F$
(CURVED TRACK, LIFT-TAMPED)

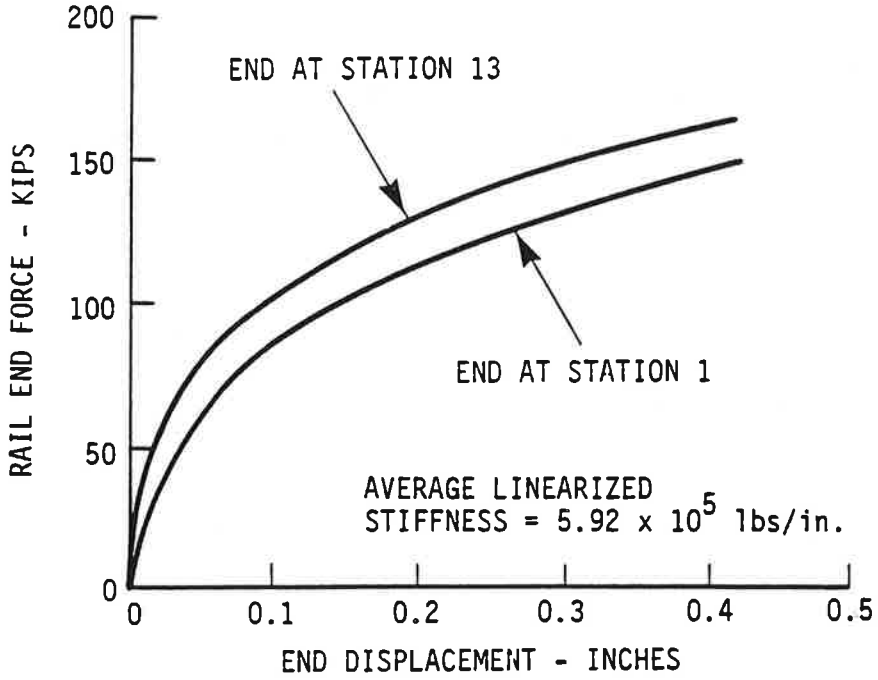

FIGURE 34. END STIFFNESS CHARACTERISTIC (TANGENT TRACK)

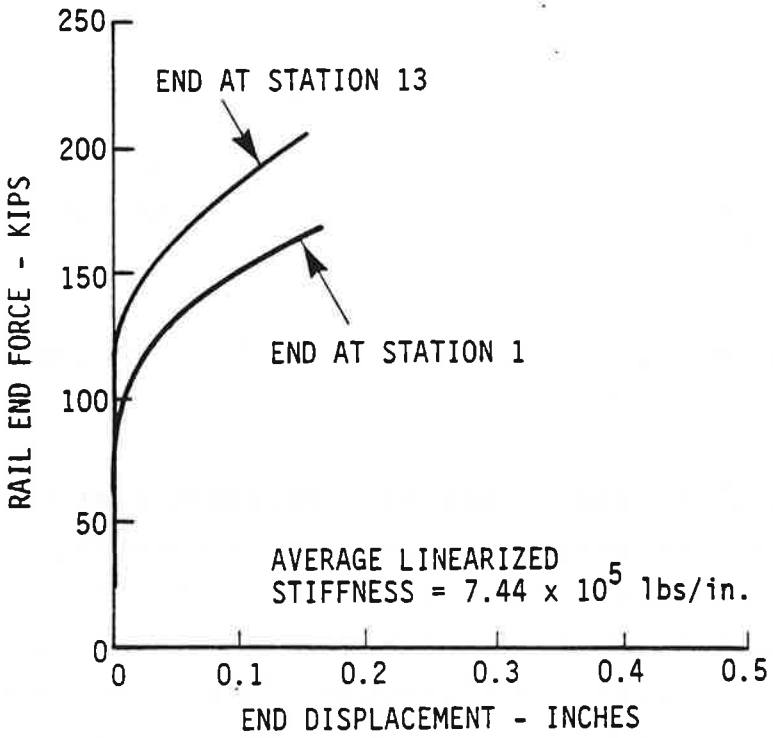

FIGURE 35. END STIFFNESS CHARACTERISTIC (CURVED TRACK)

approximations to the "infinite track." The infinite track theory can therefore be used in the analysis of Phase II results.

3.2.4 Vertical Track Modulus

The purpose of the test was not only to measure the track vertical modulus for use in the buckling analysis but also to prove that the central bending wave would create an "uplift" in the central zone, and thus reduce the lateral resistance.

A number of experiments were done both on the tangent and curved tracks. Vertical displacements of ties and rails were taken at fixed locations on the track, while the hopper car moved over the segment slowly. The measurements were made using LVDTs and also a transit.

For the partially consolidated tangent and the curved tracks, the results are shown in Figure 36. There was scatter in the results as indicated by the shaded area in the figure. Nevertheless, there seemed to be some consistency in the length of the upward rail and tie deflections region in all the experiments. This length over which the negative deflection occurred was about 14 tie spacings (7m) under the hopper car.

The maximum upward tie deflection recorded was about 0.025 in.

The scatter in the foregoing measurements of vertical deflection was not only due to naturally existing variable track conditions (spikes driven to different heights, uneven foundation modulus, etc.), but also due to the instrumentation system used. Despite the improvements made in Phase II instrumentation, it was not possible to resolve the fine accuracies involved in the measurements. Therefore, a new method (using laser optics) will be recommended in Phase III dynamic buckling tests.

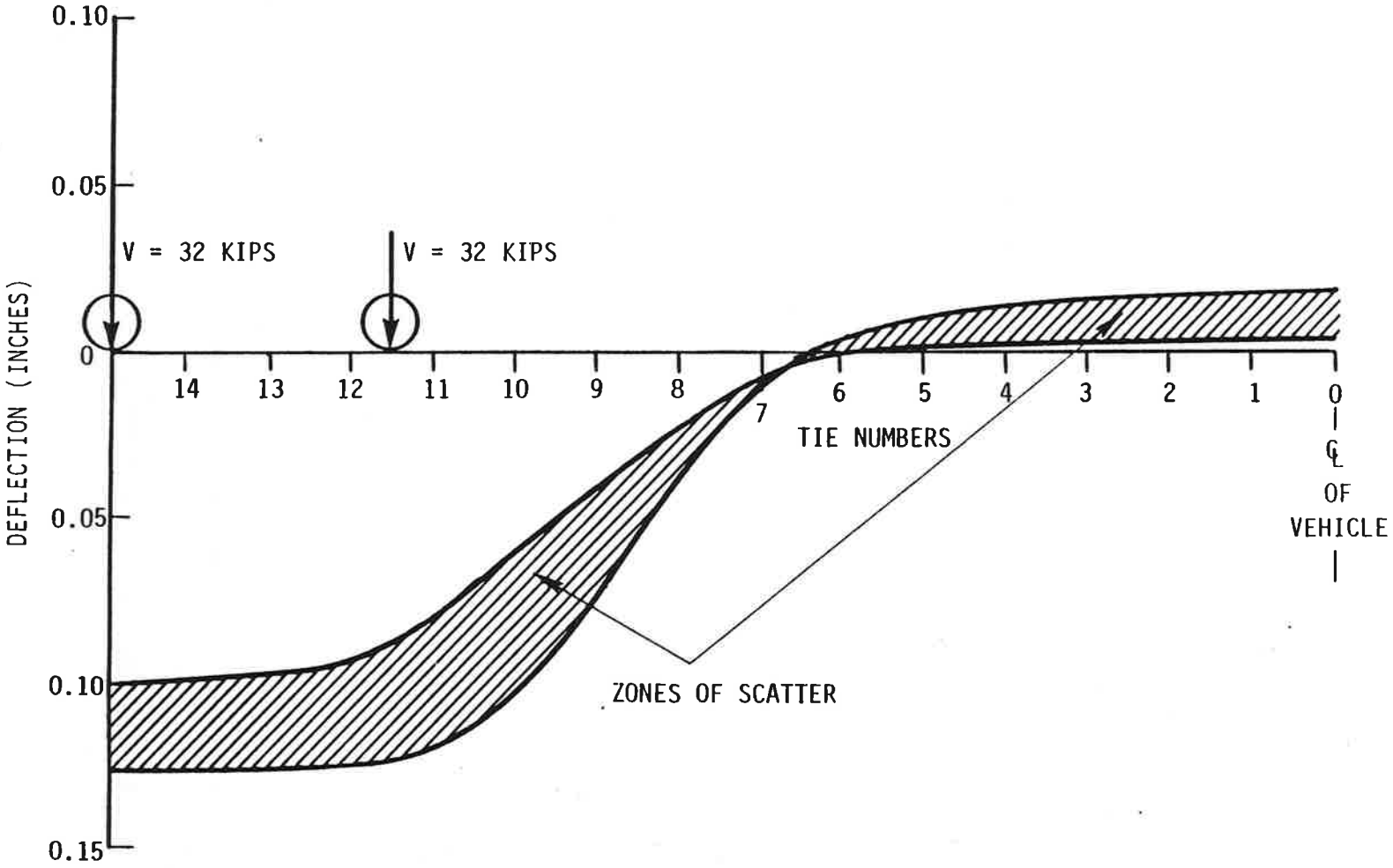

FIGURE 36. VERTICAL DEFLECTION OF TIES UNDER HOPPER CAR

The Vertical Modulus is estimated to be about 3,750 lb/in./in. in the case of partially consolidated track and 2,000 lb/in./in. for the lift-tamped curved track.

3.3 MEASUREMENTS

As in Phase I, test measurements were made in Phase II as indicated in Table 2.

The measurements included rail temperature, longitudinal rail force, lateral and longitudinal displacements, vertical and lateral loads.

The rail temperature was measured using the Resistance Temperature Detectors, which performed better than the thermo-couples used in Phase I.

The initial imperfections in the tangent and the curved track alignments were measured using the Rollordinator®, which is essentially a versine measuring device (here the offset from a 20 ft chord).

In addition to LVDTs, a transit was used in the measurement of rail/tie vertical deflections under vehicle loads.

Other measurements in Phase II were made with the same instrumentation systems as in Phase I.

3.3.1 Instrumentation Deployment

The instrumentation deployment for the major tests involved is shown in Figures 37, 38 and 39.

3.4 TESTS ON TANGENT TRACK (PHASE II)

The procedures, the test results and the theoretical predictions for the Safe Temperature and the Progressive Buckling tests conducted on the tangent track are described in the following sections.

TABLE 2. MEASUREMENTS AND INSTRUMENTATION NOTATION (PHASE II)

MEASUREMENT	METHOD	RANGE	SYMBOL ON MAP	DATA LOGGER SYMBOL	LOCATION SEE FIGS. 37 - 39	TANGENT/ CURVE	COMMENTS
Rail temperature	Rail temperature detector	0° - 350°	●	RT	1, 7, 13	Both	RTDs were better than the thermocouples used in Phase I.
Rail force	Strain gauge	±300 kips	△	SG	1 to 13	Both	Rails were assumed to carry equal forces.
Lateral rail displacement	Rotary Potentiometers	0 - 25 in. 0 - 5 in.	○	LD	7, A, B	Both	7, A, B are the major imperfection locations
Longitudinal end displacement	Rotary Potentiometers	-2.5 - 2.5 in.	⊠	ED	1, 13	Both	
Vertical displacement of rail and tie during rail heating	LVDT	-1 - 1 in.	♀	VR	7	Tangent only	
			♀	VT			
Lateral Imperfections	Rollordinator	20 ft chord				Both	
Vertical wheel load	Vertical load gauge	0 - 40 kips	A		7	Curve only	
Lateral force on rail	Lateral load gauge	0 - 20 kips	⧗	FH	7	Curve only	
Lateral force in resistance measurement		0 - 30 kips			7, A	Both	

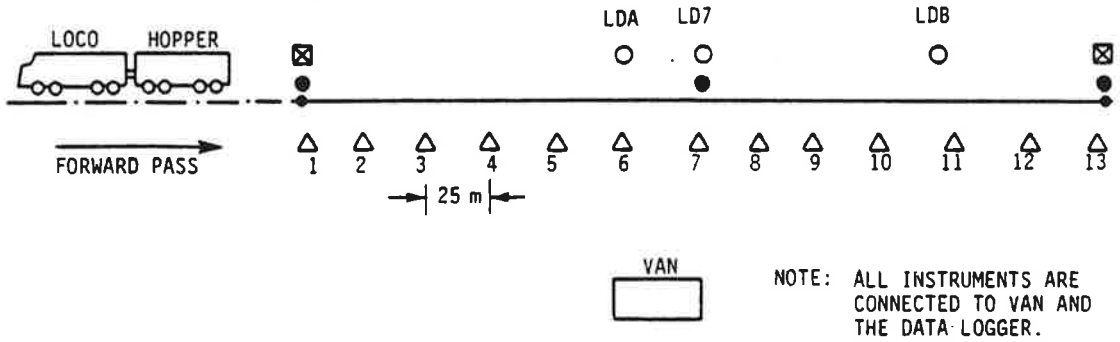

DATA OUTPUT FORMAT

TIME	SG1	SG2	SG3	SG4	SG5	SG6	SG7	SG8
TIME	SG9	SG10	SG11	SG12	SG13	RT1	RT7	RT13
TIME	ED1	ED13	-	-	-	LDA	LD7	LDB

FIGURE 37. SETUP FOR DYNAMIC SAFE TEMPERATURE VERIFICATION (TANGENT TRACK)

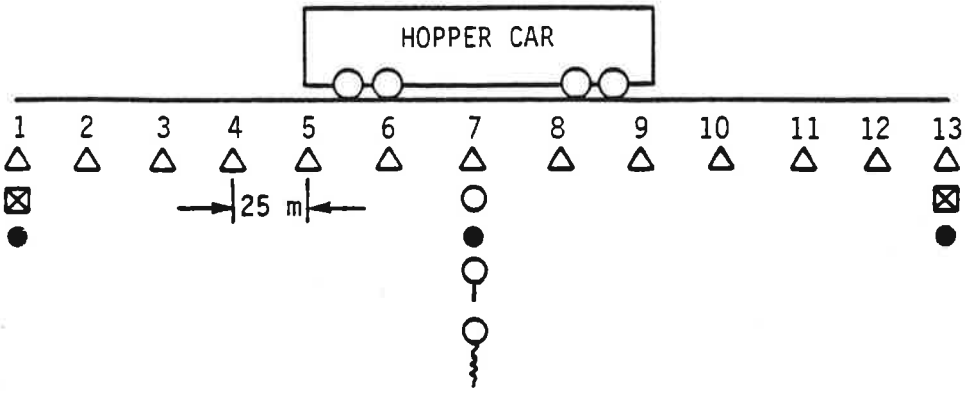

DATA OUTPUT FORMAT

TIME	SG1	SG2	SG3	SG4	SG5	SG6	SG7	SG8
TIME	SG9	SG10	SG11	SG12	SG13	RT1	RT7	RT13
TIME	ED1	ED13	VT7	VR7	-	-	LD7	-

FIGURE 38. SETUP FOR DETERMINATION OF PROGRESSIVE BUCKLING CHARACTERISTIC (TANGENT TRACK)

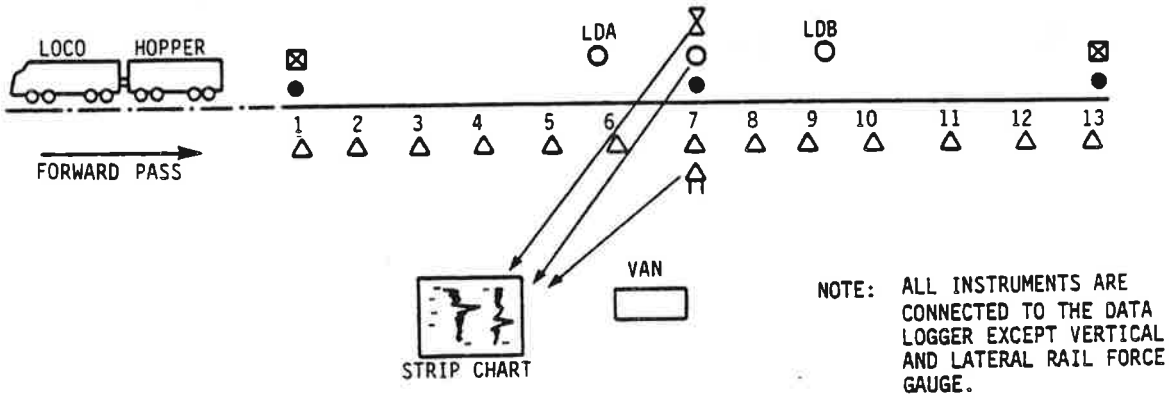

DATA OUTPUT FORMAT

TIME	SG1	SG2	SG3	SG4	SG5	SG6	SG7	SG8
TIME	SG9	SG10	SG11	SG12	SG13	RT1	RT7	RT13
TIME	ED1	ED13	-	-	FH7	LDA	LD7	LDB

FIGURE 39. SETUP FOR DYNAMIC BUCKLING RESPONSE (CURVED TRACK)

3.4.1 Safe Temperature Test

The purpose of this test was to prove that the tangent track with small initial imperfections and with adequate lateral resistance could withstand compressive forces due to the temperature rise equal to the dynamic safe temperature increase, when subjected to vehicle traffic up to speeds of 40 mph.

The initial lateral imperfections in the track were measured using the string line and the Rollordinator device. An imperfection of 0.625" over a length of 40 ft. at the center (location 7) was set intentionally. At location A, which was two tie spacings away from the station 6 (see Figure 37), a "natural" imperfection was found to be 0.25" over a length of 23 ft. At another location B (between the stations 11 and 12) there was an imperfection of 0.2 in. over a length of 22 ft. These three (7,A,B) were the significant imperfections in the track before the commencement of the safe temperature test.

The train consist of a GP-40 locomotive and a hopper car were kept outside the test zone, as in Figure 37, with the hopper car in front of the locomotive for the first forward pass.

The rails were first heated up to the theoretical static safe temperature, which was determined to be 82^{o}F above the stress free temperature (equivalent to a force of 210 kips/rail). The heating continued up to the dynamic safe temperature of 90^{o}F above the stress free, generating a force of 233 kips/rail. At this temperature level, forward and return passes of the two-car train consist were made at a speed of 5 mph. This was repeated at 25 mph, after reheating the rails to compensate for the cooling incurred due to the shutting off of the power while the train was on the heated zone. A final pass at 40 mph was made to complete the test.

Throughout the runs, the lateral rail displacements, the rail force at all the 13 locations, the rail temperature and the longitudinal displacements were monitored. (See Figure 37 for the instrumentation deployment.)

3.4.1.1 Analysis of Results - Rail heating up to the static safe temperature produced no significant lateral movements anywhere in the track. This supported the analytic prediction that the track was safe from the static stability view point.

Due to the passage of the train consist, the track showed some measurable deflections. Table 3 gives a summary of the results.

At the center location 7 and at A the imperfections grew only by 0.05 in. The largest increment of the deflection occurred at B but the overall deflection at B was still less than the value at the control location 7. This was probably due to the local buildup of the rail force at 11, as seen from the force distribution plot (Figure 31.) The force at B exceeded the safe force by about 12 kips/rail, which may be attributed to some residual forces due to nonuniform destressing of the track (subsection 3.2.1.)

Despite the large deflection increment at B, the test is indicative that tangent CWR tracks with adequate lateral resistance, even with initial imperfections, can withstand at least a limited traffic when heated to the dynamic or static safe temperatures.

3.4.2 Progressive Buckling Test

The purpose of the test was to induce a progressive dynamic buckling in order to provide a verification of the dynamic theory developed (4) and an estimate of the safe temperature that could not be determined in the explosive buckling test carried out in Phase I.

TABLE 3. TRACK MISALIGNMENT IN THE DYNAMIC SAFE TEMPERATURE TEST

Temperature Increase (^{o}F)	Location	Maximum Force/Rail (Kips)	Initial Misalignment (inches)	Increase in Misalignment (inches)	Final Misalignment (inches)
90	7	233	0.62	0.05	0.67
90	A	233	0.25	0.05	0.30
90	B	245	0.20	0.30	0.50

TRAIN PASSES

Configuration	Speed mph	Direction of Travel
L — H	5	→ ←
L — H	25	← →
H — L	40	→

L = LOCOMOTIVE

H = HOPPER CAR

To induce progressive buckling, the track was weakened by tamping and creating a large imperfection in the central zone of about 60 ft in length. The tamping reduced the lateral resistance from its previous value of 64.8 lb/in. to 53.9 lb/in., and by means of the Track Lateral Pull Test rig (TLPT) an imperfection of 5 in. was set at the center when the rail was at its neutral temperature. This imperfection, coupled with the low lateral resistance, was theoretically determined to be adequate for the progressive buckling of the track. The hopper car was spotted over the imperfection symmetrically to induce uplift, thereby simulating a quasi-dynamic condition.

As the track was heated gradually the lateral deflection at the center, the rail forces and the temperatures were monitored. See Figure 38 for the instrumentation deployment.

3.4.2.1 Analysis of Results - The temperature deflection relationship obtained in the experiment and the theoretical prediction is shown in Figure 40. The agreement is good. From this figure, it may also be seen that the safe temperature increase for a tangent track with the same parameters as the test track, but with smaller imperfections, will be of the order of 80°F.

The maximum deflection including the initial deflection of 5 in., was about 17 in. and in excellent agreement with the theory.

3.5 TESTS ON CURVED TRACKS (PHASE II)

In the following sections, the two major tests conducted on the curved site will be described. The first test was on the curve with an adequate ballast lateral resistance with margin of safety of 15°F. The track was expected to "pass" the safe temperature test. In the second test, the curve had reduced lateral resistance corresponding to zero margin of

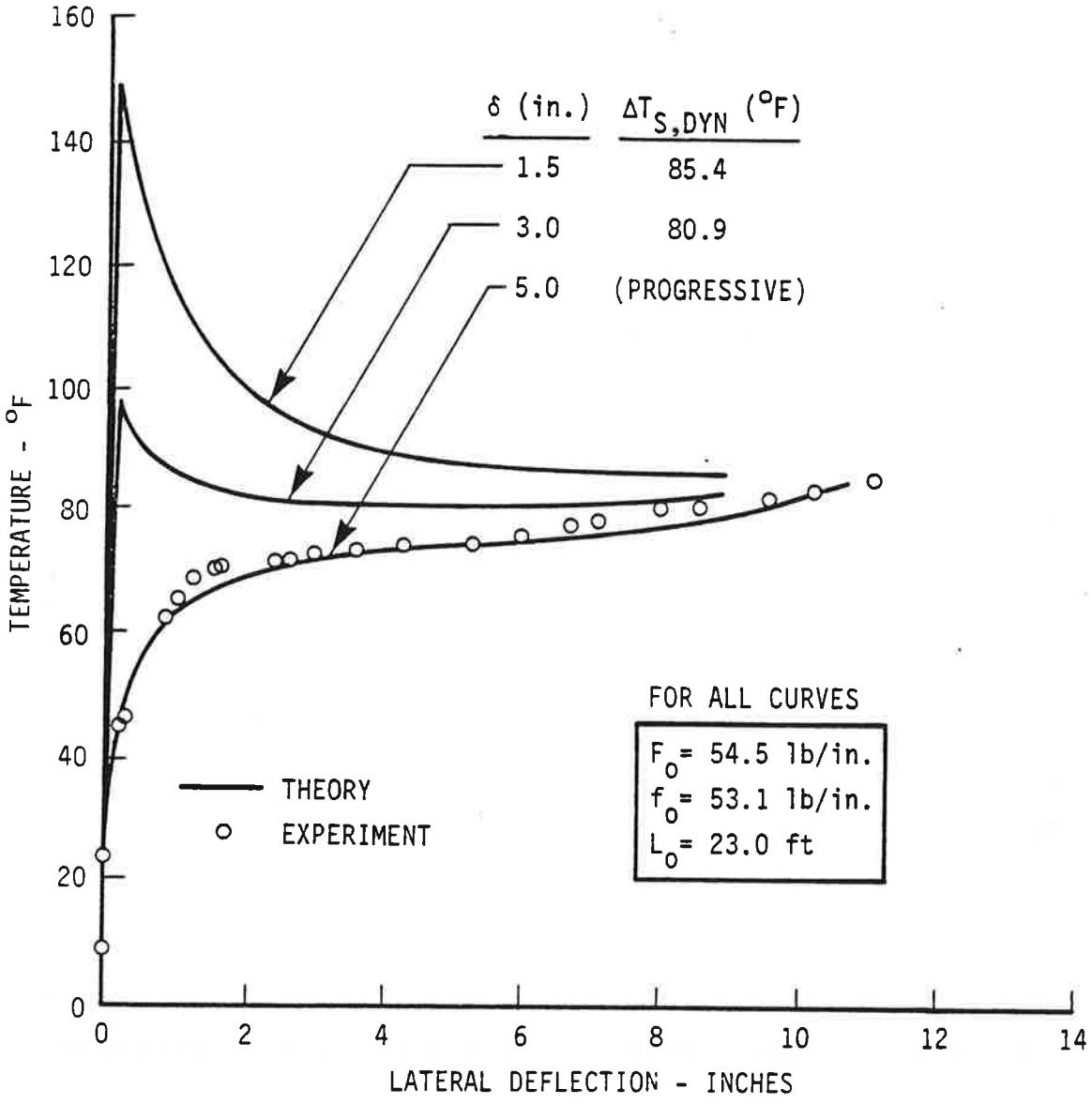

FIGURE 40. PROGRESSIVE BUCKLING OF TANGENT TRACK

safety. Rail heating test on this track was conducted to show that the track could not safely carry the traffic even at its static "safe" temperature level.

3.5.1 Curve with Finite Margin of Safety

The purpose of this test was to demonstrate that the curved track with an adequate margin of safety (at least 10°F) could be heated up to its safe temperature value and simultaneously subjected to some traffic without developing unduly large lateral misalignments.

To obtain the required minimum margin of safety, the track resistance needed to be increased. For this purpose, the track ballast was consolidated by about 0.125 MGT of traffic using the FAST consist. An imperfection of 0.375 in. was set at the center (location 7), and the rest of the track was mapped for the presence of other initial lateral imperfections using the Rollordinator. The most severe imperfections found are shown in Figure 41. The distribution of the lateral imperfection offset along the track is shown in Figure 42. As seen from this figure, the artificially set (0.375 in.) imperfection was the most severe one for the track.

3.5.1.1 Static Response - The purpose of this test was to ensure that the track would not show any significant lateral movements due to heating up to its static safe temperature value.

The track was heated up to its theoretical 'static' safe temperature value of about 75°F over the stress-free temperature. The lateral deflections at the locations 7, A and B were monitored during the heating. In addition the rail forces and temperatures were measured at the locations shown earlier in Figure 39.

LOCATION	δ_o	$2L_o$
7	0.375"	28'
A	0.200"	20'
B	0.130"	24'

$2L_o$ = LENGTH OF IMPERFECTION ZONE

δ_o = OFFSET

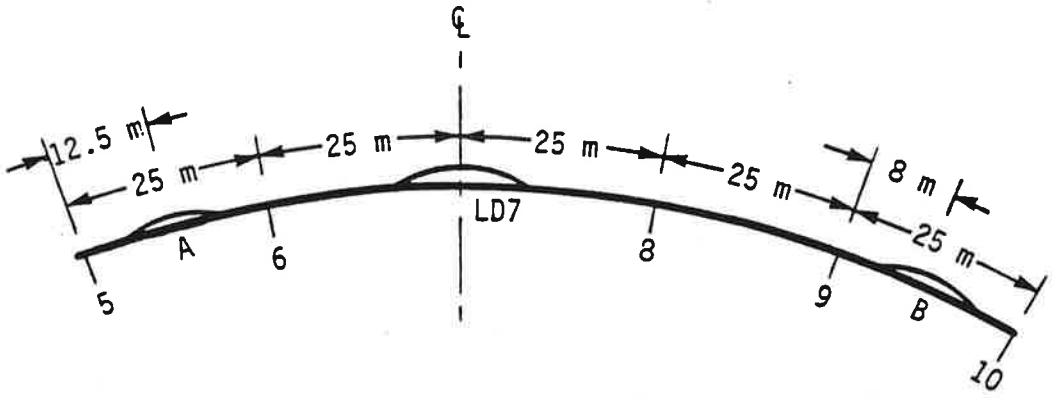

FIGURE 41. INITIAL IMPERFECTIONS OF CURVED TRACK WITH FINITE MARGIN OF SAFETY

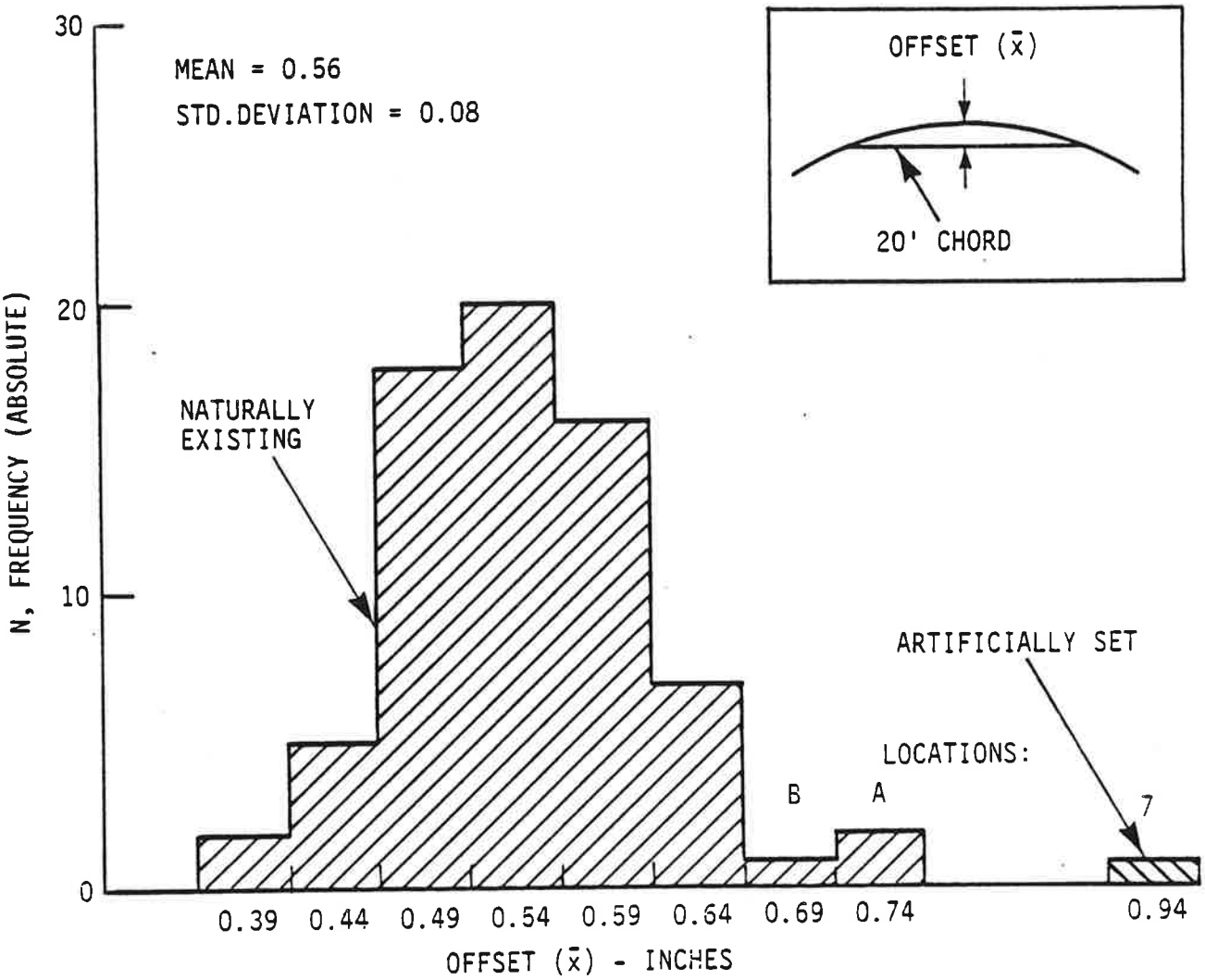

FIGURE 42. DISTRIBUTION OF CHORDAL OFFSET MEASUREMENTS (CHORD LENGTH = 20 ft)

The deflection results for the static-safe temperature increase are shown in Table 4, which clearly show that the lateral deflection increments were minimal. Therefore, the test was continued to verify the dynamic safe temperature concept, as described in the following paragraphs.

3.5.1.2 Dynamic Response - The rails were allowed to cool off naturally and then heated through increments starting from the neutral temperature. At each of the temperature increments the train consist made a pass at 5 mph. Rail heating continued till the static-safe temperature (75^{o}F over the stress-free temperature) was reached. Six passes were made with the two car consist (locomotive and hopper car) up to this temperature. Rail heating was continued further till 81^{o}F was attained. Two passes were made at this temperature, one at 25 mph and the other at 40 mph. A final ninth pass was made at 5 mph when the rail temperature was 84^{o}F above the stress-free which was slightly above the theoretical dynamic safe temperature increase.

Throughout the test, the rail force, the temperature and the displacement gages were monitored (Figure 39). In addition, the lateral and the vertical loads on the rails as the wheels negotiated the imperfection at 7 were recorded on the strip chart.

3.5.1.3 Analysis of Results - The increments of lateral deflection for each of the train passes are shown in Table 5. As seen from this table, the dynamic deflection increment at the center location 7 was reasonably small, particularly up to the static-safe temperature increase.

Figure 43 shows a graphical plot of the dynamic response at the location 7. The theoretical response is also shown in the figure. The theoretical dynamic buckling temperature increase is about 12^{o}F higher than the maximum temperature reached in

TABLE 4. STATIC RESPONSE OF CURVED TRACK (FINITE MARGIN OF SAFETY) ($\Delta T_{S,\ STATIC} = 75^{\circ}F$)

LOCATION	RAIL FORCE (KIPS/RAIL)	INITIAL MISALIGNMENT (INCHES)	INCREASE IN MISALIGNMENT (INCHES)
7	190	0.38	0.07
A	190	0.20	0.05
C	160	0.13	0.03

TABLE 5. DYNAMIC BUCKLING RESPONSE OF CURVED TRACK (FINITE MARGIN OF SAFETY)

PASS NO.	ΔT ($^{\circ}F$)	RAIL FORCE AT CENTER (KIPS/RAIL)	INCREASE IN MISALIGNMENT (INCHES)			CONFIGURATION	SPEED MPH	COMMENTS
			A	7	B			
1	24.0	62.0	0.00	0.00	0.00	H — L	5	
2	34.8	88.5	0.00	0.00	0.00	L — H	5	
3	52.0	132.0	0.02	0.00	0.00	H — L	5	
4	62.0	157.0	0.03	0.00	0.03	L — H	5	
5	69.0	176.0	0.08	0.00	0.05	L — H	5	
6	75.0	192.0	0.13	0.08	0.12	L — H	5	Static Safe Temp. at 7
7	81.0	206.0	0.22	0.15	0.19	L — H	25	
8	81.0	206.0	0.27	0.19	0.20	H — L	40	
9	84.0	213.0	0.38	0.23	0.26	L — H	5	Slightly above Dynamic Safe Temp. at 7
INITIAL MISALIGNMENT			0.22	0.37	0.13	DIRECTION OF TRAVEL →		
FINAL MISALIGNMENT			0.60	0.60	0.39			

H = HOPPER

L = LOCOMOTIVE

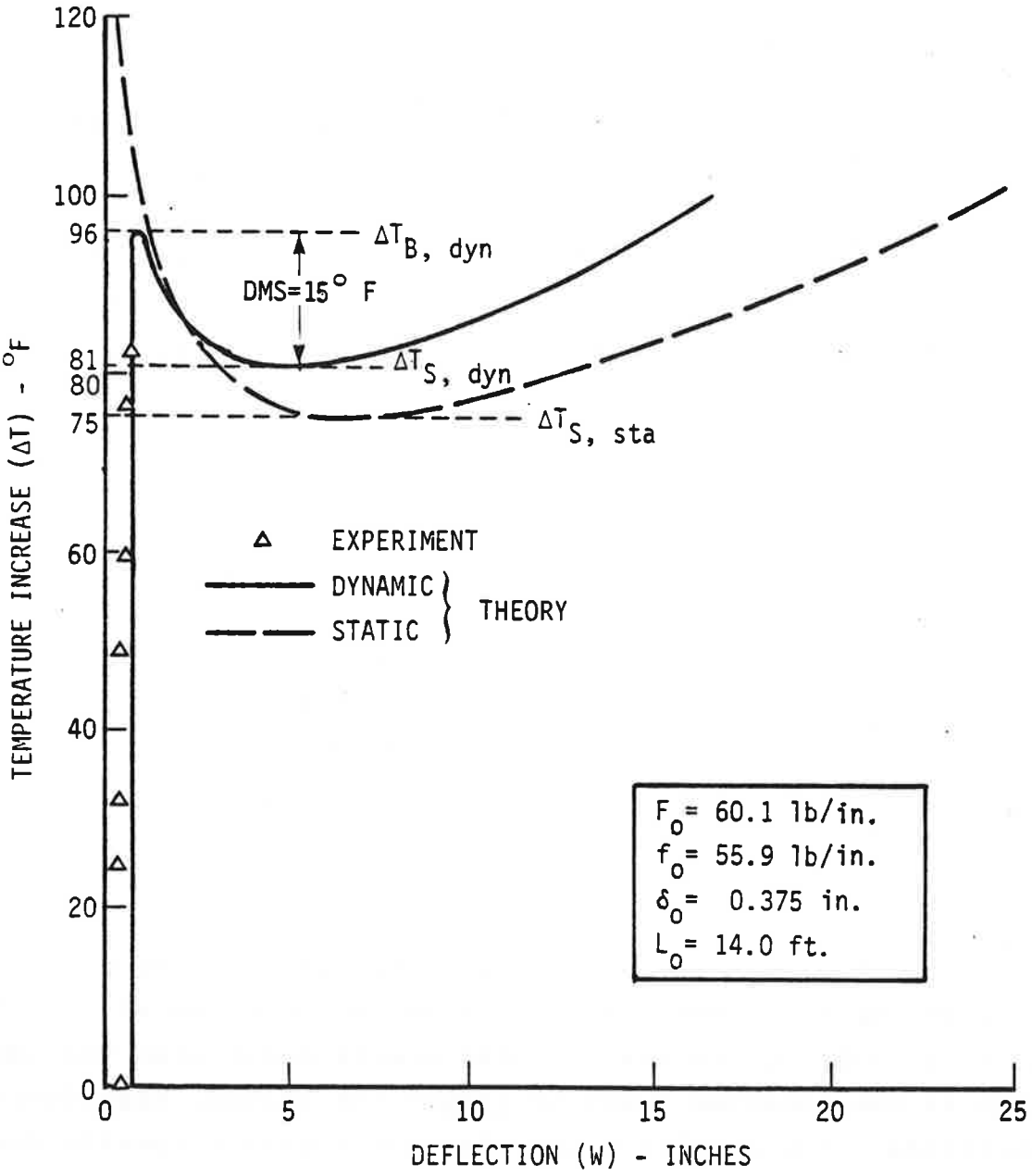

FIGURE 43. DYNAMIC BUCKLING RESPONSE AT LOCATION 7
(CURVE WITH FINITE MARGIN OF SAFETY)

the test. It can be concluded that a DMS (dynamic margin of safety) of the order of 15°F may be adequate for safe operations of the CWR track tested.

Visual inspection of the track followed by measurements with the Rollordinator soon after the test revealed that the largest lateral deflection increment occurred at the location C, which was about 6 ft from A (see Figure 44). The initial imperfection at C was less than at A, but the final imperfection at C was 0.93 in., and larger than at A.

To explain the track behavior at A and C, the local lateral resistance was measured after the rails cooled off to the neutral temperature. It was found to be about 53.9 lb/in. near A, whereas it was 60.1 lb/in. at the central location 7. Figure 44 shows the dynamic buckling response at locations A and C, where the theoretical buckling temperature increase is 83°F, whereas it is 95°F at the location 7. The maximum temperature increase reached in the test was 84°F. Hence the local buckle at A and C was due to the reduced lateral resistance.

L/V Effects

Table 6 shows the maximum (L/V) measured in the test. Inspection of the strip chart records revealed that the effect of the lateral loads on the track as the wheels negotiated the imperfection at the location 7 was to reduce the initial imperfection amplitude. The net force was directed radially towards the center of curvature (the train speed being less than the balance speed) and might have contributed to the reduction of the imperfection. However, the net increment of the lateral deflection from each pass was in the direction of the initial deflection, which was due to the central bending wave described below.

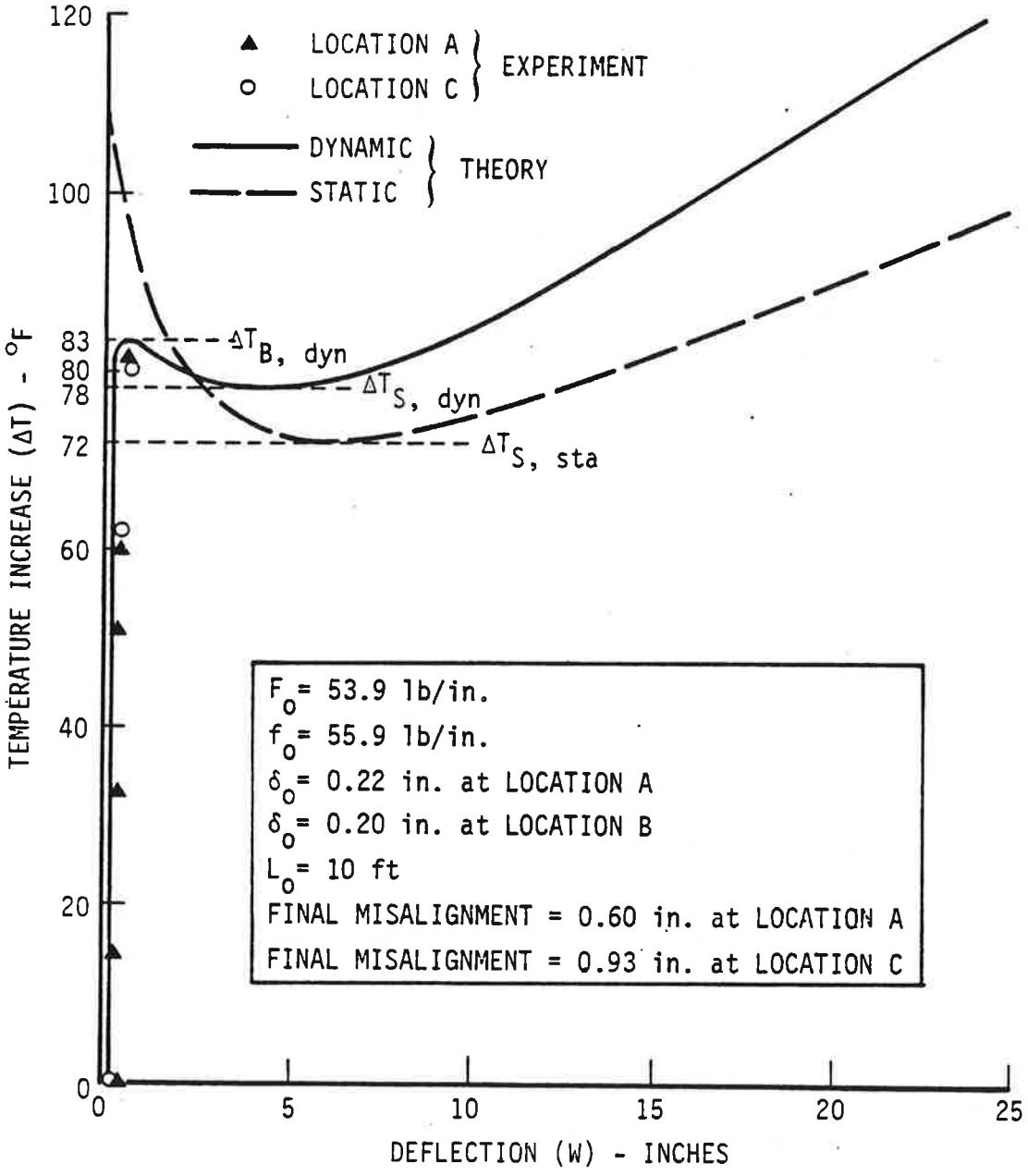

FIGURE 44. BUCKLING RESPONSE AT LOCATIONS A AND C (CURVED TRACK WITH FINITE MARGIN OF SAFETY)

TABLE 6. (L/V) FOR CURVE WITH FINITE MARGIN OF SAFETY

SERIES I RUN NO.	CONFIGURATION	SPEED MPH	$(L/V)_{max}$	LOCATION OF $(L/V)_{max}$
1	H - L	5	-0.0971	Hopper, Leading Wheel Set of Trailing Truck
2	L - H	5	+0.0976	Loco, Leading Wheel Set of Leading Truck
3	H - L	5	-0.1000	Hopper, Leading Wheel Set of Trailing Truck
4	L - H	5	+0.1512	Loco, Leading Wheel Set of Leading Truck
5	L - H	5	+0.1893	Loco, Leading Wheel Set of Leading Truck
6	L - H	5	+0.1942	Loco, Leading Wheel Set of Leading Truck
7	L - H	25	+0.1410	Loco, Leading Wheel Set of Leading Truck
8	H - L	40	+0.1911	Loco, Leading Wheel Set of Trailing Truck
9	L - H	5	+0.2279	Loco, Leading Wheel Set of Leading Truck

H = HOPPER
L = LOCOMOTIVE

DIRECTION OF TRAVEL →

Central Bending Wave Effect

A typical strip chart record is shown in Figure 45. From the strip chart records, it is concluded that the growth of the imperfection was largest when the hopper car was symmetrically situated over the imperfection; hence, the central bending wave seems to be an important factor in determining the dynamic response of the track.

For each pass, the increment in the lateral deflection due to the central bending wave was about 0.05 in. The deflection increment under the central bending wave of the locomotive was found to be less than that for the hopper car.

The experimental evidence that the central bending wave is more important than the precession and the recession wave in the development of lateral imperfection is of significant importance since the dynamic theory developed (4) is based on this phenomenon.

The test confirmed the theoretical expectation that the dynamic deflection increment due to the train consist passing over the track heated up to its safe temperature can be kept in reasonably safe limits, if the track has a reasonable margin of safety ($10^{o}F$ or greater) assured by an adequate lateral resistance and small enough misalignments.

3.5.2 Curve with No Margin of Safety

The purpose of this test was to demonstrate that the CWR track with negligible "margin of safety" was unsafe under dynamic conditions, when the rail temperature reached its "static safe temperature" (the minimum point on the temperature-deflection response curve as determined by the static buckling theory). (See the Glossary of Terms.)

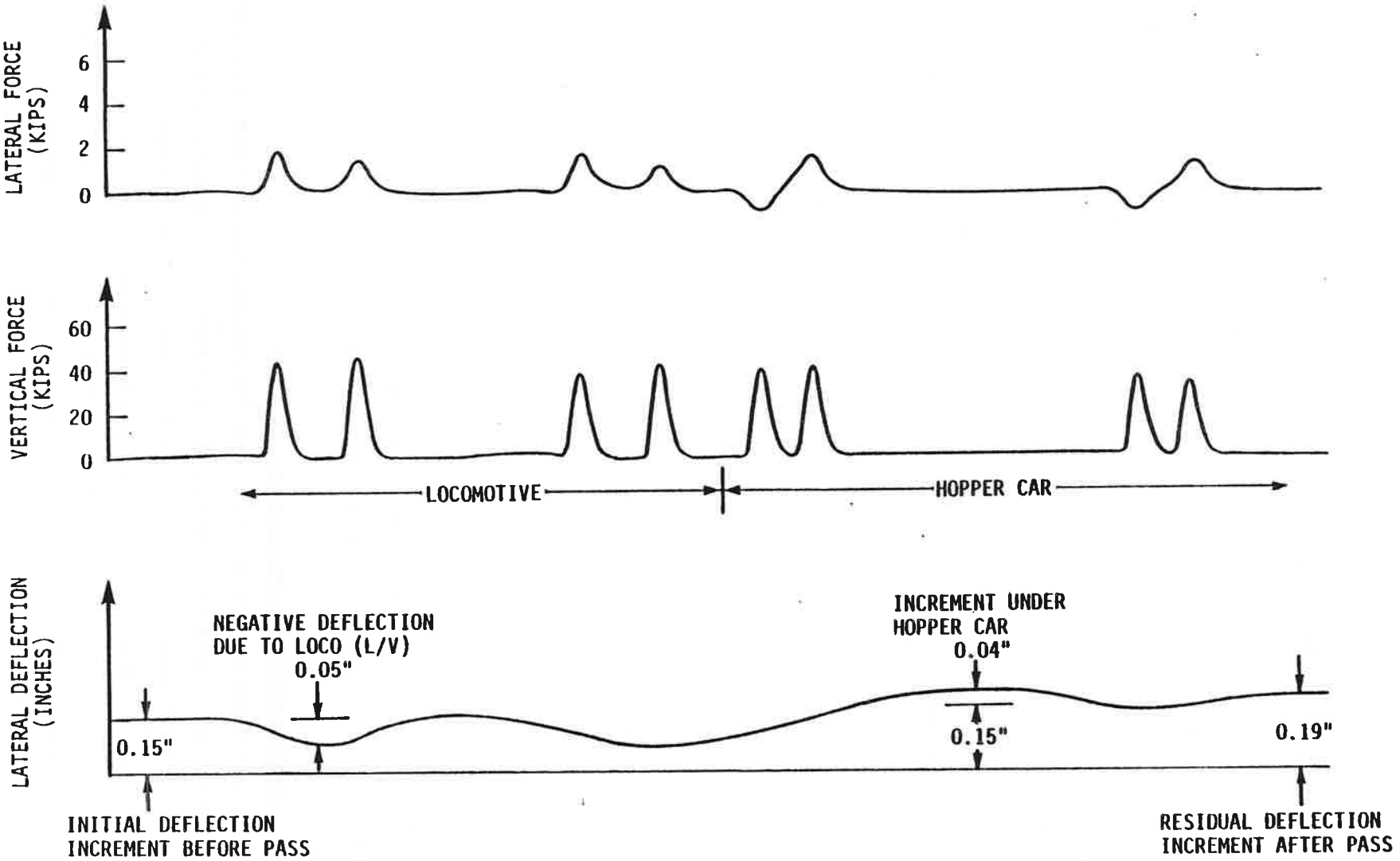

FIGURE 45. STRIP CHART RECORD FOR PASS NO.8 (CURVE WITH FINITE MARGIN OF SAFETY)

The lateral resistance in the central zone of about 500 ft was reduced by lift-tamping to condition the track for zero margin of safety. The lift level varied from its maximum value of 1.25 in. at the center (location 7) to zero at the ends of the tamped central zone. Inspection of the strain gage output before and after tamping showed that the neutral temperature did not alter significantly due to this operation. Hence, no destressing of the track was performed.

An initial lateral imperfection of 0.32 in. was set at the center, and other naturally existing imperfections were also measured using the Rollordinator. The severe imperfections were identified at the locations 7, A and B as shown in Figure 41. The respective amplitudes were 0.32, 0.18 and 0.16 in.; these were of the same order as in the previous experiment on the curve with a finite margin of safety (subsection 3.5.1). The lengths of imperfection were 28 ft at 7 (center) 20 ft at A and 28 ft at B.

3.5.2.1 Static Response - The rails were gradually heated up with the intent of studying the track static response. On the basis of the measured lateral resistance at the central location 7 after lift tamping, the static-safe temperature was computed to be 54^{o}F above the stress-free temperature of 78^{o}F. However, when the temperature was about 52^{o}F over the stress free state, a small buckle occurred at the location A. The deflection at A increased by 2 in. over the initial value. At the center location 7, the deflection increased only by about 0.3 in. The local lateral resistance at A was measured subsequently when the rails cooled down to the neutral temperature. The resistance was found to be 27.1 lb/in., whereas at the center it was 34.1 lb/in. (Figure 30). The experimental and theoretical static responses are plotted in Figure 46.

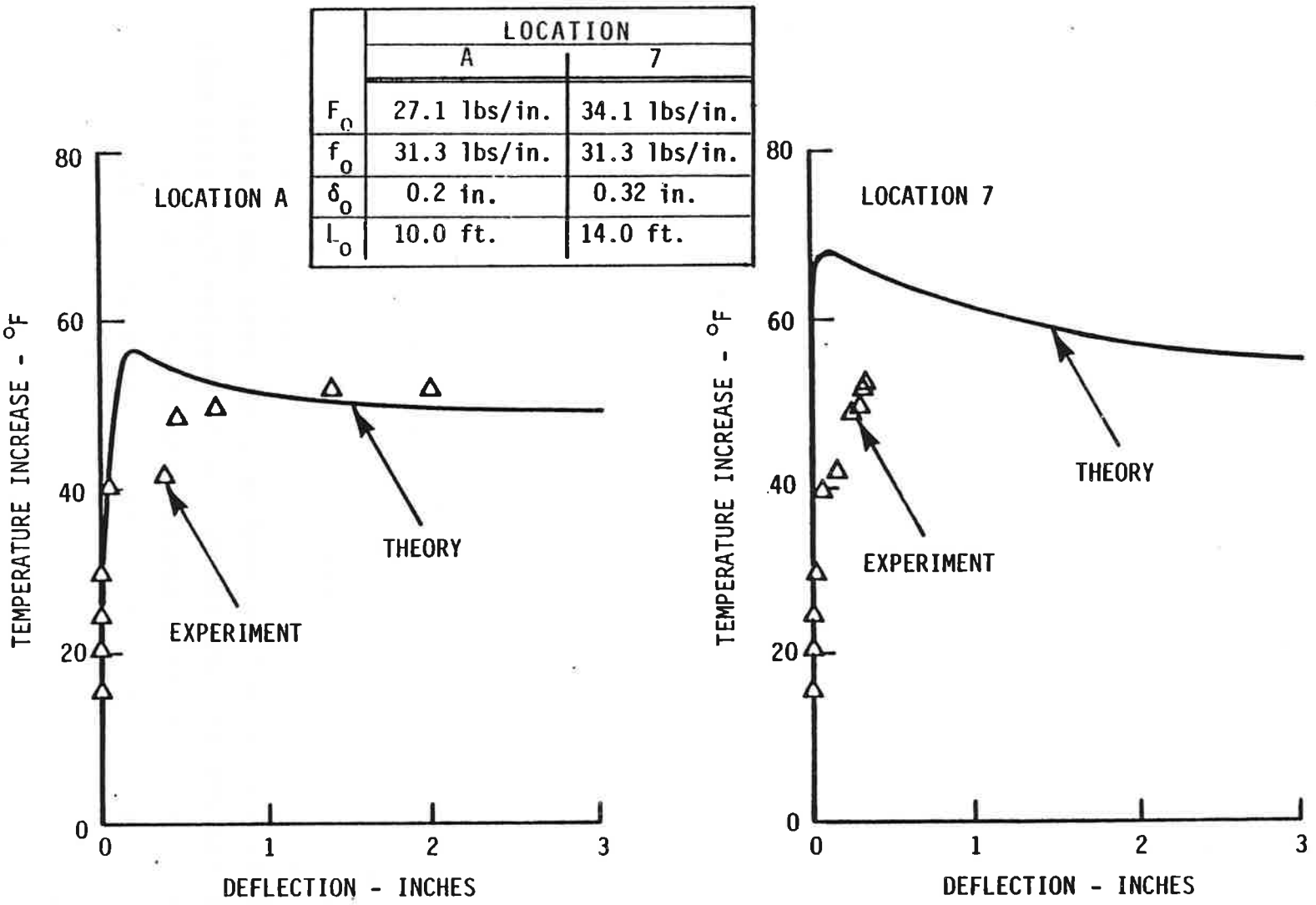

FIGURE 46. STATIC RESPONSE OF CURVED TRACK WITH ZERO MARGIN OF SAFETY

The local buckle at A was the result of inadequate lateral resistance. The static heating up to 52°F (over the stress free) clearly exceeded the theoretical static safe increase of 47°F and was quite close to the theoretical buckling temperature increase of 55°F for this location. At the location 7, the corresponding theoretical values were higher; 54°F for the static safe temperature increase and 67°F for the static buckling temperature increase.

3.5.2.2 Dynamic Response - The misalignments developed in the previous heating were corrected before the commencement of the test for the dynamic response. A truck load of ballast was dumped at the location A for a length of about 40 ft. This was to prevent undesirable deflections at this location and make the central location 7 as the main observation and control location in the track for subsequent tests.

An imperfection of about 0.32 in. was again set at location 7. The rails were heated incrementally and a total of 10 passes were made with the two car consist at the temperature intervals shown in Table 7. Each pass was at 5 mph.

After the tenth pass, the total misalignment at the center was 1.08 inches, which was considered to be unsafe for further train passes. Further heating of the rails up to 63°F temperature increase resulted in a large static buckle at the center location, with the maximum buckling deflection of 7.5 in. and the buckling length of 56 ft. The buckle reduced the compressive force at the center from the pre-buckling value of about 160 down to 128 kips/rail.

3.5.2.3 Analysis of Results - Table 7 presents the track "dynamic" response at each of the passes. Clearly, the largest misalignment growth due to the train passes occurred at the center, with negligible increments at B due to these passes, the location A being kept under control by the additional

TABLE 7. DYNAMIC BUCKLING RESPONSE FOR CURVED TRACK WITH ZERO MARGIN OF SAFETY

Pass No.	ΔT (°F)	Rail Force at Center (Kips)	Increase in Misalignment (inches)			CONFIGURATION	Speed (mph)	COMMENTS
			A	7	B			
1	13.7	34.8	0.000	0.000	0.00	L - H	5	
2	20.0	51.0	0.000	0.000	0.10	H - L	5	
3	26.0	66.0	0.000	0.010	0.15	L - H	5	
4	32.0	80.3	0.020	0.015	0.15	H - L	5	
5	37.0	94.0	0.030	0.015	0.15	L - H	5	
6	41.5	105.5	0.030	0.015	0.15	H - L	5	
7	46.5	119.0	0.065	0.070	0.15	L - H	5	
8	51.0	129.0	0.090	0.130	0.20	H - L	5	
9	55.0	140.0	0.130	0.420	0.20	L - H	5	
10	59.0	150.0	0.160	0.760	0.25	H - L	5	
No pass	63.0	160.0 ↓ 128.0	0.190	7.500	2.00	-	No Train	Static Buckling at 7
Initial Misalignment			0.180	0.320	0.16	DIRECTION OF TRAVEL →		
Final Misalignment			0.370	7.820	2.16			

L = LOCOMOTIVE

H = HOPPER CAR

ballast dumped around it. The progressive growth of the misalignment at the center location, expected from the dynamic buckling theory, was a consequence of zero margin of safety (see the dynamic response curve, Figure 47).

The static buckling at the center was not theoretically a pure static buckling phenomenon, but a cumulative result of alternating static heating and dynamic loading of the track. Therefore, the test results lie in between the two theoretical curves representing the pure static and the pure dynamic response of the track.

It must be noted that the final deflection of 2 in. at B was not due to any local weakness at B, but due to the static buckling at the center, whose influence zone (buckling length) of about 56 ft included the location B. Figure 48 shows the buckled shape of the track. The discrepancy between test and theory can be attributed to lack of perfect symmetric rail force distribution about the central tie. (See Figure 33.) Despite this discrepancy, the results are believed to provide a reasonable validation of the concept of the margin of safety as a measure of the track safety.

(L/V) Effects

As in the experiment on the stronger curved track described in subsection 3.5.1, the effect of the lateral loads generated as the wheels negotiated the imperfection, was to reduce the imperfection existing before the pass. This may be seen from a typical strip chart record shown in Figure 49. However, the net deflection increment after each pass was in the direction of the existing imperfection.

Table 8 shows the maximum (L/V) per wheel as measured in the test. The truck (L/V) was less than the values shown in this table.

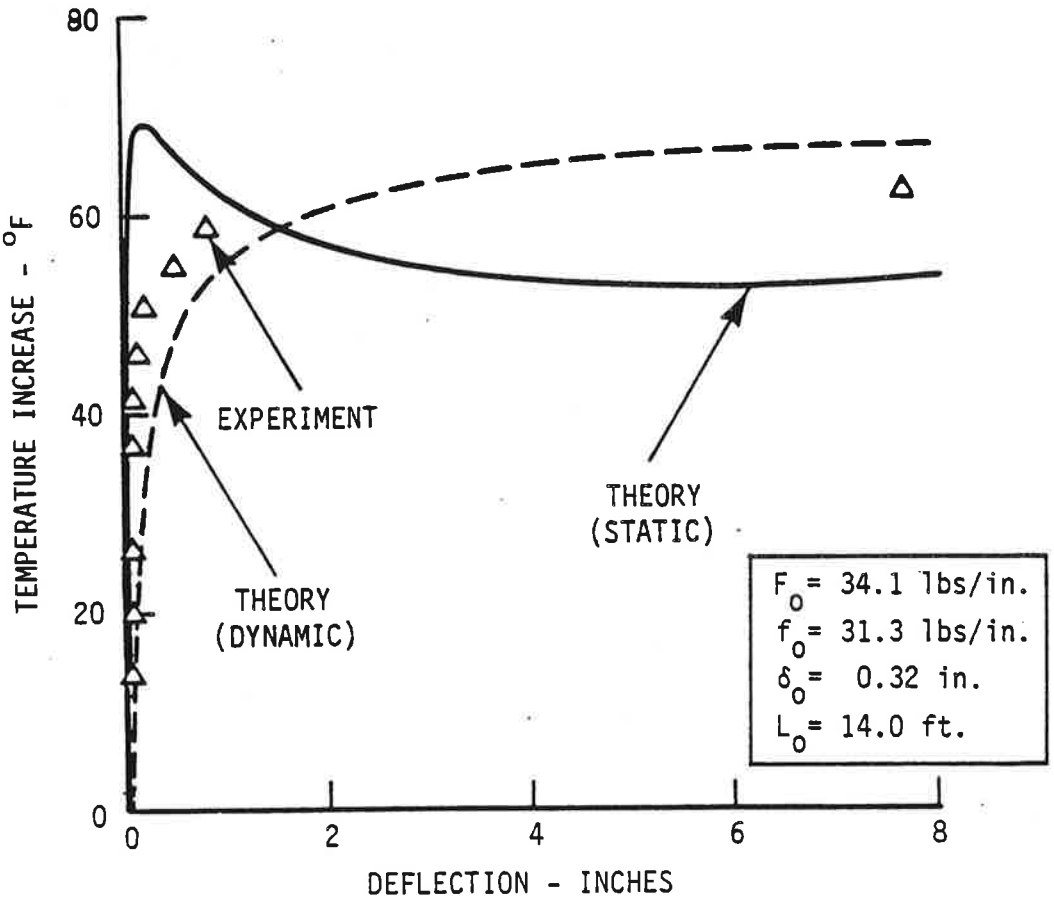

FIGURE 47. BUCKLING RESPONSE OF CURVE WITH ZERO MARGIN OF SAFETY

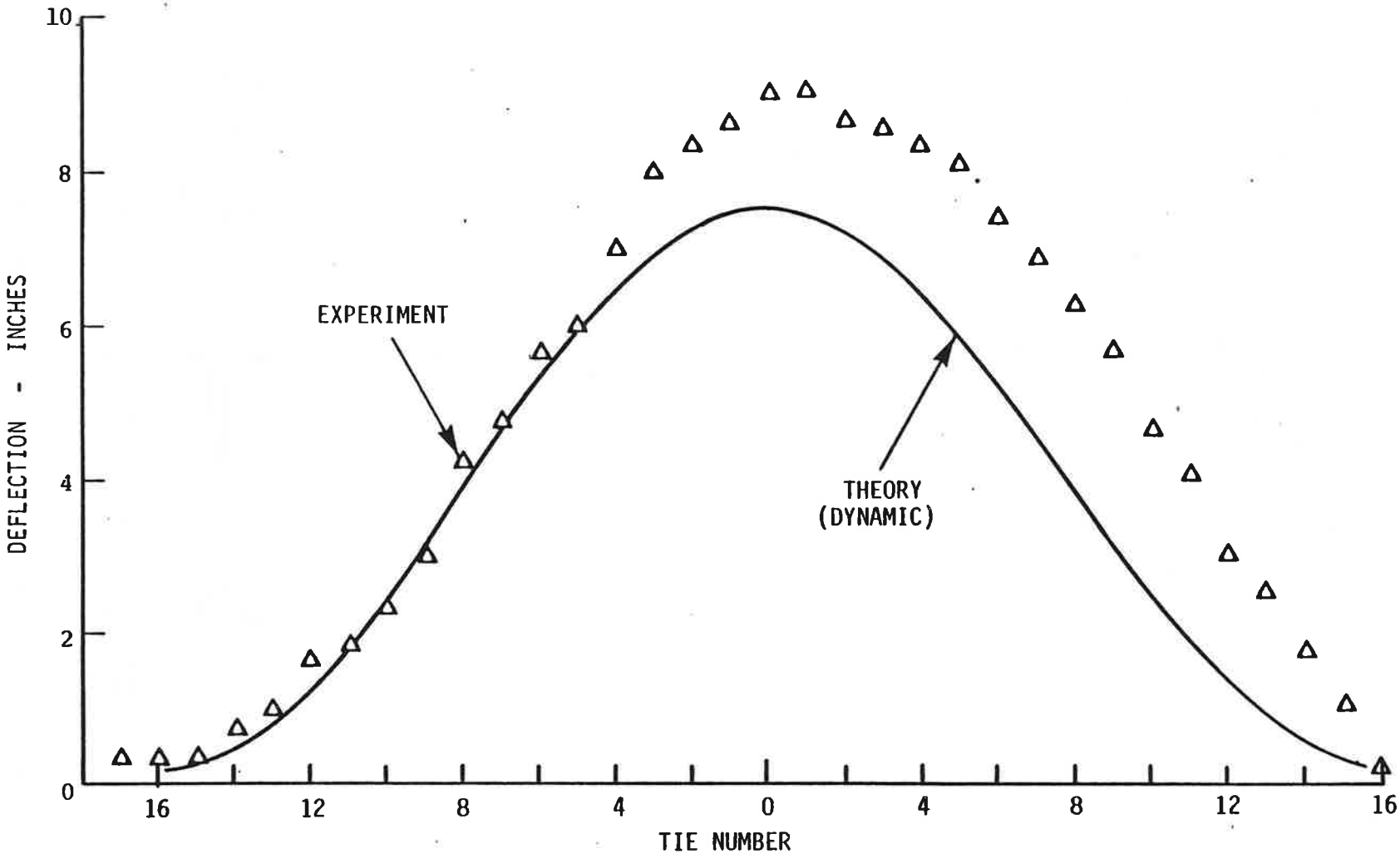

FIGURE 48. BUCKLED SHAPE OF TRACK WITH ZERO MARGIN OF SAFETY

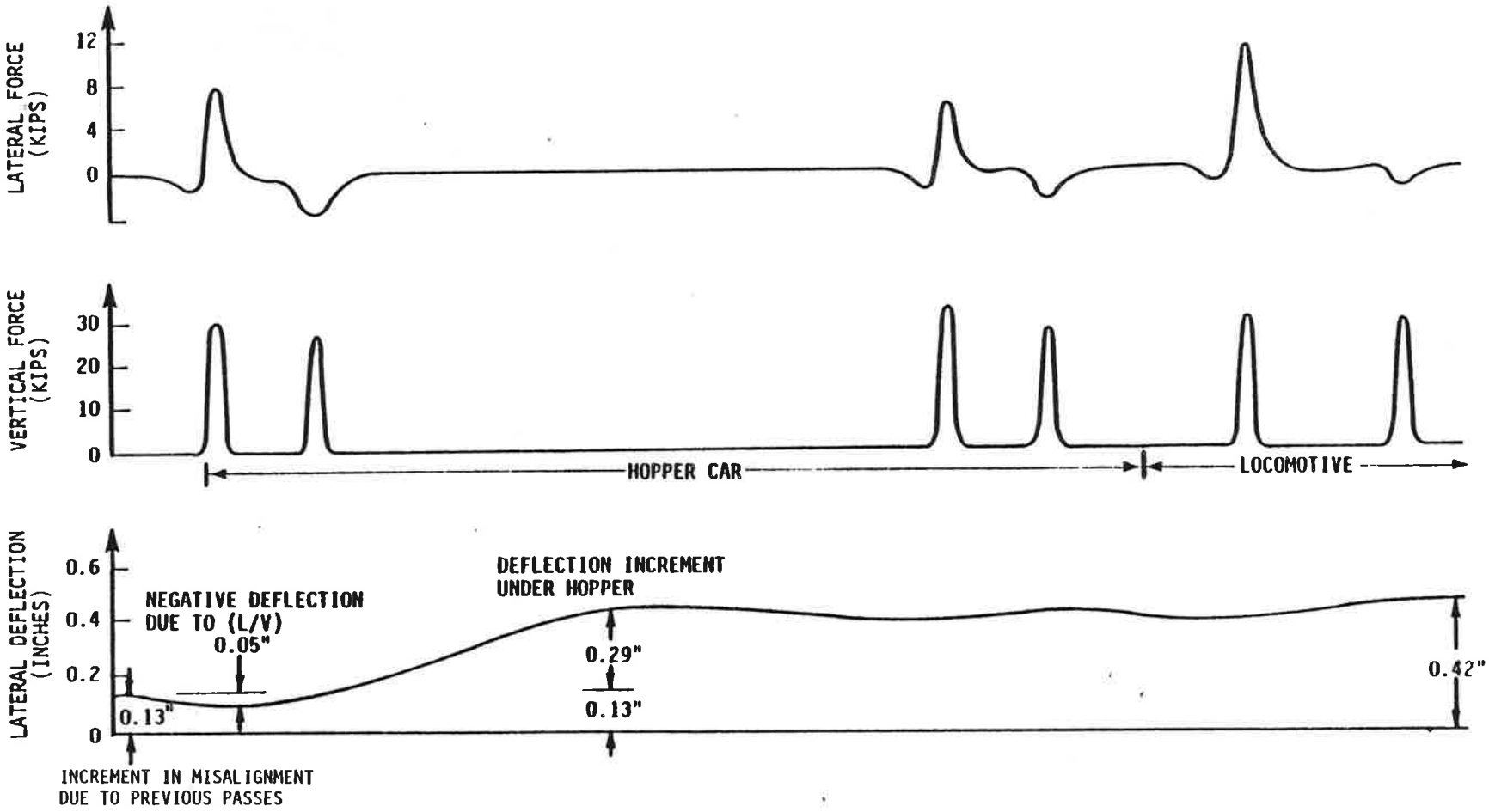

FIGURE 49. STRIP CHART RECORD FOR PASS NO.9 (CURVE WITH ZERO MARGIN OF SAFETY)

TABLE 8. (L/V) FOR CURVE WITH ZERO OF MARGIN OF SAFETY

SERIES II RUN NO.	CONFIGURATION	SPEED (mph)	$(L/V)_{max}$	$(L/V)_{max}$ LOCATION
1	H - L	5	0.2756	Loco, Leading Wheel Set of Leading Truck
2	L - H	5	0.1632	Loco, Leading Wheel Set of Trailing Truck
3	H - L	5	0.3467	Loco, Leading Wheel Set of Leading Truck
4	L - H	5	0.2048	Loco, Leading Wheel Set of Trailing Truck
6	L - H	5	0.2152	Loco, Leading Wheel Set of Trailing Truck
7	H - L	5	0.3765	Loco, Leading Wheel Set of Leading Truck
8	L - H	5	0.2190	Loco, Leading Wheel Set of Trailing Truck
9	H - L	5	0.3767	Loco, Leading Wheel Set of Leading Truck
10	L - H	5	0.2000	Loco, Leading Wheel Set of Leading Truck

L = LOCOMOTIVE
H = HOPPER
} DIRECTION OF TRAVEL →

Central Bending Wave Effect

As in the previous experiment with the "adequate ballast" curve, the growth of the imperfection was largest under the central bending wave in between the trucks of the hopper car. Figure 49 shows a typical strip chart recording for the ninth pass (Table 7). The increment due to this pass was about 0.29 in.

3.6. Observations From Phase II Results

a. The Phase II test results are, generally, in good agreement with theoretical predictions. The test track in Phase II, in regard to the length of heated zone and stiffness outside the heated zone, was a good approximation to the infinite track, when compared with the Phase I track.

b. Despite some scatter in the vertical deflection data for the central bending wave, there was some definite evidence for the existence of "lift-off" zone (i.e., zone of negative upward deflection) over a length of 14 tie spacings, as measured under a hopper car.

c. The CWR tangent track with modest initial imperfections and adequate lateral resistance can withstand limited traffic at least up to speeds of 40 mph at a temperature increase equal to the static safe temperature.

d. For a progressive growth of dynamic deflections with temperature increase, the adequately ballasted and consolidated tangent track requires unduly large initial misalignments or small lateral resistance not usually found in revenue service CWR tracks.

e. Curves are more vulnerable to progressive growth under vehicle traffic than tangent tracks; therefore a good margin of safety (about $10^{\circ}F$ or more) is essential for safe operations of curved tracks. The required minimum lateral resistance to obtain a specific margin of safety increases with curvature and is of the order of 56 lb/in. for the 5 degree curve used in the test series.

f. The precession and recession bending waves have much smaller effect on the growth of lateral imperfections compared to the central bending wave. The central bending wave influence under the hopper car is more severe than the wave under the locomotive in increasing the lateral imperfections. This is because the central bending wave under the hopper car reduces the lateral resistance to a larger extent than the precession and recession waves or the central bending wave under the locomotive. A detailed theoretical analysis of the subject is presented in Reference (4).

b. To facilitate test planning of Phase II, which included the optimization of the heated zone based on the available electric power and to design the test track so that a constant rail force in the central zone (300 ft) can be developed.

Test Track Length Requirements

Since the "end stiffness" is not known in advance and generally nonlinear, it is more convenient to express the required test track length in terms of the longitudinal resistance. Referring to Figure A-1, it can be shown that

$$\ell_2 = \frac{EA\alpha\ \Delta T}{\left(f_1 + \sqrt{f_1\ f_2}\right)} \qquad (1)$$

$$\ell_3 = \frac{EA\alpha\ \Delta T}{\left(f_2 + \sqrt{f_1\ f_2}\right)}$$

The end stiffness K_e, can be shown as

$$K_e = 2\ f_1 \sqrt{\frac{f_2}{f_1}} \left(1 + \sqrt{\frac{f_2}{f_1}}\right) \Big/ \alpha\Delta T \qquad (2)$$

Here f_1 and f_2 are the respective longitudinal resistances inside and outside the heated zones. The value of ΔT is the maximum temperature rise expected in the test series.

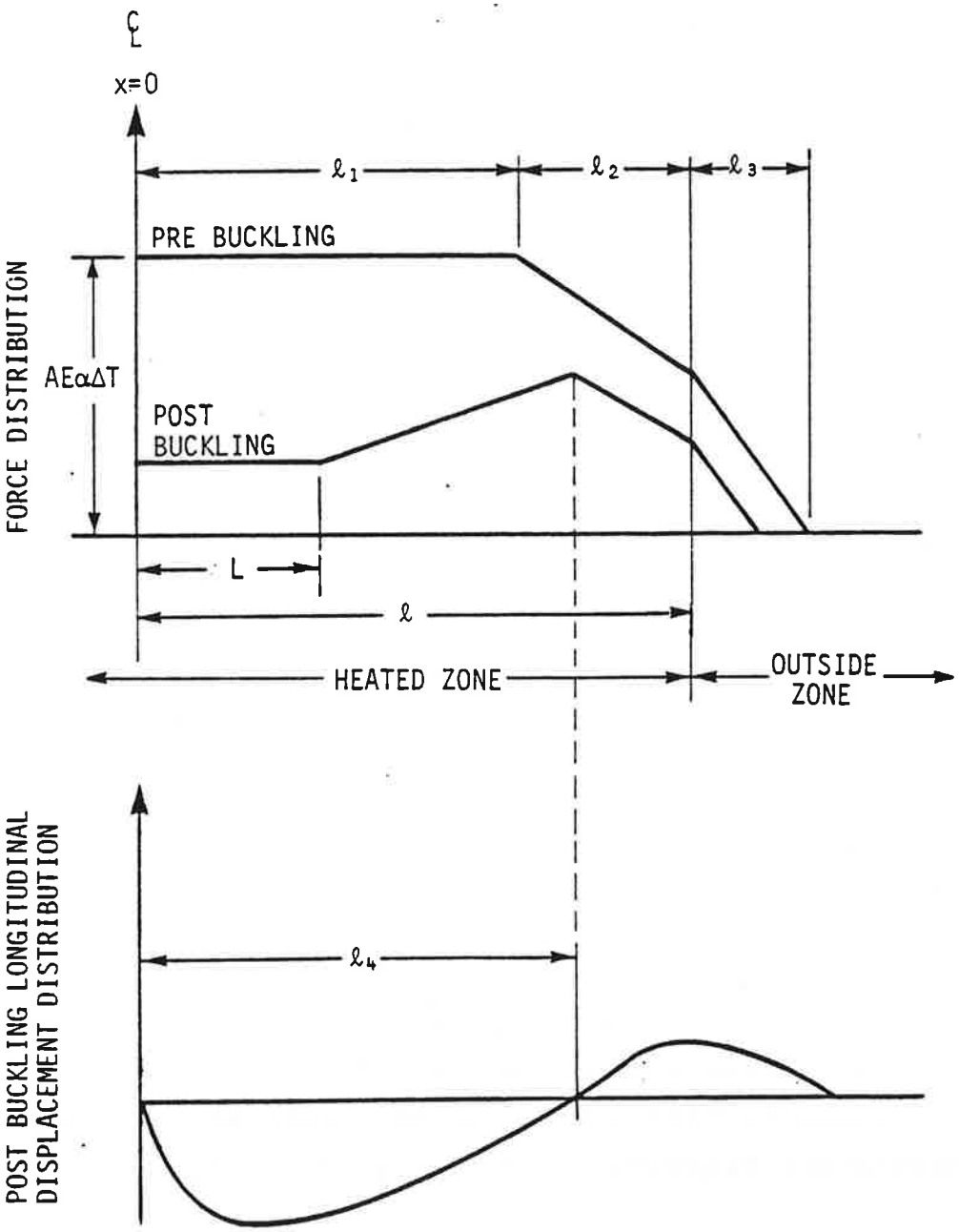

FIGURE A-1. FORCE AND DISPLACEMENT DISTRIBUTION
(TRACK HEATED OVER A FINITE LENGTH)

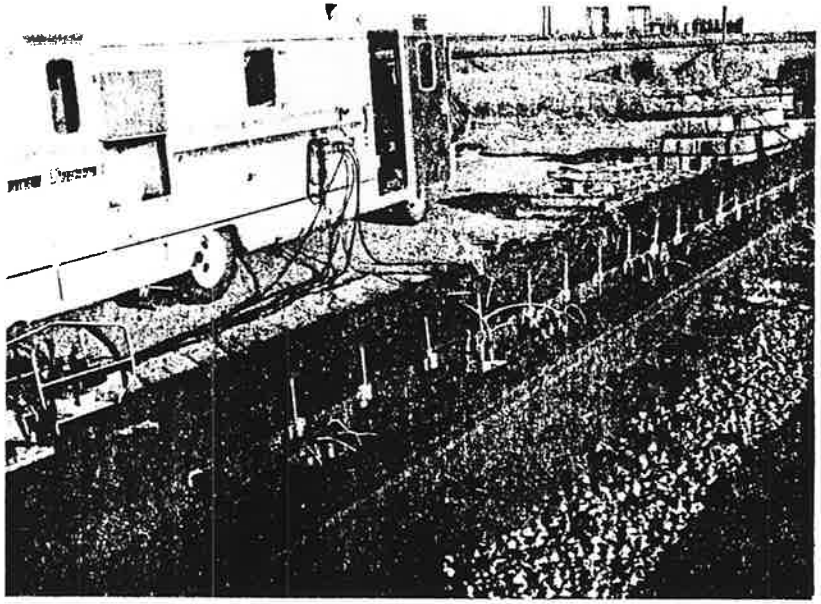

FIGURE B-1. INSTRUMENTATION VAN AND SETUP FOR UPLIFT WAVE MEASUREMENT

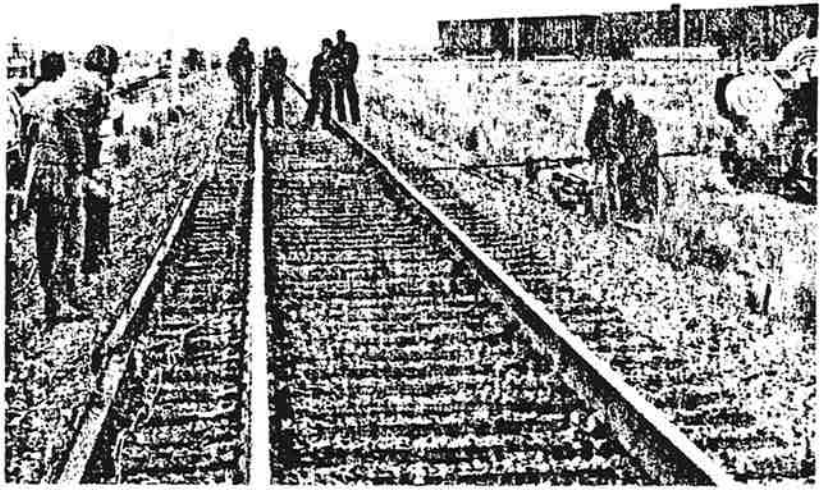

FIGURE B-2. TRACK LATERAL RESISTANCE PULL TEST

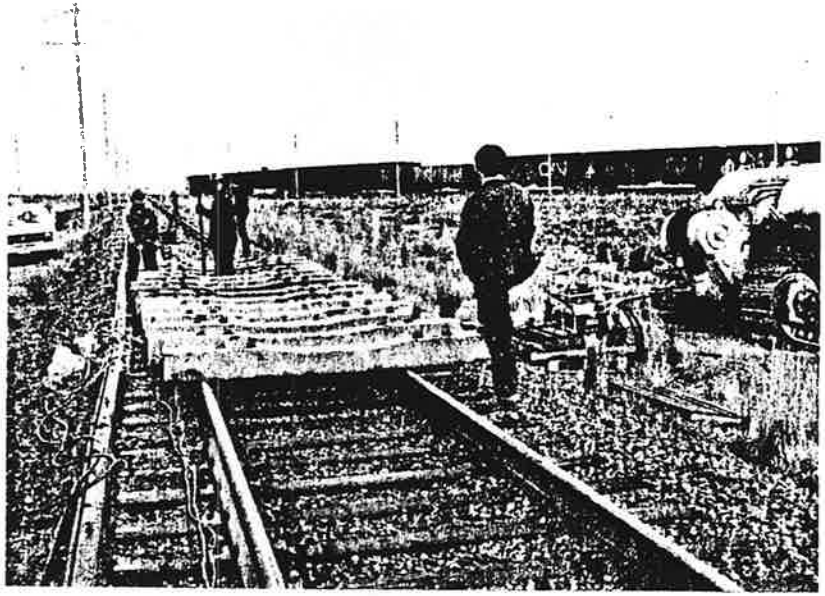

FIGURE B-3. SETUP FOR FRICTION COEFFICIENT TEST

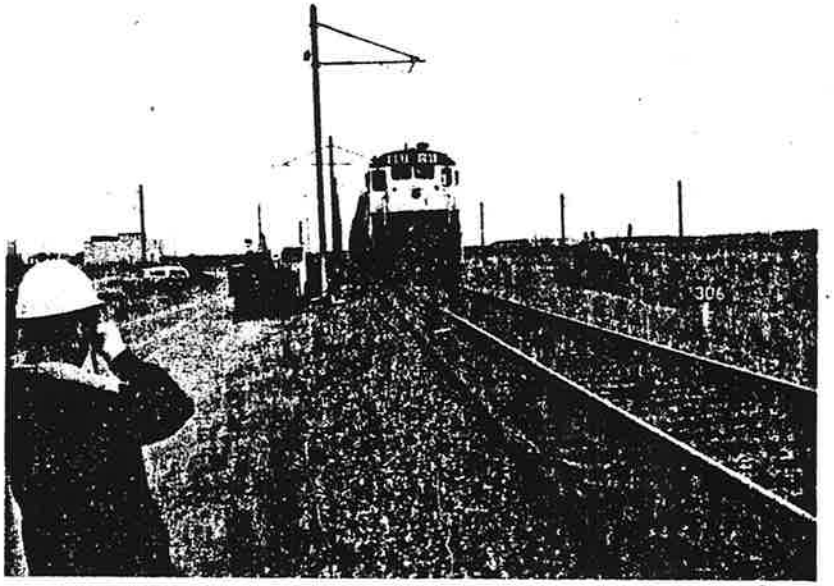

FIGURE B-4. DYNAMIC SAFE TEMPERATURE (Tangent Track)

APPENDIX C
PHOTO ILLUSTRATIONS (PHASE II BUCKLING TESTS)

(These are copies of the original photographs taken at TTC during the tests.)

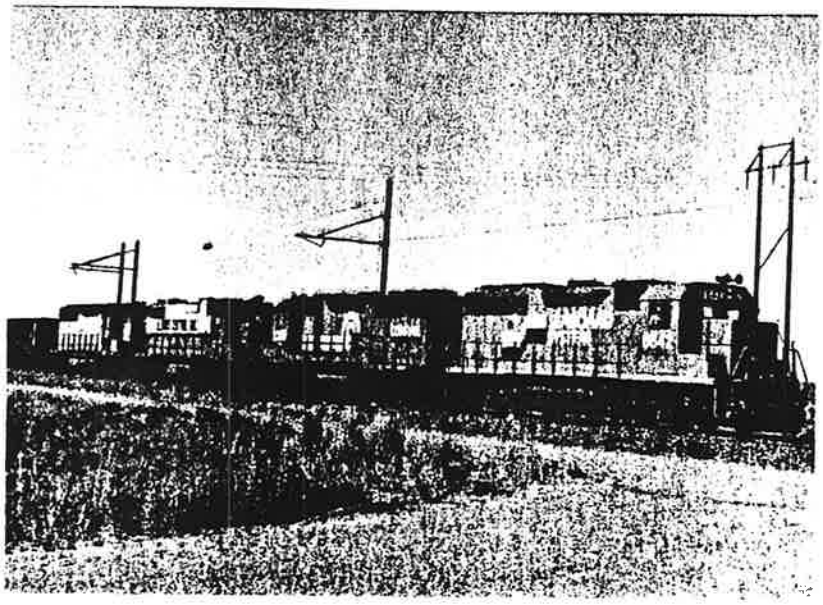

FIGURE C-1. FAST CONSIST TO CONSOLIDATE TRACK

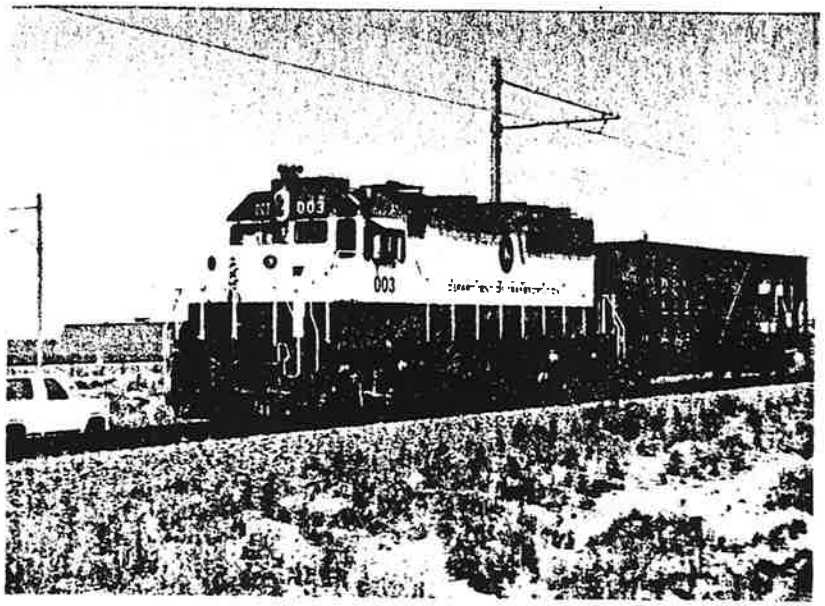

FIGURE C-2. LOCOMOTIVE AND HOPPER CONSIST USED IN DYNAMIC BUCKLING TEST

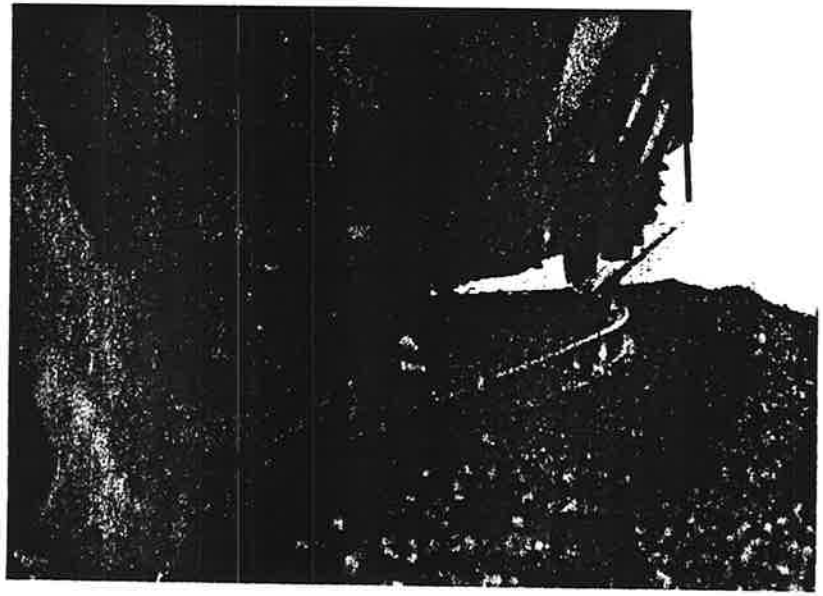

FIGURE C-3. PROGRESSIVE BUCKLING TEST UNDER HOPPER

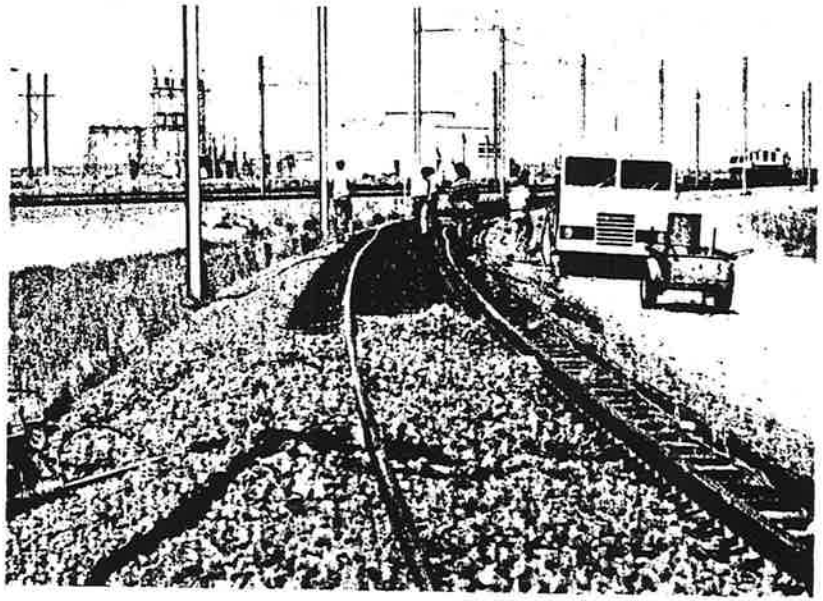

FIGURE C-4. ADDITIONAL BALLAST DUMPED TO CONTROL BUCKLING

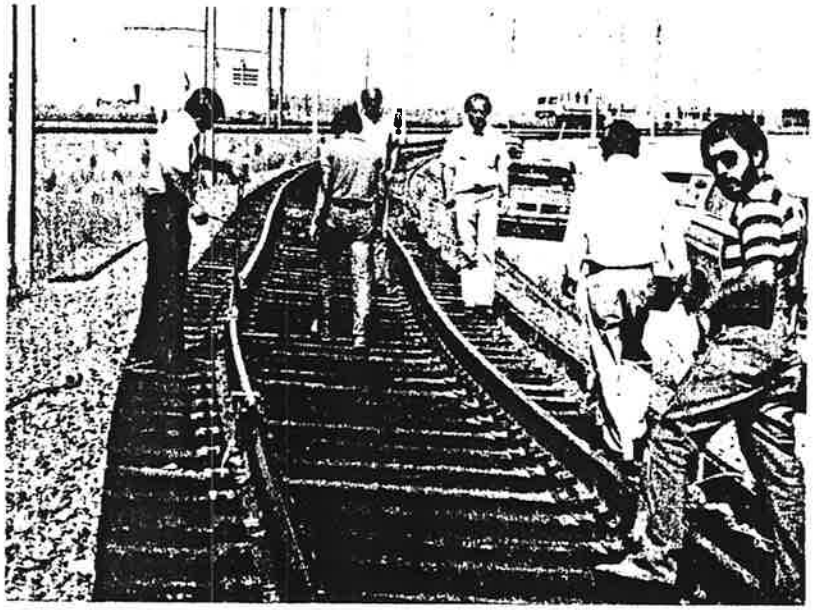

FIGURE C-5. BUCKLED CURVED TRACK

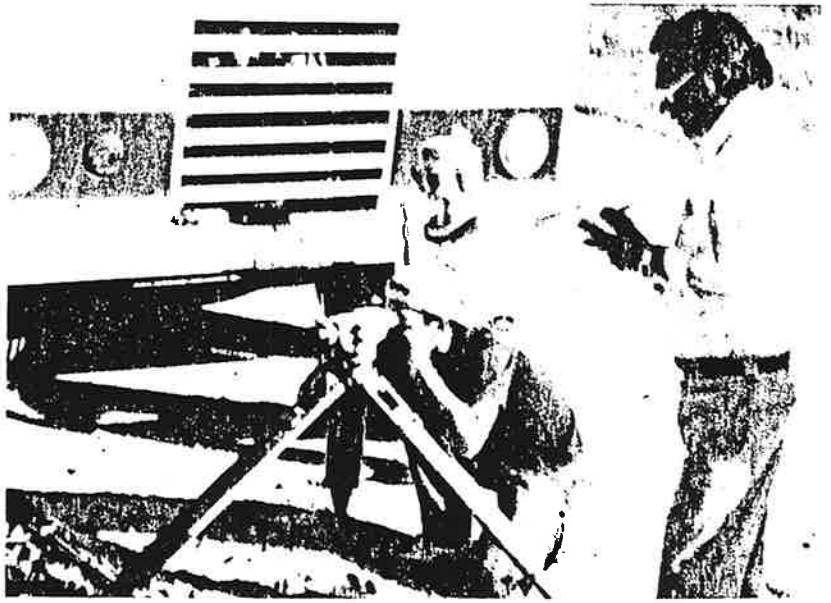

FIGURE C-6. TRANSIT TO MEASURE VERTICAL DEFLECTIONS

FIGURE C-7. ROLLORDINATOR TO MEASURE IMPERFECTIONS

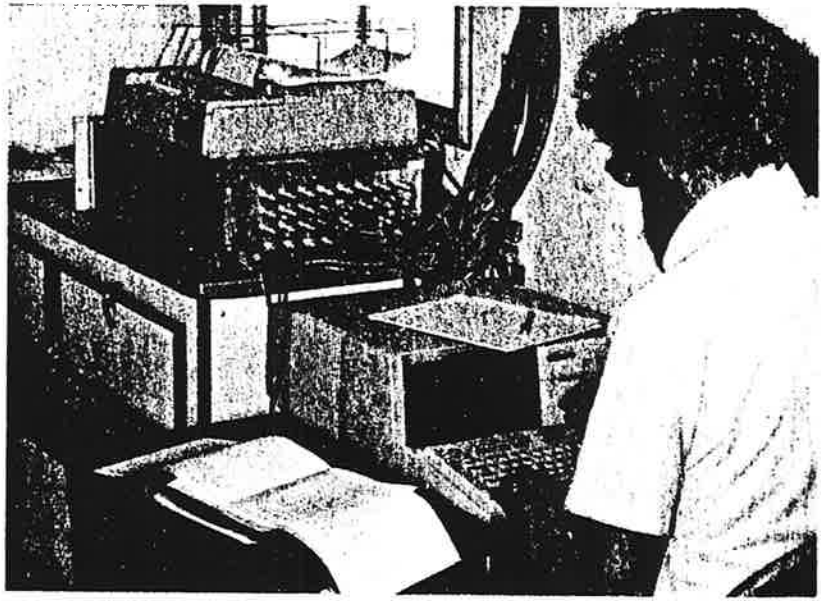

FIGURE C-8. DATA LOGGER IN INSTRUMENTATION VAN